ION EXCHANGE KINETICS OF CESIUM FOR VARIOUS REACTION DESIGNS USING CRYSTALLINE SILICOTITANATE, UOP IONSIV® IE-911

A Dissertation

by

SUNG HYUN KIM

Submitted to the Office of Graduate Studies of
Texas A&M University
in partial fulfillment of the requirements for the degree of

DOCTOR OF PHILOSOPHY

December 2003

Major Subject: Chemical Engineering

ION EXCHANGE KINETICS OF CESIUM FOR VARIOUS REACTION DESIGNS USING CRYSTALLINE SILICOTITANATE, UOP IONSIV® IE-911

A Dissertation

by

SUNG HYUN KIM

Submitted to Texas A&M University
in partial fulfillment of the requirements
for the degree of

DOCTOR OF PHILOSOPHY

Approved as to style and content by:

Rayford G. Anthony (Chair of Committee)	Aydin Akgerman (Member)
David Ford (Member)	F. Michael Speed (Member)
	Kenneth R. Hall (Head of Department)

December 2003

Major Subject: Chemical Engineering

ABSTRACT

Ion Exchange Kinetics of Cesium for Various Reaction Designs Using Crystalline Silicotitanate, UOP IONSIV® IE-911. (December 2003)

Sung Hyun Kim, B.S., Korea University;

M.S., Korea University

Chair of Advisory Committee: Dr. Rayford G. Anthony

Through collaborative efforts at Texas A&M University and Sandia National Laboratories, a crystalline silicotitanate (CST), which shows extremely high selectivity for radioactive cesium removal in highly concentrated sodium solutions, was synthesized.

The effect of hydrogen peroxide on a CST under cesium ion exchange conditions has been investigated. The experimental results with hydrogen peroxide showed that the distribution coefficient of cesium decreased and the tetragonal phase, the major component of CST, slowly dissolved at hydrogen peroxide concentrations greater than 1 M.

A simple and novel experimental apparatus for a single-layer ion exchange column was developed to generate experimental data for estimation of the intraparticle effective diffusivity. A mathematical model is presented for estimation of effective diffusivities for a single-layer column of CST granules. The intraparticle effective diffusivity for Cs was estimated as a parameter in the analytical solution. By using the least square method, the effective diffusivities of $1.56 \pm 0.14 \times 10^{-11}$ m^2/s and $0.68 \pm$

0.09x 10^{-11} m^2/s, respectively, were obtained. The difference in the two values was due to the different viscosities of the solutions. A good fit of the experimental data was obtained which supports the use of the homogeneous model for this system.

A counter-current ion exchange (CCIX) process was designed to treat nuclear waste at the Savannah River Site. A numerical method based on the orthogonal collocation method was used to simulate the concentration profile of cesium in the CCIX loaded with CST granules. To maximize cesium loading onto the CST and minimize the volume of CST, two design cases of a moving bed, where the fresh CST is pulsed into the column at certain periods or at certain concentration of cesium, were investigated. Simulation results showed that cesium removal behavior in the pilot-scale test of CCIX experiment, where the column length is 22 ft and the CST is pulsed 1 ft in every 24 hours, was well predicted by using the values of the effective diffusivities of 1.0 to 6.0 × 10^{-11} m^2/s.

ACKNOWLEDGEMENTS

First, I would like to express my deepest appreciation to my research advisor, Dr. Rayford G. Anthony for all his sincere support and guidance throughout the course of this research.

I would also like to thank my committee members, Dr. Aydin Akgerman, Dr. David Ford, and Dr. F. Michael Speed, for their valuable advice and assistance.

I am grateful to the members of the kinetics, catalysis and reaction engineering group for their excellent advice and support.

I would like to thank Korean students in Chemical Engineering for the help they gave me.

Finally, I cannot adequately express my appreciation for my family-my wife and my son, my brother, my parents, brothers in law, and parents in law-for their love, encouragement and emotional support during my study.

TABLE OF CONTENTS

CHAPTER Page

LIST OF FIGURES

FIGURE Page

FIGURE Page

FIGURE Page

LIST OF TABLES

CHAPTER I

INTRODUCTION

1.1 Background

During World War II, the United States built a complex of top-secret nuclear production and research facilities across the country to face with Nazi Germany. At that time, many handling and disposal technique were considered state-of-the-art, but they were not enough to prove adequate to protect the hundreds of thousands of employees and environment (U. S. Department of Energy, 1994). After the war, the former alliance, the United States and the Soviet Union, started the nuclear arms race, as the Cold War era began in the late 1940s. The Cold War era stretched from the late 1940s to the late 1980s, ending in 1990 with the dissolution of the Soviet Union and the fall of communist governments throughout Eastern Europe. The facilities at sites across the country to produce the nuclear weapons and conduct research generated radioactive waste and contaminated some areas of the production and research sites. After the Cold War era, the U. S. Department of Energy (DOE) faced the challenge to clean-up and manage the radioactive waste rather than produce the nuclear materials. The environmental management program is an enormous and complex effort requiring constant advances in technology. Unfortunately, the development of waste treatment technologies is far behind the development of waste generating technologies.

This dissertation follows the style and format of *AIChE Journal.*

Furthermore, the disposal of these radioactive wastes is very expensive, so the DOE have chosen to store these wastes at various facilities throughout the Unite States. For example, at the Hanford Reservation in Richland, Washington, currently stores 65 million gallons of radioactive wastes in 177 underground storage tanks. Sixty seven of these 177 tanks are presumed to be leaking and potentially contaminating surface and ground waters (Marsh et al., 1993). Thus, one mission of DOE is to clean-up these hazardous wastes and to develop technologies to treat and dispose of wastes at each storage location.

The DOE has focused its research and technology development in areas where new technology is currently needed to solve clean-up problems. In many cases, there is no effective, proven, long-term waste management or cleanup technology for the DOE's wastes or sites. The development of new technologies is essential to the success of the environmental management program. Thus, the goals of the technology development program are to (U. S. Department of Energy, 1994):

- development technologies that will minimize the volume and toxicity of wastes,
- manage unavoidable waste more safely and efficiently,
- accomplish faster, cheaper, better, and safer cleanup of contamination and waste problems, and
- achieve safe, permanent disposal of waste within regulatory guidelines.

Over the long term, many researchers have provided needed technologies for environmental management to achieve the goals.

1.2 Tank Waste Clean Up Technology

Within the DOE complex, 287 underground storage tanks have been used to process and store radioactive and hazardous waste in the form of solid, sludge, liquid, and gas generated from weapon materials production and researchers. Collectively, these tanks hold over 90 million gallons of wastes containing approximately 650 million curies of radioactivity (U. S. Department of Energy, 2000). The bulk of the wastes is stored at 4 major sites across the United States, including Hanford Site, Savannah River Site (SRS), Oak Ridge, and Idaho National Engineering and Environmental Laboratory (INEEL). Table 1.1 summarizes the tanks and quantities of each site.

Table 1.1. Tank summaries at four major sites

Characteristics	Hanford	SRS	Oak Ridge	INEEL
No. of tanks	177	49	40	18
Waste Volume (million gallons)	54	35	0.43	2.4
Radiations (million curies)	200	420	0.013	25

Most of the wastes is alkaline and contains various chemicals including nitrate and nitrite salts, hydrated metal oxides, and phosphate precipitates. Much of radioactivity in the wastes is primarily due to the presence of isotopes of ^{137}Cs and ^{90}Sr, which are present at ppm levels. The primary component in these wastes is ^{137}Cs because it is a

gamma emitter, which is the most penetrating radiation and can pass through many materials including human body, and has a high mobility in the biosphere (Moore, 1993).

In 1994, the DOE's Office of Environmental Management established the Tank Focus Area (TFA) to manage and carry out the integrated national program of technology development for tank waste remediation. The TFA focused on the following five key process steps (U. S. Department of Energy, 2000):

1) Safe Waste Storage,
2) Retrieval,
3) Closure,
4) Pretreatment,
5) Immobilization.

Within the Safe Waste Storage process, the TFA is developing systems to identify chemical and physical characteristics of the waste inside the tank, to monitor the tank integrity, to prevent tank corrosion, and to ventilating tanks.

The TFA is developing waste retrieval devices capable of dislodging the solid, sludge, and saltcake fractions of the wastes and conveying them from the tanks that can be deployed with remotely controlled equipments. The TFA is also developing methods that mobilize solid waste at the tank bottoms without adding water, while still enabling optimal treatment and transfer properties.

The Closure of tank waste is demonstrating cost-efficient methods to remove saltcake and solid waste at the tank bottoms and close a high-level waste tank. The TFA

is developing characterization solutions to support the determination of closure criteria within regulatory constraints and tank cleaning methods that enabling cleanup with minimal water and chemicals.

To reduce costs and the required volumes of high-level waste disposal, the pretreatment technique will separate tank wastes into low-level and high-level fractions. Therefore, the TFA is developing waste minimization solutions to separate waste types and reduce high-level waste volumes. These techniques include the design of a Cesium Removal Demonstration (CsRD) unit and a mobile evaporator to concentrate tank waste.

To prevent release of radioactivity or hazardous chemicals to the environment, the wastes must be immobilized into solid stable forms. The highly radioactive waste is melted into a vitrified form and the less hazardous radioactive waste is immobilized through vitrification or grouting. The TFA continues to develop the technique to improve melter and waste product performance and enhance glass and grout formulations. Cesium-loaded separation media from the CsRD will also be treated and vitrified by immobilization technique.

1.3. Pretreatment Technology

DOE has stored about 90 million gallons of high-level and low-level waste in tanks at four primary sites within the DOE complex. Although each tank has different compositions, the total volume of waste is considered high-level wastes, which is neither cost-effective nor practical to treat and dispose of all of the wastes to meet the requirements of the high-level wastes repository program. Hence, the wastes need to be

separated into low and high-level wastes. Tank wastes at INEE are acidic, and stored in stainless steel tanks. Much of it has already been calcined at high temperature to a dry powder form. Wastes at Oak Ridge are small in volume and radioactivity compared to other major sites. At Hanford, several different nuclear fuel processes for weapons production were used, which resulted in different waste volumes and chemical compositions. Fuel processing at the SRS did not changed substantially from the beginning of operations. Although the wastes at SRS are fairly uniform, they still required pretreatment to separate the low-level waste from high-level waste before immobilization. The saltcake and liquid forms, which are the largest source of high-level wastes, contain mostly sodium nitrate and sodium hydroxide salts. The radioactive components such as cesium and strontium can also be present in varying concentration. Mostly, only a small fraction of the waste, by weight, contains radioactive components. The radioactive components must be removed or reduced below the Nuclear Regulatory Commission (NRC) limit, which enables large portion of waste to be treated and disposed of as low-level wastes and with a small portion of that is to be considered as high-level waste. Therefore, the primary object of the removal of cesium is to reduce the overwhelmingly large volume of high-level wastes and minimizing the radiation exposure hazards to the environment and personnel during treatment and disposal of the waste.

DOE has investigated several new technologies for separating and stabilizing the radioactive constituents in high-level waste. Chemical precipitation, solvent extraction, ion exchange, evaporation, and membrane separation have all been considered as

potential technologies. Chemical precipitation typically requires sodium tetraphenylborate (NaTRB), which precipitates cesium, aiding in the decontamination of high-level radioactive waste solution (Lee and Kilpatrick, 1982; Walker and Schmitz, 1984). However, the low stability of NaTPB has been observed in acidic solutions through acid hydrolysis (Fowler, 1983). Even in strongly basic solution, NaTPB decomposes with certain component or conditions, which include copper (II), light, and temperatures greater than normal temperature. As a generic separation technique for separation of radioactive constitutes from aqueous solution, solvent extraction has been used successfully in the nuclear industry (Ritcey and Ashbrook, 1984). Although it has a lot of advantages including high selectivity, flexibility, and adaptability for remote control, solvent extraction requires additional equipment for stripping and stabilizing the radioactive constitute into a stable solid form. The hazardous organic solvent, requires additional treatment prior to disposal, is also involved. Evaporation technology has been used extensively in industry to efficiently remove water from liquid solutions for many years. Evaporation technology offers the possibilities of removing water from tank waste, thus reducing the volume of radioactive wastes stored in tanks at the DOE facilities. Large scale and stationary evaporator facilities have also been used at SRS and Hanford sites (Fowler and Perona, 1993). However, operating evaporators are energy intensive and difficult to optimize. The resulted solid phase from an evaporator is the mixture of all other salts with radioactive wastes, which needs separation and decontamination. The high-level waste sludges at Hanford and SRS contain large quantities of sodium salts, which can be recovered as sodium hydroxide and also be

recycled. The membrane technology has been used to remove sodium ions from liquid stream, which contains high concentration of salt. Although membrane technology is effective to remove the component selectively from the waste tank, it requires large pressure drop and efficient separation becomes increasingly difficult as the fouling problem is intensified by the complexity of high-level waste.

Currently, the most accepted options for cesium removal from high-level waste before final disposal are ion exchange technology, organic solvent extraction, and precipitation method (Fink et al., 2002). Among them, ion exchange technology has several advantages. For example, the processes are flexible, efficient enough to achieve decontamination factors of several orders of magnitude, simple, compact, and not requiring any hazardous organic solvents (Miller and Brown, 1997). Several different sorbents, both inorganic and organic ion exchangers, are being considered for use in the cesium removal processes. These include resorcinol formaldehyde resin, zeolites, Duolite CS-100, CST, potassium cobalt hexacyanoferrete (KCoCF), pillared clays, and ammonium molybdophosphate (AMP).

The inorganic ion exchangers offer many advantages over the organic ion exchangers. First, inorganic ion exchangers offer more resistant than organic ion exchangers to chemical, physical, and radiation degradation. Second, the inorganic ion exchangers have a uniform structure, which lead to remarkable selectivity. Third, the simple single-pass operation is possible because of the high selectivity and efficient operation of inorganic ion exchangers. Next, a number of options for disposal of radioactive waste loaded inorganic ion exchangers are possible after the separation

process is finished. Finally, contrast to the inorganic ion exchangers, it has been reported that organic exchangers lose around 3 % of their capacity per cycle, which could not be used after 20 to 30 cycles (Kurath et al., 1994). In addition, re-generable organic ion exchangers require additional processing equipment to handle the regeneration liquid and the Cs loaded eluent (Miller and Brown, 1997). Among the inorganic ion exchangers, the clays are not selective at high sodium solution and zeolites and metal salts tend to decompose in highly alkaline solutions (Anthony et al., 1994). Because of concerns regarding the potential for a hazardous exothermic reaction between the nitrates and ferrocyanides, KCoCF may not be considered for use at Hanford and SRS (Walker and Youngblood, 1995). Furthermore, KCoCF has been shown to begin to dissolve or decompose in the highly alkaline tank solution, at pH values greater than 12 (Collins et al., 1995). Although the ability of AMP to remove cesium from acid solution and to retain its capacity in excess sodium solution, AMP is also not be used at pH values greater than 6 because it tend to decompose at high pH value. Since the channel size of CST is close to the diameter of Cs ions, ion exchange of Cs ions is almost irreversible (Philip and Anthony, 2000). That's why the CST can not be regenerated after the ion exchange process of Cs ions.

CST is considered to be a primary candidate for use in the cesium removal process due to its chemical and physical stability and relatively good loading characteristics across a wide pH range and ability to be converted into a stable waste form for disposal (Bunker, 1994).

1.4. TAM-5 as an Ion Exchanger

Amorphous hydrous titanium oxide (HTO), developed at Sandia National Laboratory in the 1960s, was tested as an ion exchanger to convert high-level waste into a stable ceramic form in 1975 (Johnstone, 1978). The HTO can be used as an ion exchanger for most cationic radioactive constituents, for example strontium and plutonium, but had essentially no affinity for cesium, which is the most dangerous constituent because it is a gamma emitter and has a high mobility in the biosphere. As a result of effort to treat the cesium, a new class of ion exchangers called TAM5, a particular CST, which has a large affinity for cesium and strontium in the presence of high sodium concentrations across a wide pH range, was prepared by Anthony et al. (1993). Under a Cooperative Research and Development Agreement (CRADA) between Sandia, Texas A & M University and Universal Oil Products (UOP), subsequent product development and commercialization was conducted by UOP. In 1994, UOP prepared the first large-scale batch of TAM5 powder, which is nearly identical to materials prepared at the laboratory scale. This is given the name IONSIV® IE-910, commercial name of powdered form of TAM5. The engineered form, which combines the powdered form with binder to form a larger granular form, is essential for practical use in a fixed-bed column arrangement proposed for continuous processing of radioactive waste. IONSIV® IE-911, commercial form of engineered TAM5, was developed in 1995. According to the study at Los Alamos National Laboratory (LANL), the use of IE-911 for the Hanford cleanup effort would result in over 300 million dollars in savings over the baseline process (DeMuth, 1996). Eventually, these results led to the designation of

IONSIV® IE-910 and 911 as "one of the 100 most technologically significant products of the year " and the inventions and works receive the 1996 R & D 100 award (Miller and Brown, 1997).

From the cesium removal experiments of SRS simulants and actual waste, McCabe reported that the TAM-5 is very effective for cesium removal from SRS high-level waste (McCabe, 1995,1997). As a sorbent selection process, the full-scale demonstration of cesium removal, which uses approximately 116,000 L of supernate and 265 L of sorbent, has been conducted at Oak Ridge National Laboratory (ORNL) (Walker et al., 1999; Lee et al., 1997). In an evaluation of several ion exchangers, which were selected from state-of-art ion exchange material, Walker et al. (1999) concluded that IONSIV® IE-911 was the only sorbent with no limiting operation problems and was rated first on all discrimination criteria except for kinetic performance as the best for use in cesium removal technology.

CHAPTER II

THEORIES AND LITERATURE REVIEW

2.1 Ion Exchange Equilibrium

The ion exchange reaction, by common definition, is a stoichiometric process in which an ion in one phase is replaced by an equivalent amount of number of ions from the other phase. The exchangeable ions may be either cation or anion and the two different phases are usually a solid phase and liquid phase. A typical reaction can be described by the following general equation:

$$\nu_A A^{z_A} + \nu_B \overline{B}^{z_B} \Leftrightarrow \nu_B B^{z_B} + \nu_A \overline{A}^{z_A} \qquad (2.1)$$

where A and B are the ions in the liquid phase, overbar represents the solid phase, ν_A and ν_B are the stoichiometric coefficients, and Z_A and Z_B are the charge values. The electric charge balance requires $\nu_A Z_A$ equals $\nu_B Z_B$.

The thermodynamic equilibrium constant is described as follows:

$$K_{eq} = \frac{\overline{a}_A^{\nu_A} a_B^{\nu_B}}{\overline{a}_B^{\nu_B} a_A^{\nu_A}} \qquad (2.2)$$

where the K_{eq} is the thermodynamic equilibrium constant, overbar represents the solid phase, a_A and a_B are the activities in the liquid phase. By multiplication of concentration

and an activity coefficient, the activity of component of i is calculated. Thus, equation (2.2) can be represented as follows:

$$K_{eq} = K_C K_\gamma \qquad (2.3)$$

where

$$K_C = \frac{Q_A^{\nu_A} C_B^{\nu_B}}{Q_B^{\nu_B} C_A^{\nu_A}} \qquad (2.4)$$

$$K_\gamma = \frac{\bar{\gamma}_A^{\nu_A} \gamma_B^{\nu_B}}{\bar{\gamma}_B^{\nu_B} \gamma_A^{\nu_A}} \qquad (2.5)$$

and Q_A and Q_B are the concentrations of A and B in the solid phase, C_A and C_B are the concentrations in the liquid phase, γ_A and γ_B are the activity coefficients in the liquid phase, and the overbar represents the solid phase.

If the solid phase is ideal, which is commonly assumed for some zeolites (Barrer and Sammon, 1955; Barrer and Falconer, 1956), the rational selectivity, the thermodynamic equilibrium constant without solid-phase activity coefficients, is the same as the thermodynamic equilibrium constant. If both solid phase and liquid phase are ideal, the K_c is the same as the thermodynamic equilibrium constant. However, the electrolytic solution of liquid phase cannot be assumed ideal because the activity coefficients are mostly affected by the ionic strength of the solution (Pitzer, 1991).

The widely used distribution coefficient, which represents the performance of an ion exchanger, is defined as the ratio of the equilibrium concentration in the solid phase to that in the liquid phase:

$$K_{dA} = \frac{Q_A}{C_A} \qquad (2.6)$$

where K_{dA} is the distribution coefficient of ion A.

The heat of reaction for ion exchange is related to the ion exchange equilibrium constants by Van't Hoff's equation (Holland and Anthony, 1989) as follows:

$$\left(\frac{\partial \ln K_{eq}}{\partial T}\right)_P = \frac{\Delta H^\circ}{RT^2} \qquad (2.7)$$

where T and P are the temperature and pressure, ΔH^o is the enthalpy change of the ion exchange, which can be considered constant if the temperature range is not wide, and R is the gas constant, which is 8.314 J/mol K.

The equilibrium concentration relationship between the liquid and solid phase can be represented by a simple form of isotherm equation. The isotherm equation is as follows:

$$Q_A = f(C_A) \qquad (2.8)$$

A lot of adsorption isotherms have been developed for explaining the adsorption phenomenon. While ion exchange is a stoichiometric process involving electrostatic forces within a solid matrix, adsorption is not necessarily stoichiometric and involves

both electrostatic and van del Waals forces at the solid phase. Despite the differences between adsorption and ion exchange, both processes can be predicted by similar mathematical equations. Thus, some authors have employed adsorption isotherms into ion exchange to represent the relationship between the liquid and solid phase (Crittenden el al., 1980; Gu el al., 1990; Polzer and Fuentes, 1988; Polzer et al., 1992; Zheng et al., 1995).

Activity coefficients for the liquid phase are commonly available from many references (Robinson and Stokes, 1970; Bromley, 1973; Zemaitis et al., 1986; Horvath, 1985, Pitzer, 1991; Lide, 1996) both in tabulated and model estimated forms. The activity coefficients of electrolytes can be correlated with ionic strength, which is defined as follows:

$$I = \sum_i \frac{1}{2} m_i Z_i^2 \qquad (2.9)$$

where I is the ionic strength, m_i is the molality of ion i, and Z_i is the valence of ion i.

Denbigh (1981) proposed the empirical equation (Eq. 2.10) for estimating activity coefficient of electrolytes up to ionic strengths of 0.1 mol/kg, which was an improved version of the Debye-Huckel limiting law.

$$\log \gamma_{\pm} = - \frac{A_m \left| Z_M Z_A \right| I^{0.5}}{1 + I^{0.5}} \qquad (2.10)$$

where $\gamma_{\pm}$ is the mean activity coefficient of an electrolyte in the liquid, A_m is the Debye-Huckel constant which equals 0.511 $kg^{0.5}/mol^{0.5}$ at 25 ^oC, and Z_M and Z_A are the number of the charges of cation M and anion A.

A single-parameter equation for estimation of activity coefficients of individual ion in a mixture of strong aqueous electrolytes, i.e., ionic strength is up to 6 mol / kg, proposed by Bromley (1973) as follows:

$$\log \gamma_i = -\frac{0.511\, z_i^2\, I^{0.5}}{1 + I^{0.5}} + F_i \qquad (2.11)$$

where subscript i denote cations, and F_i is calculated from the following equations.

$$F_i = \sum_j C_{i,j} Z_{i,j}^2 m_j \qquad (2.12)$$

$$C_{i,j} = \frac{(0.06 + 0.6\, B_{i,j})\left|Z_i Z_j\right|}{\left(1 + \frac{1.5}{\left|Z_i Z_j\right|} I\right)^2} + B_{i,j} \qquad (2.13)$$

$$Z_{ij} = \frac{\left|Z_i\right| + \left|Z_j\right|}{2} \qquad (2.14)$$

where subscript j denote anions, Z_i and Z_j are the number of the charges of caions i and anions j, m_j is the molality of anion j, B_{ij} is the Bromley's model parameter, which is calculated by following equation.

$$B_{ij} = B_i + B_j + \delta_i \delta_j \qquad (2.15)$$

where B_i and B_j, and δ_i and δ_j are Bromley parameters for individual ions and their value at 25 ^oC are given by Bromley (1973).

Pitzer et al. (1991) proposed the 8 parameter model, which can be used for solution greater than 6 mol/kg of ionic strength. Although Pitzer's model is little more accurate than Bromley's model for the mixture of aqueous electrolytes, many parameters make it difficult to use for complex solutions.

Polzer et al. (1992) used combined modified Langmuir isotherm for ion exchange on volcanic tuff media with Gains and Thomas theory (1953), which satisfies the Gibbs-Duhem equation and implicitly includes the activity coefficients for the solid phase, to predict the parameters of modified Langmuir isotherm.

Zheng et al. (1995) claimed that they could predict the distribution coefficient of cesium with a high degree of accuracy in complex electrolytic solutions for a variety of solution concentrations by using Polzer's method. However, when competitive effect exists the predicted distribution coefficient is higher than the observed value because the model does not take into account the competitive effect of the competitive cations. The

activity coefficients for cesium and sodium cations were calculated by using Bromley's model.

Although activity coefficient of the solid phase can be calculated from the excess Gibbs energy, only a few methods, which are highly empirical and difficult to estimate, have been developed (Smith and Van Ness, 1987). An ion exchanger, which is rigid, does not swell and has relatively small changes in water content between different cationic forms of the solid, is commonly considered to follow the ideal solid phase behavior (Amphlet, 1964). Zheng et al. (1996) reported that the solid phase could be treated as an ideal solid for TAM5 ion exchanger in a double shell slurry feed (DSSF) simulant at Hanford waste. They also found that the existence of two types of ion exchange sites, one of which exhibited preference for Cs^+ and Rb^+ ions and the other exhibited preference for H^+, K^+, and $SrOH^+$ ions (Zheng et al., 1997).

A ZAM (Zheng-Anthony-Miller) model of the ion exchange reaction based on TAM5 powder, was proposed for ion exchange between H^+, Na^+, K^+, Rb^+, and Cs^+ by Zheng et al. (1997). To predict the activity coefficients of the liquid phase, Bromley's model was used. The equilibrium compositions and distribution coefficients of the counterions were calculated for complex solutions by solving the equilibrium equations, whose equilibrium constants were estimated from experiments with simple ion exchange system, and material balance equations. They concluded that the predictions match the experimental results within 10 % for all of the solutions used.

2.2 Diffusion Modeling

2.2.1 Mass Transfer in the Liquid Phase

An adsorption or ion exchange process is composed of three mass-transfer steps, i.e., mass transfer in the liquid phase, interphase mass transfer, and intrapellet mass transfer.

The resistance to mass transfer in the liquid phase, which may become important in cases where the liquid is contacted with pellets in relatively slow motion, as in the case of a fixed-bed, moving bed, or fluidized bed operation, is related to the diffusion and mixing of ions in the liquid phase between the pellets. As a result of ion concentration gradients and the non-uniformity of fluid flow in the fixed-bed operation, diffusion and mixing of ions in the liquid phase could occur. These effects result in the dispersion of ions, which takes place along both the direction of main flow, i.e., axial dispersion, and the direction transverse of main flow, i.e., radial dispersion. Several theories and models have been proposed to describe the diffusion and mixing in terms of dispersion coefficients. It is generally recognized that radial dispersion is ignored because the bed diameter is almost always several orders of magnitude greater than the pellet diameter in the fixed bed process.

Suzuki and Smith (1972) proposed the following relationship for the axial dispersion coefficient in beds of small particles whose diameters ranged from 0.1 to 1 mm.

$$\frac{D_L}{D_m} = 0.44 + 0.83 \frac{u}{D_m} \qquad (2.16)$$

where D_L is the axial dispersion coefficient in cm^2/s, D_m is the molecular diffusivity in cm^2/s, and u is the superficial velocity in cm/s. The molecular diffusivity at infinite dilution for cesium was reported as 2.05×10^{-9} m^2/s (Lide, 1996). The first term, is due to molecular diffusion, is dominant at low velocities, and the second term, is due to convective mixing, is dominant at high velocities.

Latheef (1999) performed residence time distribution (RTD) experiments using a small-scale ion exchange column to compare the axial dispersion correlation with the experimental values. The correlations developed by Suzuki and Smith (1972), Wakao and Kaguei (1982), and Wen and Fan (1975) were compared with the experimental results and concluded that the Suzuki and Smith (1972) correlation provided the best estimate of the experimentally measured values. The Latheef (1999)'s experimental results for ion exchange column can be applied to the axial dispersion correlation using dimensionless analysis. The results are shown in equation 2.17

$$D_L = 1.171\frac{ud_p}{\varepsilon} + 21.037\frac{d_p^2 u^2 \rho}{\mu\varepsilon} \qquad (2.17)$$
$$0.1 \le N_{\mathrm{Re}} \le 100$$

where u is superficial velocity, ρ and μ are the density and viscosity of the fluid, and ε is the porosity of the pellets.

2.2.2 Interphase Mass Transfer

Interphase diffusion refers to the transport of ions from bulk of the liquid phase to the external surface of ion exchange pellets, which depends on the hydrodynamic condition outside the pellets. The main driving force is the gradients of concentration across the boundary layers. But, because the diffusing species are charged ions, the electric potential is also considered as a driving force.

When the electric potential is ignored, the interphase mass transfer rate may be expressed as follows:

$$N_i = k_f (c_i - c_{i,s}) \qquad (2.18)$$

where N_i is flux at the particle surface, k_f is the mass transfer coefficient, c_i is the concentration of ion i in the bulk solution, and $c_{i,s}$ is the concentration of ion i at the surface of the pellet. Although there is no method for directly measuring the film mass transfer coefficient, numerous investigations have been conducted to establish correlations for the mass transfer coefficient.

Sherwood et al. (1975) summarize the approximation expression for mass transfer coefficient in agitated vessels graphically in terms of j factor, J_M, and Reynolds number, N_{Re}, which are defined as follows:

$$J_M = (\frac{k_f}{u})(\frac{\nu}{D_M})^{2/3} \qquad (2.19)$$

$$N_{\mathrm{Re}} = \frac{d_p u}{\nu} \qquad (2.20)$$

where u is superficial velocity, ν is kinematic viscosity of the fluid, D_M is ion diffusivity in the bulk phase, and d_p is the particle diameter.

By using dye test for ion exchange on TAM-5 in a batch reactor, Huckman (1999) has shown that film resistance is insignificant at a setting of 4 on a model 4650-50 Spincadet (Cole-Parker) stirrer.

Wakao and Funazkri (1978) and Suzuki (1990) reported the comparison of mass transfer correlations in a fixed-bed column and plotted the results in terms of the Reynolds number and the Sherwood number, N_{Sh}, which is defined as follows:

$$N_{Sh} = \frac{k_f d_p}{D_M} \qquad (2.20)$$

An expression for mass transfer coefficient commonly used by researchers in liquid systems is based on the earlier correlation of Wilke and Hougen (1945), and is given as follows:

$$k_f = \frac{2.62\,(D_m u)^{0.5}}{a_p (d_p)^{1.5}} \qquad (2.21)$$

where u is the superficial velocity, a_p is the external surface area of the particle per packed volume, which is $3/R_p$ for the sphere, and d_p is particle diameter.

2.2.3 Intrapellet Mass Transfer

Because adsorption or ion exchange take place almost exclusively within the pore of the pellets, the diffusion of adsorbates or ions into the interior of the pellets is inevitably required. For the simple case of pore diffusion, where the pellet is assumed to consist pore and a solid phase diffusion through the pore may be represented as shown in equation 2.22.

$$\varepsilon_p \frac{\partial C_{pi}}{\partial t} + (1 - \varepsilon_p) \frac{\partial q_i}{\partial t} = \frac{\varepsilon_p D_e}{r^2} \frac{\partial}{\partial r} (r^2 \frac{\partial C_{pi}}{\partial r}) \qquad (2.22)$$

where ε_p is the particle porosity, C_{pi} is the concentration of i in the pore fluid, q_i is the concentration of i in the solid phase, t is the time, D_e is the effective diffusivity, and r is the radial distance from the center of the particle. Fick's law is used in equation 2.22 for constitutive equation because of the high total ionic concentration of the solution due to the sodium cation. The solution of equation (2.22) requires the proper initial and boundary conditions as well as an additional relationship between C_p and q.

A common feature of pellets is their tortuous path from the surface to the center of the particles. Consequently, the diffusion must follow the tortuous path. The most commonly accepted semi-empirical relationship between effective diffusivity and molecular diffusivity may be expressed as

$$D_e = \frac{D_m \varepsilon_p}{\tau} \qquad (2.23)$$

where τ is tortuosity factor, which accounts for the fact that the diffusion take places along the tortuous path rather than along the radial direction. Satterfield (1970) investigated many common catalysts and concluded that the tortuosity factor varied from 2 to 6. According to the random pore model, parallel cross linked pore model, and pore network model τ varies as the inverse of porosity, 3, and 4, respectively.

If there is strong interaction between the adsorbate and adsorbent, surface diffusion is usually neglected. Sladek el al. (1974) developed a general correlation of surface diffusivity for gas adsorption. This correlation relates the value of m, which varies with the nature of the bond between the adsorbate molecules and the adsorption site as well as the substrate material, and the heat of adsorption with surface diffusivity. Komiyama and Smith (1974) developed the theory for correlating the surface diffusivity in terms of the heat of adsorption and the free energy of activation for forming a vacant site adjacent to an adsorbed molecule. Surface diffusivities were predicted to increase as the heat of adsorption decreases and as the bond becomes weaker between solvent molecules and the adsorbent surface. Yoshida el al. (1994) presented the parallel transport of a bovine serum albumin (BSA) by surface and pore diffusion within two different strongly basic chitosan, a highly porous ion exchanger, using the shallow bed method. Ma et al. (1996) developed multicomponet, two phase homogeneous column

models incorporating parallel constant pore and surface diffusion to examine the effects of pore and surface diffusion on the shape of ion exchange column breakthrough curves for several hypothetical cases. They concluded that only for systems with a linear isotherm yield symmetric breakthrough curves both surface and pore diffusion. Koh et al. (1998) extended the model of Ma et al. (1996) to a fluidized bed using Duolite C-20 cation-exchange resin for sorption of L-phenylalanine and suggested that both pore diffusion and surface diffusion are important intraparticle transport mechanisms. They also proposed a systematic method to estimate the pore diffusivity and surface diffusivity independently. However, this technique requires column breakthrough data under various conditions, which is slower and inefficient than the traditional batch method.

2.3 Modeling of Bidisperse Particles

Commercial CST granules, IONSIV® IE-911, are formed by combining the CST crystals, IONSIV® IE-910, with a binding material, which provides the macropores for transport of ions to the micropores with the crystals. Since the resistances to mass transfer within the crystals, micropores, and those through the binding material, macropores, are different, they require different treatment in explaining the overall intrapellet diffusion process. The particle balance equation for diffusion within a micro-porous crystal is given as

$$\frac{\partial q_i}{\partial t} = -\frac{1}{s^2}\frac{\partial}{\partial s}\left[s^2 J_i^s\right] \qquad (2.24)$$

where s is radial distance from the center of the crystal, and J^s_i is the mass flux into the crystal phase. The macropore diffusion equation is

$$\varepsilon_P \frac{\partial C_{Pi}}{\partial t} + (1-\varepsilon_P)\frac{3}{R_C} J_i^S\Big|_{s=R_C} = -\frac{1}{r^2}\frac{\partial}{\partial r}\left[r^2 J_i\right] \qquad (2.25)$$

where Rc is the crystal radius, and the superscript S refers to the crystal phase.

Ruckenstein et al. (1971) considered the competing effects of macropore and micropore diffusion in a shallow bed, which provided an infinite source of sorbate solution such that the concentration at the surface of the sorbate particle remained constant. They assumed an isothermal condition and a linear isotherm, which could be applied for the condition of a dilute solution. They solved the micro-macro balance equation as follows:

$$\frac{C_i - C_i^o}{C_i^\infty - C_i^o} = 1 + \frac{4\pi}{\eta\beta}\sum_{k=1}^{\infty}\sum_{q=1}^{\infty}\frac{(-1)^k k \sin(k\pi\eta)\exp(-\alpha\xi_{qk}^2\tau_i)}{\xi_{qk}^2\left[\frac{\alpha}{\beta}+1+\cot^2\xi_{qk}-(1-\frac{k^2\pi^2}{\beta})\frac{1}{\xi_{qk}^2}\right]} \qquad (2.26)$$

where C_i is the concentration in the macropore fluid phase, C^o_i is the initial concentration in the macropore fluid phase, C^∞_i is the equilibrium concentration in the macropore fluid

phase, τ_i is dimensionless time, η is dimensionless macrosphere radial position, ξ_{qk} are the roots of the transcendental equation

$$\beta(1 - \xi_{qk} \cot \xi_{qk}) + \alpha\xi_{qk}^2 = k^2\pi^2 \qquad (2.27)$$
$$k = 1, 2, 3 ..... \infty$$

where the parameters α and β are defined as follows:

$$\alpha = \frac{D_c R_s^2}{D_s R_c^2} \qquad (2.28)$$

$$\beta = \frac{3(1 - \varepsilon_a)\varepsilon_c}{\varepsilon_a} \alpha \frac{(1 + \frac{S_c H_c}{\varepsilon_c})}{(1 + \frac{S_s H_s}{\varepsilon_s})} \qquad (2.29)$$

where subscript c and s refers to micropore and macropore, respectively, D is effective diffusivity, R is radius, ε is porosity, S is surface area, H is Henry's law constant. They suggested that large values of α, i.e., larger than 100, mean that the macropore diffusion process is rate limiting and very small values of α, i.e., less than 0.001 indicate that micropore diffusion is rate controlling. They also suggested that the large values of the ratio, β/α, mean that the macropore uptake is negligible and the very small value of the ratio, β/α, indicate that the micropore uptake is negligible. They concluded that the two-

stage process occurs when neither macropore diffusion nor micropore diffusion is dominant. If the two-stage process occurs, a relatively rapid initial uptake is due to the macropore sorption without sorption in the microparticle. Thus rapid uptake is followed by the slow uptake, which is due to penetrating the crystalline particles.

Huckman (1999) suggested that a crystal resistance parameter could be used to determine dominant resistance between the liquid filled pores and the solid phase, which is defined as:

$$N_{Cr} = \frac{\varepsilon_s}{3(1-\varepsilon_s)} \frac{D_e R_c^2}{D_s R_s^2} \frac{C^0}{F(C^0)} \qquad (2.30)$$

where D_s is the crystal-phase diffusivity and $F(C^o)$ is the evaluation of the equilibrium isotherm function at the initial concentration $C = C^o$. The crystal resistance parameter is the inverse of the Ruthven and Laughlin (1972) number, divided by three, and averaged over all possible concentrations. Ma and Lee (1976) and Ma (1978) considered the boundary condition which arises when the bidisperse particles are immersed in a well-stirred batch reator and obtained the expression for the uptake curve.

Although Furusawa and Smith (1973) demonstrated that the single effective diffusivity can be related to the macropore diffusivity, the micropore diffusivity, or both diffusivities, they did not clarified the relationship between the single effective diffusivity and the macropore and micropore diffusivities. Kim (1990) investigated a moment analysis of the modeling equation for diffusion in a bidisperse particle with two

diffusivities and a single diffusivity. He concluded that except when the adsorber is extremely short in length, or flow through the bed is extremely fast, the simple single effective diffusivity model can be advantageously used to account for the diffusivity within the bidisperse solid instead of the complex micro-macro model.

Robinson et al. (1994) investigated ion exchange reaction of the bidispersed chabazite zeolites in binary and multicomponent solutions containing Cs, Sr, Ca, and Mg using the finite batch reactor. They found that the uptake rate for the small particles was significantly faster than for the large particles and that the selectivity for the cations was Cs > Sr > Ca > Mg > Na. Although they showed that the simplified mathematical models including constant diffusivity, parallel or series micro-macropore diffusion, and parabolic concentration profile inside particle could be used predict the experimental uptake, they concluded that only the model accounting for micropore and macropore diffusion occurring in series accurately predicted the multicomponent data using diffusivities from the binary system.

DePaoli and Perona (1996) developed a different model, which employed the two phase homogeneous model containing the film resistance, for the data originally obtained by Robinson et al. (1994). The film mass transfer coefficients were determined by fitting the initial experimental uptake curve with the model, which is used by Fettig and Sontheimer (1987), Weber and Wang (1987), and Simith and Weber (1988), and which gave the value of on the order of 10^{-5} m/s for this system. They obtained the value of 4.8×10^{-9} m^2/s as the effective diffusivity for cesium multicomponent system in the bidispersed chabazite zeolites.

Recently, Silva and Rodrigues (1999) studied the adsorption process in a bidisperse solid in a transient state considering linear, Langmuir, and irreversible isotherms only for microporous particles, which is an extension of Ruckenstein et al. (1971)'s work to nonlinear adsorption equilibrium with negligible macropore adsorption. They concluded that the analytical solution for the linear system and the numerical solution for the nonlinear systems, which was obtained by using orthogonal collocation, were well matched each other. They also provided the criterion to identify the controlling mechanism using Turner (1958)'s pore structure. The parameters, i.e., pore length, number of micropores per unit area of the macropore surface, are difficult to obtained.

2.4 Research Objectives

The main objectives of this research are to investigate the effect of various chemicals on the cesium loading of IONSIV® IE-910 and to develop a mathematical model to simulate ion exchange performance for cesium ion using the UOP IONSIV® IE-911 granules in various reactor systems such as counter-current ion exchange (CCIX) column and single-layer column reactor. In order to accomplish these objectives, the previous equilibrium model developed by Zheng et al.(1997), which was developed based on data collected for experiments with IE-910 powder, will be used to predict the ion exchange performance of IE-910 for cesium and its distribution coefficient for radioactive simulants. This model will be further extended for IE-911 granules to predict the performance of commercialized CST in the radioactive solutions. Analytical and numerical solutions of single-layer column will be provided. Experimental data

from ion exchange single-layer column will be compared with model simulations to determine the effective diffusivity of the particle. The CCIX model also will be offered to compare with the result of the pilot-scale CCIX experiment.

CHAPTER III

THE EFFECT OF CHEMICAL COMPOUNDS ON CESIUM LOADING OF CST

3.1 Introduction

In 1990, a new crystalline silicotitanate, (TAM5) was synthesized by hydrothermal synthesis using sodium hydroxide and the alkoxides of titanium and silicon (Anthony et al., 1993, 1994, 2000, 2002). The crystalline structure of TAM5 is similar to that of Sitinakite, a rare Russian mineral, whose structure consists of the Ti octahedra, Si tetrahedral, and Na octahehedra. TAM5 has straight uniform channels of approximately 3.5 Å diameter, and belongs to a new class of materials similar to zeolites. Typical crystal sizes are in the range of 0.1 – 0.4 μm. Sodium ions are ion exchangeable with protons and also with other alkali metal ions without affecting the crystal structure. Since the channel size of TAM5 and the diameter of Cs ions are very close, ion exchange with Cs ions is almost irreversible (Philip and Anthony, 2000). The TAM5 was proven stable toward cesium desorption even at temperatures up to 55 ^{o}C, i.e., only two percent or less of total cesium irreversibly desorbed during an experiment for a two week period at 55 ^{o}C (Walker, 2000).

Replacing about 25% of the titanium atoms with niobium atoms modifies TAM5 but the crystal structure is still tetrahedral. The resulting product was tested extensively to enable its use as an inorganic ion exchanger for the removal of radioisotopes, especially ^{137}Cs, from highly alkaline nuclear waste solutions. TAM5, also labeled as a

CST, has been synthesized from inorganic precursors in aqueous solutions without the use of any organics, such as alkoxides. Additionally, alternative alkali metal hydroxides can replace the use of sodium hydroxide, which produces different products. The alkali metal ion that is used controls the channel diameter, as well as, whether the channel network is parallel as in TAM5 or intercepting at right angles as in TAM4, which forms a cubic crystal.

A variety of liquid wastes with significant variation in composition are produced and stored at waste sites across the United States. Therefore, the ion exchanger should remove cesium over a wide range of chemical elements including carbonate, oxalate and the radiolysis byproduct peroxide. The oxalate comes primarily from previous additions of oxalic acid in various cleaning operations. The production of gases by radiolysis was speculated to have an effect on the selective ion exchange of cesium. Hydrogen peroxide was used in testing at ORNL to generated gas to determine the effect of gas production on column operation. These experiments raised the question of a possible effect of hydrogen peroxide on the selective removal of cesium using the CST. Therefore, this study examined the cesium loading performance of CST in simulated wastes containing carbonate, oxalate and peroxide.

3.2 CST Crystal Structure

TAM5 is structurally related to a rare Russian mineral, Sitinakite, from the Kibinskii alkaline massif. The idealized formula for the mineral is $Na_2(H_2O)_2Ti_4O_5(OH)(SiO_4)_2K(H_2O)_{1.7}$. Similarly the formula for TAM5 is

$Na_2(H_2O)_2Ti_4O_5(OH)(SiO_4)_2Na(H_2O)_{1.7}$. The presence of potassium is the major distinction between Sitinakite and TAM5. Sitinakite may also contain up to 5 weight % of niobium, as well as small amounts of other elements.

Sokolova et al. (1989) revealed the crystal structure of Sitinakite by single crystal XRD work. They pictured that the crystal consists of a) a column built with clusters of four octahedral Ti atoms linked with oxygen and b) a string of alternating Si tetrahedra and Na octahedra. When four columns are attached with four strings, a straight channel of 3.5 Å is created, where the columns and strands are parallel to each other. Potassium ions and water molecules occupy the channels in Sitinakite while sodium ions and water molecules occupy the channels in TAM5.

Philip et al. (2003) revealed that the TAM5 structure is illustrated as a parallel channel and a section of TAM5 structure shows the Ti_3Nb clusters linked with tetrahedral silicates. In the XY projection, cubes are bridged with silicate groups to form the TAM5 structure. Within the cubes Ti and O occupy alternate corners. In the Z-axis direction silicate groups are linked by sodium ions to form a straight $(–O\text{-}Si\text{-}O\text{-}Na\text{-})_n$ strand. In TAM5, the cubes are linked by oxygen in the Z-axis direction. TAM5 has parallel channels of 3.5 Å diameter, which is perpendicular to the XY projection.

During the hydrothermal synthesis, high alkalinity with sodium hydroxide is critical for the formation of the TAM5 structure. The alkali hydroxide plays a template role during the synthesis of TAM5. Once the crystals are synthesized, the alkali metal ions are easily ion exchanged with protons using a strong acid e.g. (2 M HCl) while keeping the crystal structure intact (Philip and Anthony 2000). H-form TAM5 can be

loaded with other alkali metal ions, which are larger than a Na ion. Larger ions can only occupy the channels.

The analysis of an earlier batch indicated that the performance of a CST as an ion exchanger was very difficult to predict. The TEM of CST indicated a major phase with high crystallinity that is structurally similar to Sitinakite. The remaining solid is consisted of a silicate-rich second phase and a niobate-rich third phase. The powder XRD patterns of CST and elemental compositions of CST, which have a good Cs loading capacity, are similar.

3.3 Experiments

3.3.1 Experimental Methods

The distribution coefficient for 100 ppm Cs in a solution of 5.1 M NaOH and 0.6 M $NaNO_3$ was initially used to determine the quality of each batch products. The DOE wastes have some typical properties such as high alkalinity, very high concentration of sodium ion. These wastes contain various other ions and the composition varies by location. To reduce the effect of other ions while keeping common properties of real wastes, a standard nuclear waste simulant (5.1 M $NaNO_3$, 0.6 M NaOH, 100 ppm Cs) was utilized. Generally, 100 mg of CST and 10 ml of standard simulant were transferred to a plastic vial, closed, and then shaken continuously for 48 hours using a Burrel Wrist-Action shaker. The vial was then centrifuged, using an IEC EXD Centrifuge (Damion/IEC Division), at 60% power for 10 minutes. The clear supernatant liquid was separated from the vial, and then the Cs levels in the supernatant

liquid and a control (basic salt solution without the CST) were determined using a Varian AA 30 Atomic Absorption Spectrometer. The corresponding cesium concentration in the solid phase, q, was calculated by the following equation:

$$q = (C_0 - C)\frac{V}{W} \qquad (3.1)$$

where Co and C are the initial and equilibrium cesium concentration in the liquid phase, V is the volume of the liquid, and W is the weight of the solid.

The Cs distribution coefficient (K_d) was calculated by using equation (2.6) and the quality of TAM5 was determined using the K_d. The amount of Ti, Si, and Nb in the supernatant liquid was determined by elemental analysis using an Inductively Coupled Argon Plasma Spectrometer (ICAP, Thermo Jarrel Ash Model Poly Scan 61E). The very low level of Ti, barely above the background, indicated that no TAM5 is present in the supernatant liquid. Membrane filters with 0.2-micron pores were also tested to separate the CST from the supernatant liquid; it was observed that centrifuging was as effective as filtration using membrane filters.

3.3.2 CST Samples and Simulants

IONSIV® IE-910 (crystalline form) from UOP, LLC (UOP), TAM5 prepared by Ding Gu (DG141), and TAM5 (TAM5-4 and TAM5-5) are the four CST samples used in the study. UOP and DG141 were 6 years old samples. Both TAM5-4 and TAM5-5 were synthesized in June 2000. The samples were heated at 400°C overnight and weight

losses were determined. Since TAM5-4 and TAM5-5 were air-dried samples, they experienced 25% weight loss. They lost water and acetone during heating. The samples from UOP and from DG141 experienced 8% and 12% weight loss respectively. All CST samples were composed of similar size crystals and used 'as received'. Seven simulants were prepared by varying the composition of our standard simulants by adding sodium carbonate and hydrogen peroxide. These studies were used to evaluate the effect of carbonate, oxalate, and hydrogen peroxide on the K_d and the leaching of Si, Ti, and Nb from the CST during the equilibration experiments. The experiments were conducted in duplicates. K_d and leaching of Si, Ti, and Nb were determined as previously discussed.

Seven simulants were prepared by adding sodium carbonate, oxalic acid, and hydrogen peroxide into the standard nuclear simulant (5.1 M $NaNO_3$, 0.6 M NaOH, 100 ppm Cs). The compositions of seven simulants are listed in the Table 3.1. Potassium permanganate titration was used to estimate the contents of oxalate and hydrogen peroxide in the simulant before and after ion exchange experiments. Oxalic acid was difficult to dissolve in the standard simulant. Only 0.0016 M of oxalate was prepared, which is below that of the previously reported value of 0.015 M at ionic strength of 6.55 mol/kg (Kilpatrick, 1984). Initial hydrogen peroxide concentration in simulant 2 was 0.0025 M. Simulant 6 and simulant 7 had hydrogen peroxide concentrations of 0.1 M and 1 M. Hydrogen peroxide in the simulant decomposed continuously and the presence of CST did not have any significant effect on the rate of decomposition of H_2O_2 to H_2O and O_2. In 9 days, H_2O_2 concentrations dropped from 1M to about 0.1M. Any

experiments specifically to monitor the catalytic effect of CST on H_2O_2 decomposition were not conducted.

Table 3.1. The chemical composition of simulants

	$NaNO_3$ (M)	NaOH (M)	Na_2CO_3 (M)	$H_2C_2O_4$ (M)	H_2O_2 (M)	CsCl (M)
#1	4.78	0.6	0.16			0.000753
#2	4.78	0.6	0.16		0.0025	0.000753
#3	4.14	0.6	0.48			0.000753
#4	4.78	0.6	0.16	0.0016		0.000753
#5	4.78	0.6			0.0025	0.000753
#6	5.1	0.6			0.1	0.000753
#7	5.1	0.6			1.0	0.000753

The ion exchange experiment was conducted by shaking 100mg of each CST with 10 ml of simulant for periods of 1-, 2- and 5-days. The 2-day experiments did not show any catalytic effect on H_2O_2 by the CST. 1-day and 5-day experiments showed a slight trend towards decomposition of H_2O_2 by CST. Since CST did not show vigorous catalytic activity, it has been concluded that CST by itself does not significantly promote the decomposition of H_2O_2.

3.3.3 Analysis Methods

Cesium was analyzed by atomic absorption using a Varian AA 30 atomic absorption spectrometer. The nuclear waste simulants were diluted 1:3 by adding water so that the capillary and the burner would not become clogged by the salt. The instrument was calibrated with cesium standard solutions and a blank with a similar matrix composition. The elemental analysis of Si, Ti and Nb in the nuclear waste simulant samples was performed using an Inductively Coupled Argon Plasma (ICAP) spectrometer (Thermo Jarrel Ash Polyscan 61E). The simulants were diluted 1:3 by adding water in order to enhance the aerosol formation. A Scintag XDS 2000 X ray spectrometer was used to obtain the powder X ray diffraction (XRD) pattern of solid samples. After equilibration with nuclear simulants, the CST solids were separated by a centrifuge, washed with water and acetone, air-dried and scanned for the XRD patterns. One hundred-mg sample of CST was dissolved in 1 ml 50% HF, water was added to make 10 ml solution, and it was further diluted as needed for the ICAP.

3.3.4 Determination of Oxalate and Hydrogen Peroxide by Titration

A stock solution of 0.1 M was prepared by dissolving 15.8 g of potassium permanganate in a one-liter volumetric flask and adding water to make one liter of solution. This solution was diluted a hundred-fold to obtain 0.001M potassium permanganate. Both solutions were used for the titration. Oxalic acid was used to standardize these solutions. The titration was performed by warming 1 ml of simulant and 10 ml of 2 M sulfuric acid in a 250 ml Erlenmeyer flask on a hot plate. Potassium

permanganate solution was added from a 50-ml burette. Since the reaction between hydrogen peroxide and potassium permanganate is slow at room temperature the solution was maintained at 65 to 85°C during the titration. A pink color lasting longer than 30 seconds indicated the end point.

3.4 The Effect of Carbonate

To evaluate the effect of carbonate, the cesium distribution coefficients of simulant 1, which contains 0.16 M of carbonate, was compared with simulant 3, which contains 0.48 M of carbonate for period of 1-, 2- and 5 days. The ZAM model (Zheng et al., 1997), which is based on TAM-5 powder, also was used to compare the experimental data with the simulation data. Figure 3.1 shows the change of K_d values along with the time in simulant 1.

The K_d values of simulant 1 were increased with increasing time, which means that the TAM5 powder and simulants do not reach equilibrium after 1 day. After two days, there is very little change in the cesium distribution coefficient for TAM5-4 and TAM5-5 and DG 141. If one compares the distribution coefficients for TAM5-4, TAM5-5, and DG 141 the differences are well within the standard deviations. These three batches were prepared using the same procedures, while the UOP samples were synthesized at a lower temperature than the other three samples.

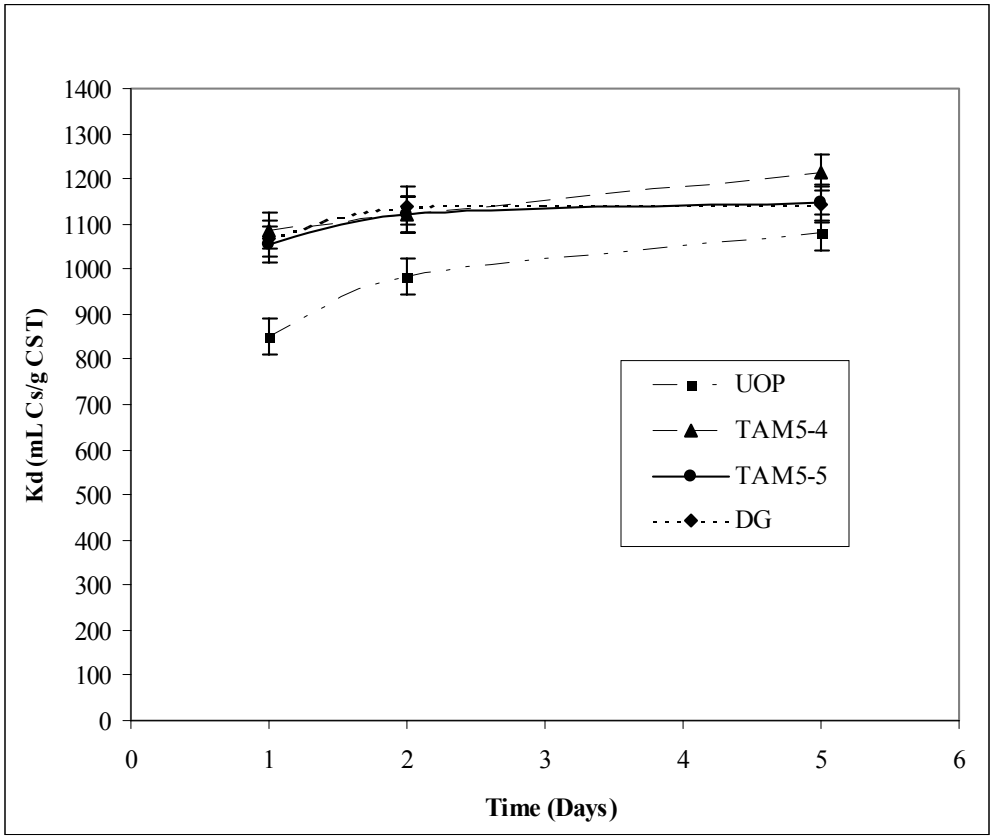

Figure 3.1. The change of K_d values along with the time in simulant 1. The error bar represents 2σ, 95 % confidence interval.

Figure 3.2 shows the comparison of K_d values between simulant 1 and simualnt 3. In silmulant 1, the ZAM model well predicted the cesium distribution coefficient after one day. However, the estimated K_d values of CST materials after two days were smaller than that of experimental data. The predicted K_d values for the simulant 3 were larger than that of experimental data prior to two days. For 5 days, however, the predicted values were close to the values from the experimental data. These results showed that the higher carbonate content may need more time to reach the equilibrium state. The differences of cesium distribution coefficients between simulants 1 and 3 were larger as the equilibration time was increased. After 5 days, one easily could notice that the higher carbonate content resulted in higher cesium K_d values for CST material.

One should note that the sodium concentration of simulant 3 maintains 5.7 M, which is the same sodium concentration as simulant 1. As the concentration of carbonate is increased the ionic strength is also increased. To eliminate the effect of ionic strength, the K_d values was calculated using ZAM model with the variation of carbonate while the ionic strength was maintained as 7.675 mol/kg by reducing the content of sodium nitrate. Figure 3.3 shows the simulation results. Figure 3.3 affirms the simulation result of the increasing cesium K_d values with increasing carbonate content in the same ionic strength. Obviously, this calculation indicates the cesium K_d value for simulant with 0.48 M carbonate is larger than the corresponding value for simulant with 0.16 M carbonate both with the same sodium content and same ionic strength. One may reach the same general conclusion that the cesium K_d value has positive correlation with carbonate content.

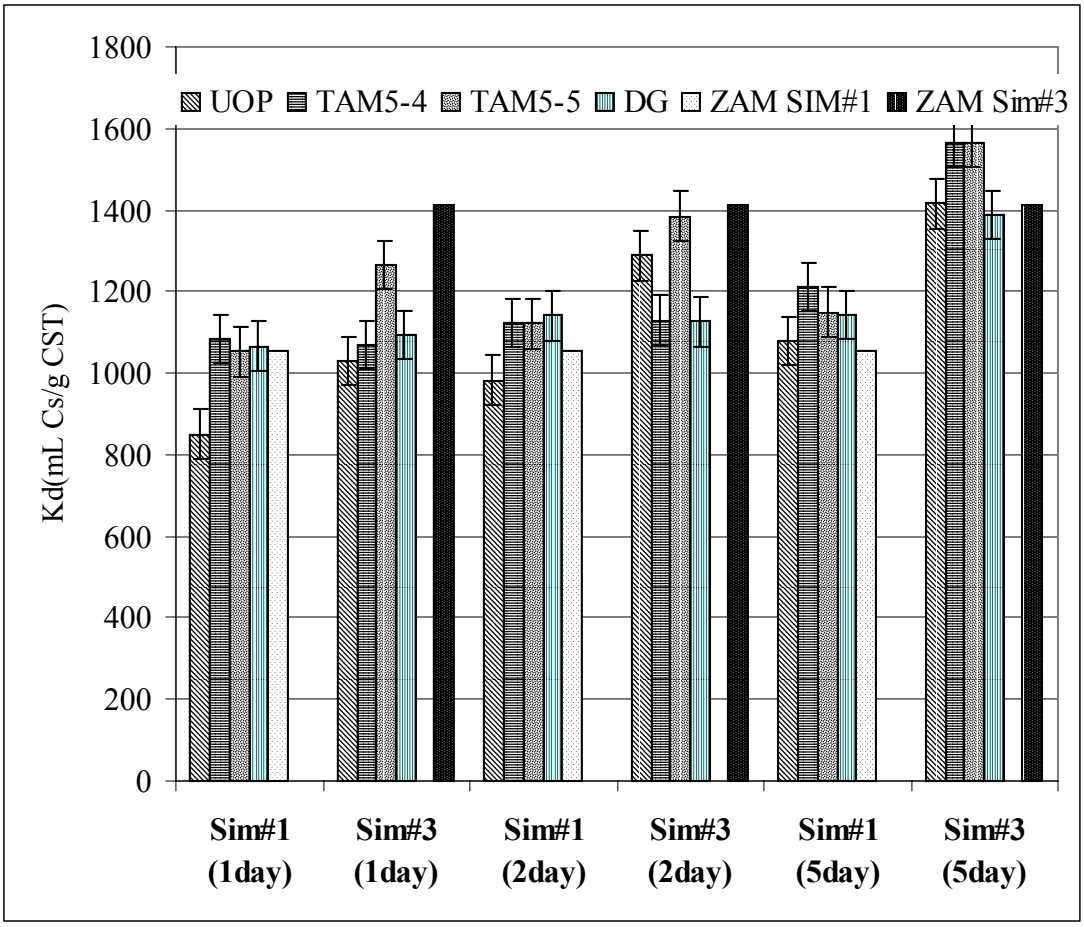

Figure 3.2. The effect of carbonate on cesium distribution coefficients. Simulant 1 contains 0.16 M of carbonate and simualnt 3 contains 0.48 M of carbonate.

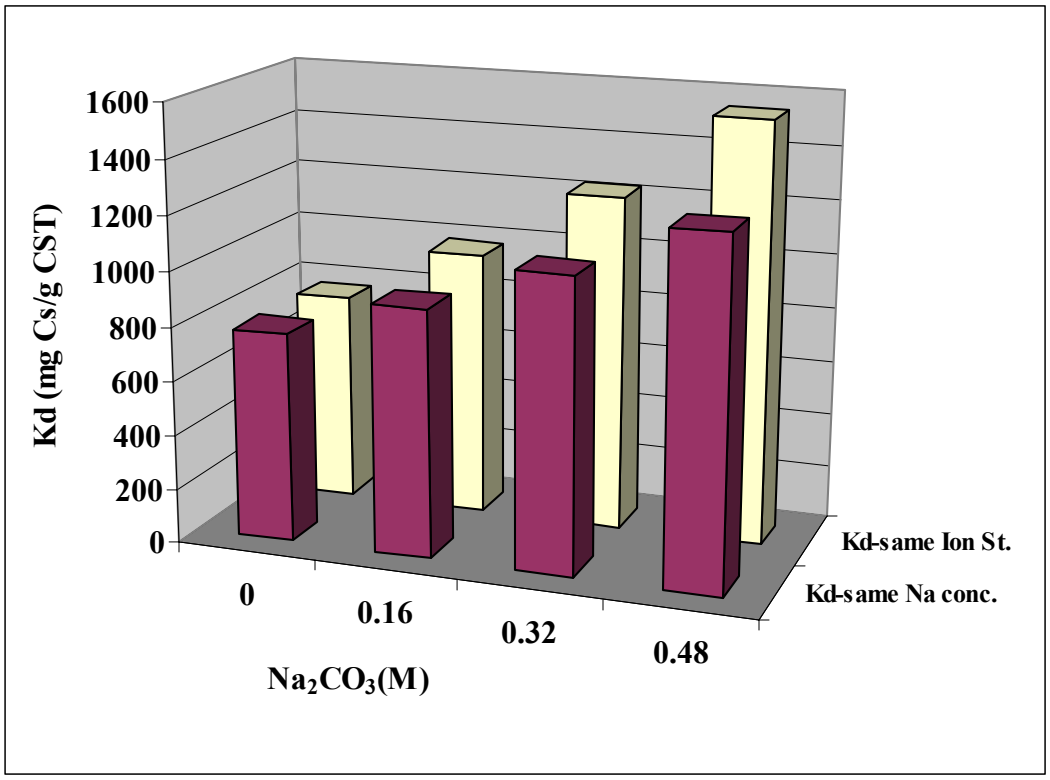

Figure 3.3. The simulation results that shows the effect of carbonate on cesium K_d values.

In this work, the simulants were separated from the solids by a centrifuge and analyzed by ICAP to estimate the leaching amounts of Si, Ti, and Nb from CST as a result of shaking with simulants. Figure 3.4 and 3.5 show the results, which illustrates the weight percent of Si, Ti, and Nb that dissolves in the solution from the CST. This percent is based on gram of Si, Ti, and Nb per gram of CST charged to the ion exchange experiment times 100. The elemental analysis of the simulants 1 and 3 do not show any significant loss of Ti, indicating that the CST phase with the sitinakite structure is very stable. Leaching of a small amount of the silicate and niobate phases is indicated by the presence of dissolved Si and Nb species in the simulant.

3.5 The Effect of Oxalate

Figure 3.6 shows the effect of oxalate on cesium removal from the simulant solution by comparing the simulants 1 and 4. As shown in Figure 3.6, simulation predicted that the cesium K_d values of simulant 1 and simulant 4 were almost same. Furthermore, these predicted K_d values were close to the experimental data of 5 days. From this result one can conclude that the oxalate concentration has no effect on the cesium removal process.

The ICAP analysis, which showed leaching of Ti, Si, and Nb from the CST as a result of shaking with simulant 4, is shown in Figure 3.7.

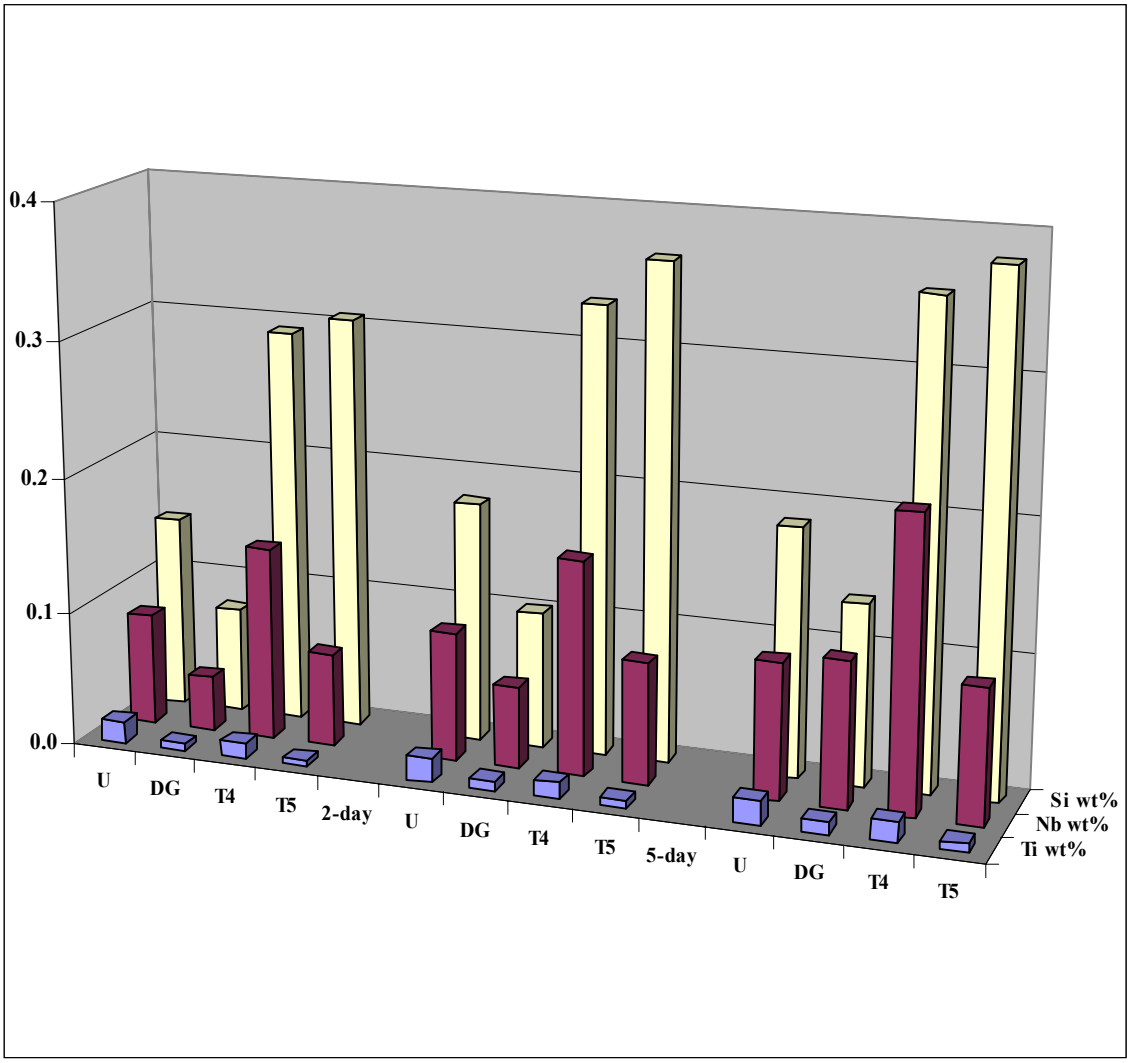

Figure 3.4. Leaching of Si, Ti, and Nb from CST as a result of shaking with simulant 1 (basic solution with 0.16 M $NaCO_3$).

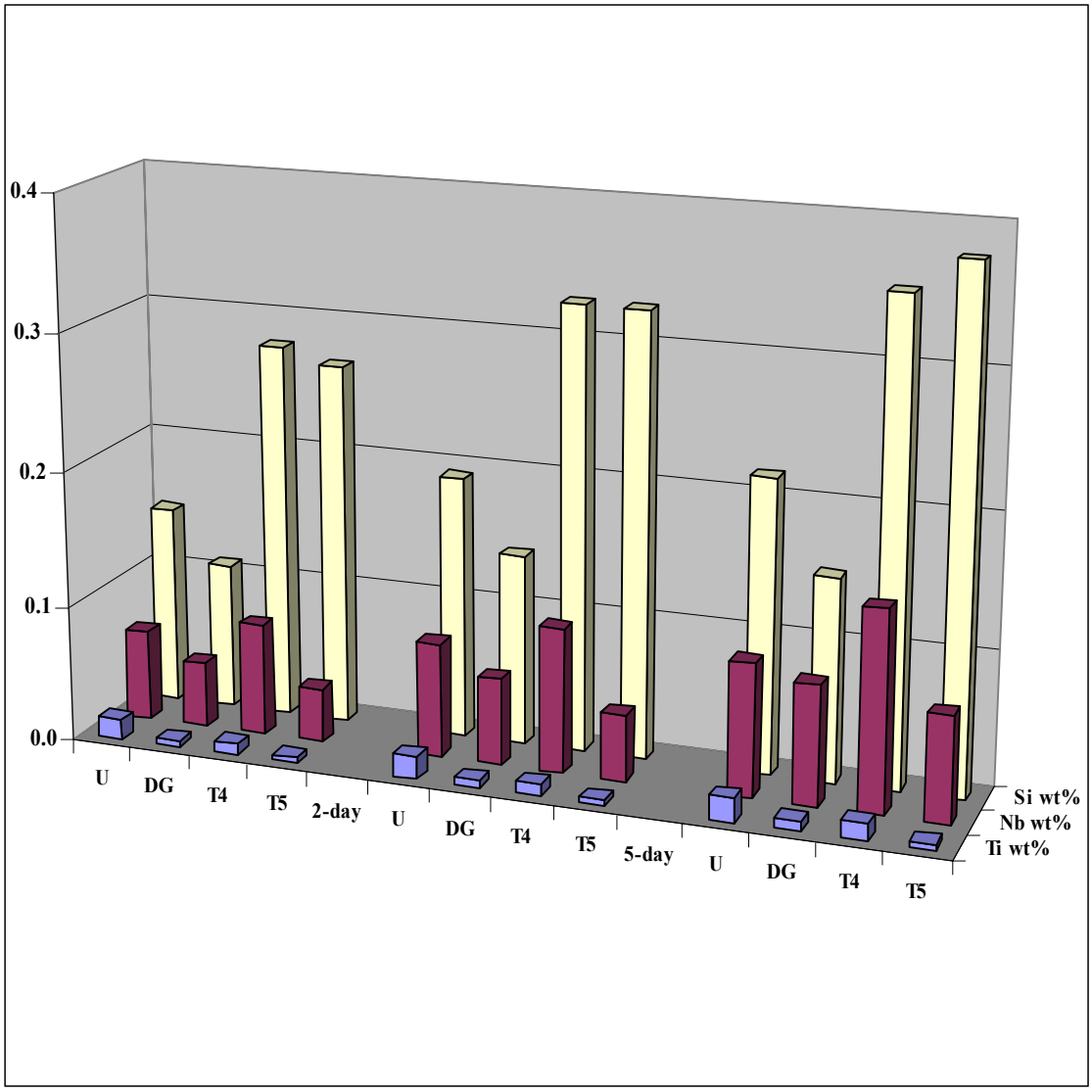

Figure 3.5. Leaching of Si, Ti, and Nb from CST as a result of shaking with simulant 3 (basic solution with 0.48 M $NaCO_3$).

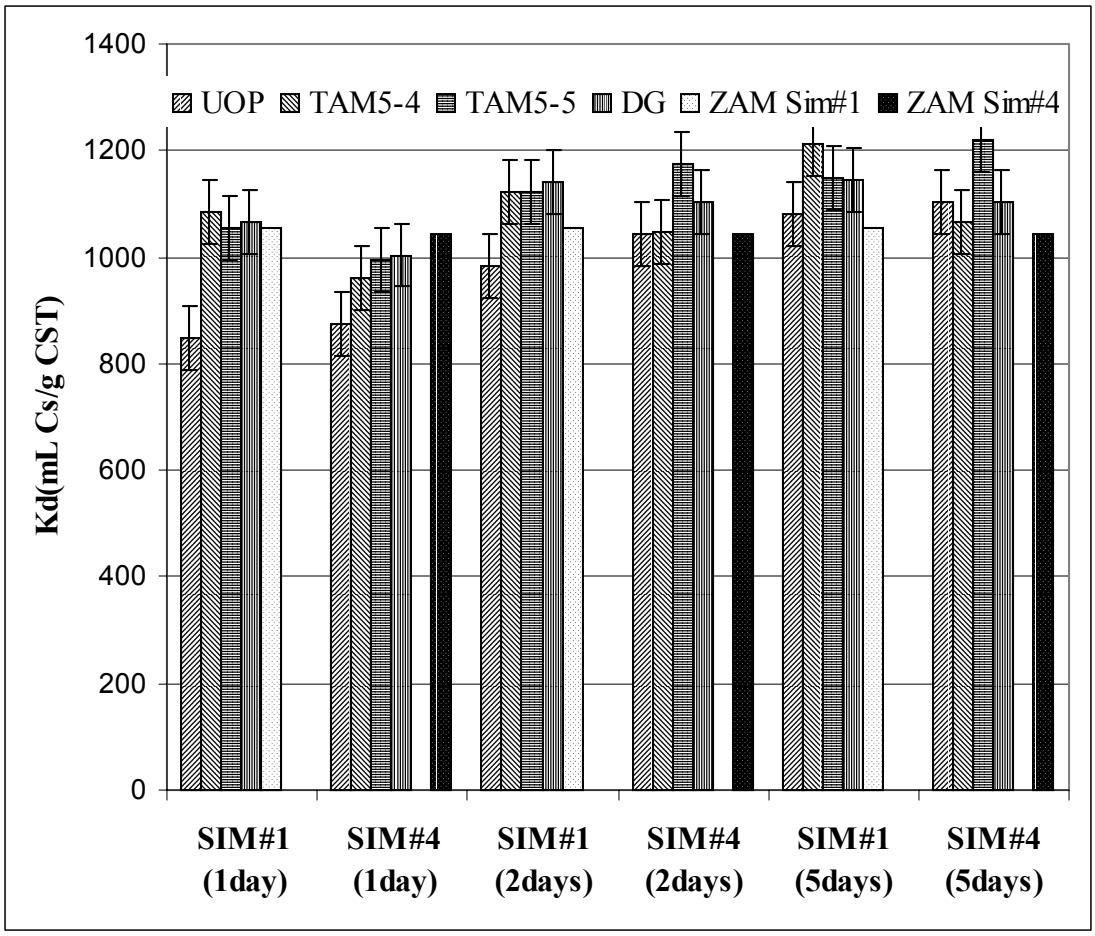

Figure 3.6. The effect of oxalate on cesium distribution coefficients. Simulant 1 contains 0 M of oxalate and simualnt 4 contains 0.0016 M of oxalate.

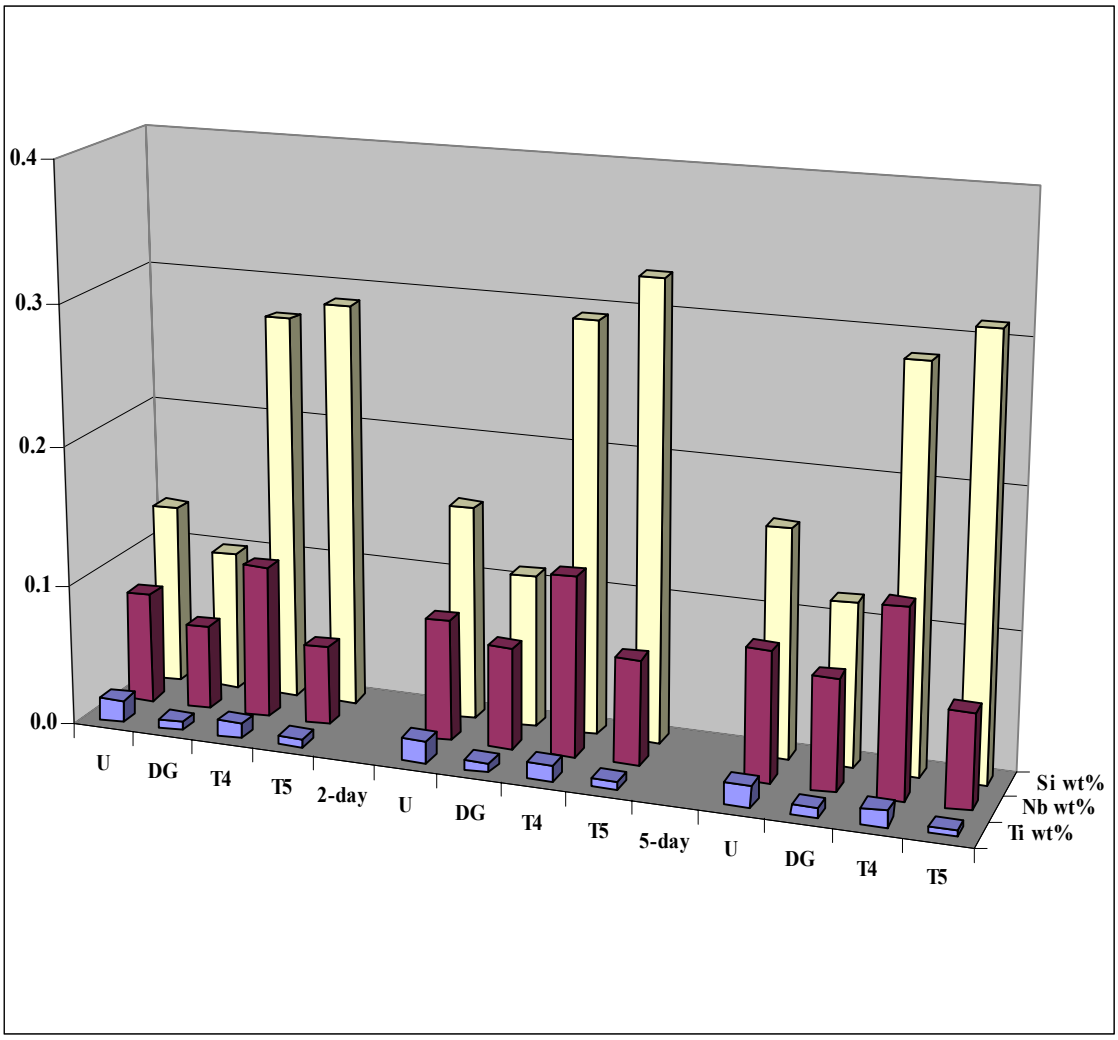

Figure 3.7. Leaching of Si, Ti, and Nb from CST as a result of shaking with simulant 4 (basic solution with 0.0016 M $H_2C_2O_4$).

The result of Figure 3.7 indicates that the simulant 4 does not show any significant amount of Ti loss, indicating that increase of oxalate concentration up to 0.0016 M has no effect on the stable CST phase with a sitinakite structure.

3.6 The Effect of Hydrogen Peroxide

To evaluate the decomposition rate of hydrogen peroxide, the titration of hydrogen peroxide was performed with potassium permanganate. Figure 3.8 shows the results of titration simulant 7, which initially contained 1 M of hydrogen peroxide. The result indicates that almost 50 % of hydrogen peroxide is decomposed within 1 day and almost 90 % of hydrogen peroxide is decomposed within 5 days.

Figure 3.9 shows the effect of small amount of hydrogen peroxide (0.0025 M) on the K_d value with the carbonate amount of 0.16 M. When samples of CST were equilibrated with Simulant 1 and 2, containing carbonates, cesium K_d values increased with equilibration time. At least in simulants with low concentrations of hydrogen peroxide, carbonate apparently inhibits the effect of hydrogen peroxide. Carbonate is structurally similar to silicate and titanate and has the ability to inhibit their dissolution from the CST. Thus, carbonate is a stabilizing agent for the CST.

Figure 3.10 and 3.11 show the effect of hydrogen peroxide at 0.1 and 1 M concentrations on cesium K_d values over five days of equilibration. At the end of five days of equilibration, a 40 % decrease of cesium K_d was observed in simulant 6. In simulant 7, which contained 1 M hydrogen peroxide, the cesium K_d values dropped as much as 95%.

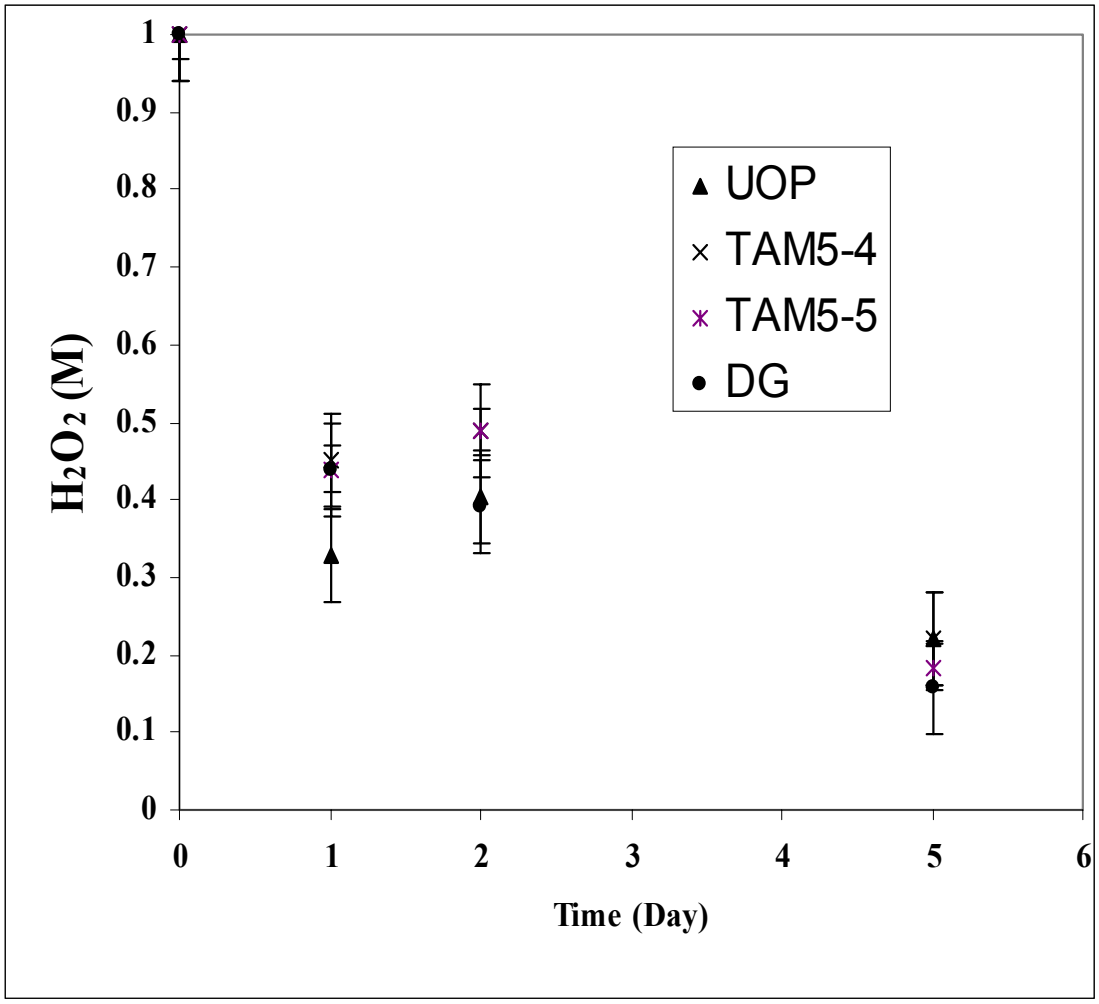

Figure 3.8. The titration result for simulant 7 (Basic solution with 1 M hydrogen peroxide).

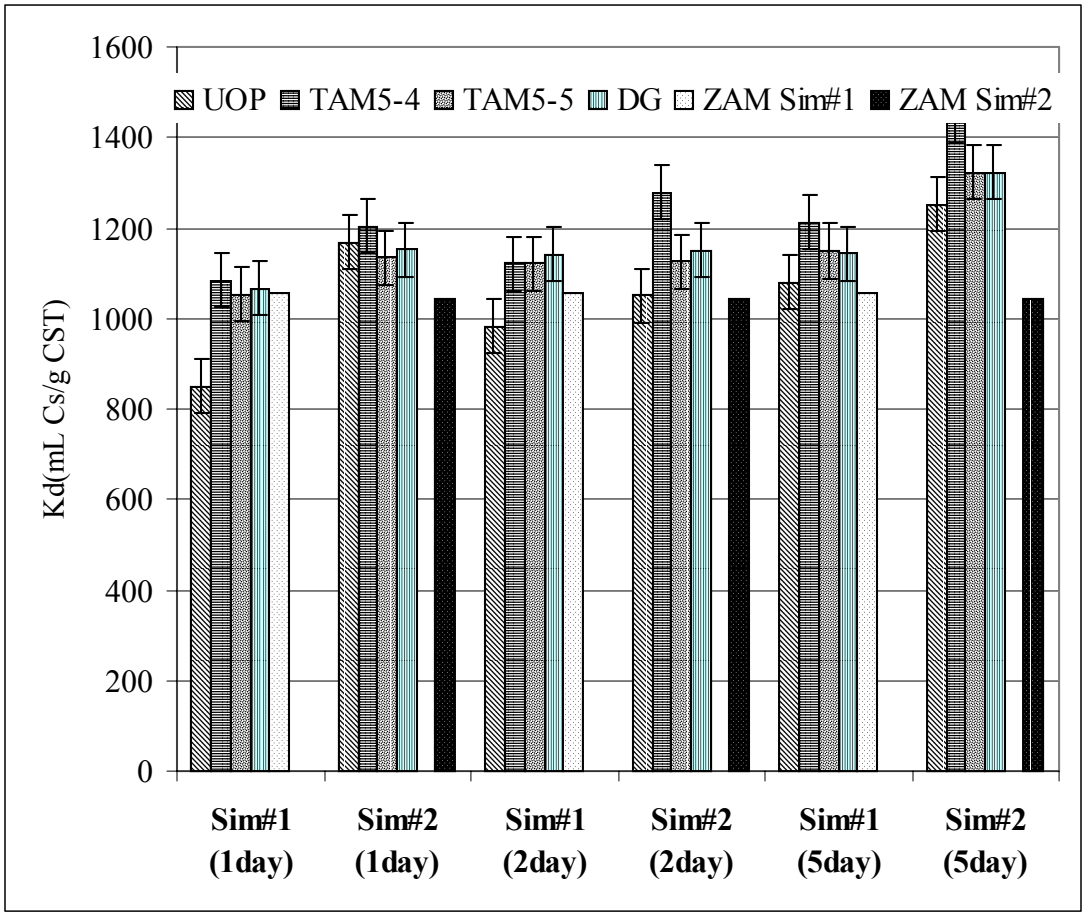

Figure 3.9. The effect of 0.0025 M hydrogen peroxide on cesium distribution coefficients with 0.16 M carbonate. Simulant 1 contains 0 M of hydrogen peroxide and simulant 2 contains 0.0025 M of hydrogen peroxide.

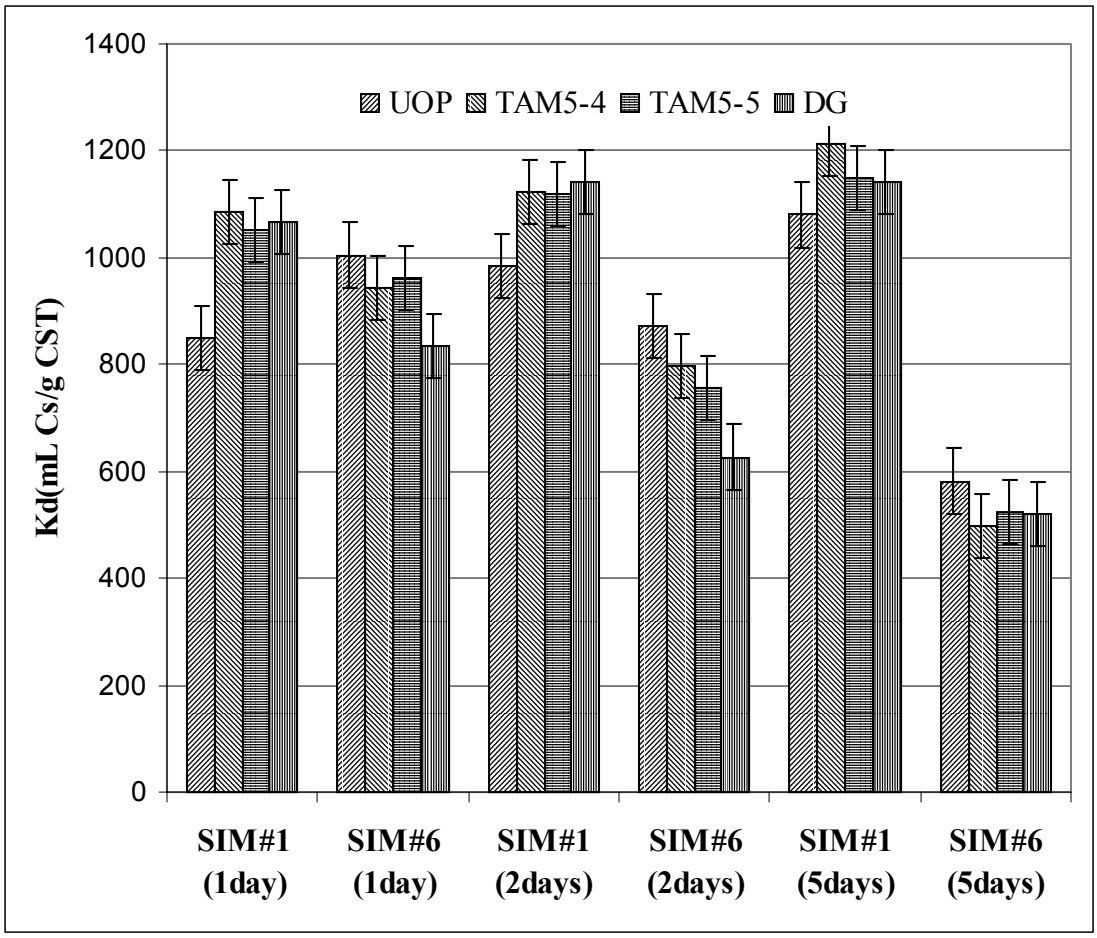

Figure 3.10. The effect of 0.1 M hydrogen peroxide on cesium distribution coefficients. Simulant 1 contains 0 M of hydrogen peroxide and simulant 6 contains 0.1 M of hydrogen peroxide.

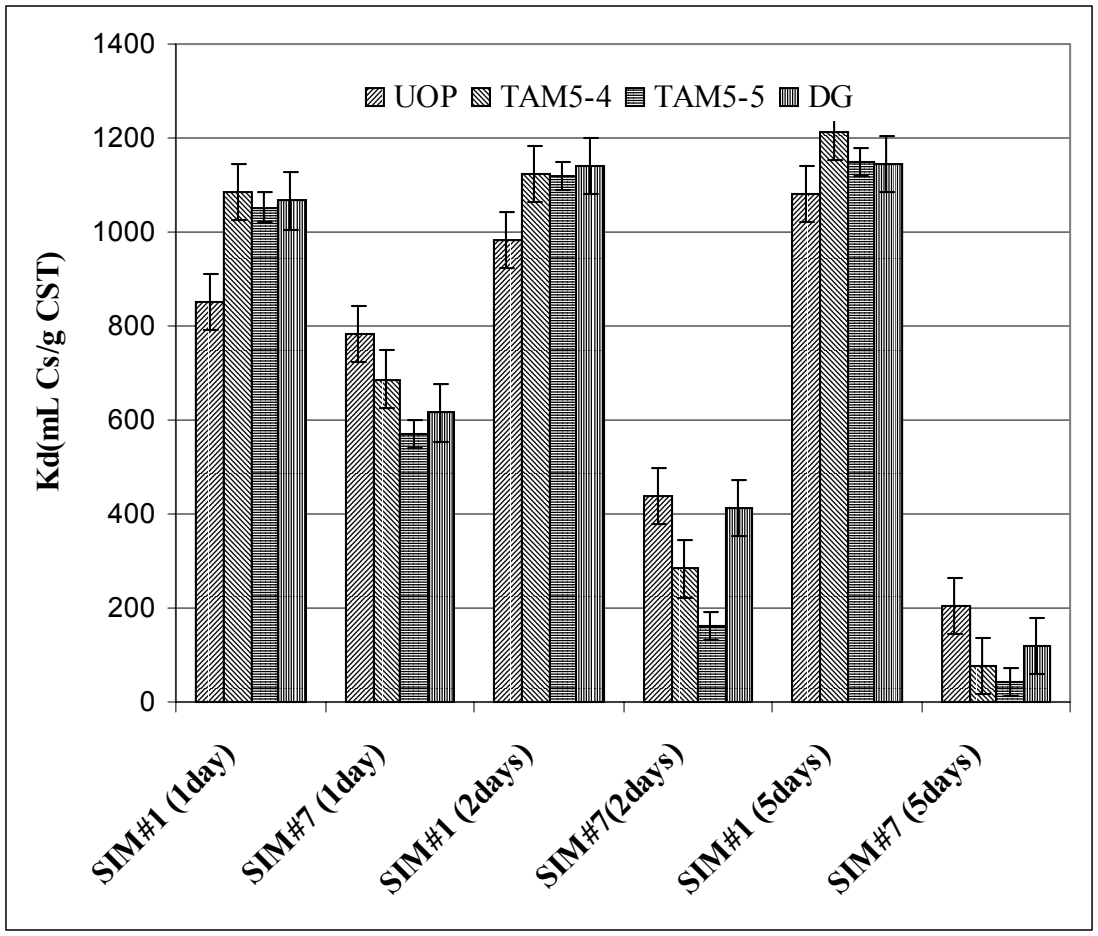

Figure 3.11. The effect of 1 M hydrogen peroxide on cesium distribution coefficients. Simulant 1 contains 0 M of hydrogen peroxide and simulant 7 contains 1 M of hydrogen peroxide.

The weight percentage of CST dissolved in the five simulants is listed in Table 3.2-3.6. In five days, about 1 wt % of CST dissolved in simulants 1and 2 while slightly more dissolved in simulant 5. In simulant 6 with 0.1M H2O2, as much as 35 wt% of CST dissolved in five days. As much as 75% of CST was dissolved in simulant 7 with 1 M H_2O_2 after five days equilibration.

Table 3.2. Leaching of TiO_2, SiO_2, Nb_2O_5, and Na_2O from CST as a result of shaking with simulant 1 (Basic salt solution with 0.16 M carbonate)

Name	SiO_2wt%	TiO_2 wt%	Nb_2O_5 wt%	Na_2O	Wt% Dissolved
1-day					
UOP	0.31	0.03	0.12	0.10	0.55
DG141	0.17	0.01	0.06	0.05	0.28
TAM5-4	0.63	0.02	0.20	0.19	1.04
TAM5-5	0.65	0.01	0.10	0.18	0.94
2-days					
UOP	0.38	0.03	0.14	0.12	0.67
DG141	0.22	0.01	0.09	0.07	0.38
TAM5-4	0.71	0.02	0.23	0.21	1.17
TAM5-5	0.78	0.01	0.13	0.22	1.14
5-days					
UOP	0.40	0.03	0.15	0.12	0.70
DG141	0.29	0.02	0.15	0.10	0.55
TAM5-4	0.76	0.03	0.31	0.24	1.34
TAM5-5	0.81	0.01	0.14	0.23	1.20

Table 3.3. Leaching of TiO_2, SiO_2, Nb_2O_5, and Na_2O from CST as a result of shaking with simulant 2 (Basic salt solution with 0.16 M carbonate, 0.0025 H_2O_2)

Name	SiO_2wt%	TiO_2 wt%	Nb_2O_5 wt%	Na_2O	Wt% Dissolved
1-day					
UOP	0.33	0.03	0.12	0.10	0.58
DG141	0.22	0.01	0.08	0.07	0.37
TAM5-4	0.53	0.01	0.12	0.15	0.82
TAM5-5	0.59	0.01	0.08	0.16	0.84
2-days					
UOP	0.38	0.03	0.12	0.12	0.65
DG141	0.25	0.01	0.11	0.08	0.46
TAM5-4	0.61	0.02	0.18	0.18	0.98
TAM5-5	0.71	0.01	0.13	0.20	1.04
5-days					
UOP	0.42	0.03	0.15	0.13	0.74
DG141	0.29	0.02	0.15	0.10	0.56
TAM5-4	0.69	0.02	0.24	0.21	1.16
TAM5-5	0.76	0.01	0.16	0.22	1.15

Table 3.4. Leaching of TiO_2, SiO_2, Nb_2O_5, and Na_2O from CST as a result of shaking with simulant 5 (Basic salt solution with 0.0025 M carbonate)

Name	SiO_2wt%	TiO_2 wt%	Nb_2O_5 wt%	Na_2O	Wt% Dissolved
1-day					
UOP	0.33	0.04	0.14	0.11	0.62
DG141	0.27	0.01	0.07	0.08	0.43
TAM5-4	0.71	0.01	0.11	0.20	1.04
TAM5-5	0.73	0.01	0.06	0.20	0.99
2-days					
UOP	0.41	0.04	0.16	0.13	0.73
DG141	0.32	0.01	0.10	0.10	0.53
TAM5-4	0.79	0.02	0.16	0.23	1.19
TAM5-5	0.83	0.01	0.08	0.23	1.14
5-days					
UOP	0.51	0.04	0.18	0.16	0.89
DG141	0.35	0.02	0.14	0.11	0.62
TAM5-4	0.90	0.03	0.24	0.26	1.43
TAM5-5	0.96	0.01	0.12	0.26	1.36

Table 3.5. Leaching of TiO_2, SiO_2, Nb_2O_5, and Na_2O from CST as a result of shaking with simulant 6 (Basic salt solution with 0.1 M H_2O_2)

Name	SiO_2wt%	TiO_2 wt%	Nb_2O_5 wt%	Na_2O	Wt% Dissolved
1-day					
UOP	1.87	1.84	1.85	1.06	6.62
DG141	1.83	2.02	2.21	1.12	7.18
TAM5-4	1.68	1.56	2.08	0.98	6.30
TAM5-5	2.01	1.76	2.28	1.13	7.19
2-days					
UOP	3.76	4.70	3.79	2.32	14.57
DG141	5.91	5.32	5.97	3.25	20.46
TAM5-4	4.39	3.77	4.87	2.43	15.45
TAM5-5	5.05	3.82	5.22	2.65	16.75
5-days					
UOP	7.88	11.59	8.03	5.22	32.73
DG141	6.51	8.41	6.78	4.10	25.80
TAM5-4	8.41	11.59	10.31	5.62	35.93
TAM5-5	7.43	9.38	8.70	4.75	30.26

Table 3.6. Leaching of TiO_2, SiO_2, Nb_2O_5, and Na_2O from CST as a result of shaking with simulant 7 (Basic salt solution with 1 M H_2O_2)

Name	SiO_2wt%	TiO_2 wt%	Nb_2O_5 wt%	Na_2O	Wt% Dissolved
1-day					
UOP	6.66	8.15	7.20	4.14	26.14
DG141	8.43	8.06	8.70	4.75	29.94
TAM5-4	8.05	5.10	8.36	4.04	25.55
TAM5-5	9.15	5.91	9.28	4.59	28.93
2-days					
UOP	7.34	7.86	6.73	4.20	26.14
DG141	12.96	8.41	11.06	6.27	38.69
TAM5-4	12.70	8.61	11.89	6.34	39.54
TAM5-5	14.62	6.49	11.55	6.38	39.04
5-days					
UOP	15.13	24.60	17.38	10.70	67.82
DG141	16.21	27.13	20.70	11.86	75.90
TAM5-4	14.33	23.55	19.80	10.58	68.26
TAM5-5	15.36	22.02	19.14	10.47	66.98

The lowering of cesium K_d value parallels the dissolution of CST in the simulants. However, overall percentage decreases in cesium K_d outpaced wt % dissolution of CST. There are three phases that exist in a typical sample of CST. Only a tetragonal phase, which accounts for at least 90% of the CST, is known to have high cesium ion exchange capacity. This is the first indication that hydrogen peroxide causes the selective dissolution of the tetragonal phase in basic simulants. Figure 3.12, 13, 14, and 15 show the result of the ICAP analysis of simulant 2, 5, 6 and 7 respectively, which show the weight percentage of Si, Ti, and Nb dissolved from CST in the 4 different simulants. Hydrogen peroxide attacks the tetragonal phases and solubilizes its components. As a result, the CST structure as well as the ion exchange capacity, is lost. Table 3.7 shows the variation of Nb/Ti ratio when CST is shaken with simulant 7 containing 1 M hydrogen peroxide, which shows that Nb/Ti ratio of the solid increases from 0.4 to 1.

Table 3.7. The variation of Nb/Ti as a result of shaking with simulant 7 (Basic salt solution with 1 M H_2O_2)

CST- exposure	Nb/Ti
UOP-1day	0.38
UOP-2days	0.45
UOP-5days	0.60
DCG-1day	0.46
DG-2days	0.56
DG-5days	0.96
TAM5-4-1day	0.46
TAM5-4-2days	0.59
TAM5-4-5days	1.12
TAM5-5-1day	0.38
TAM5-5-2days	0.51
TAM5-5-5days	0.83

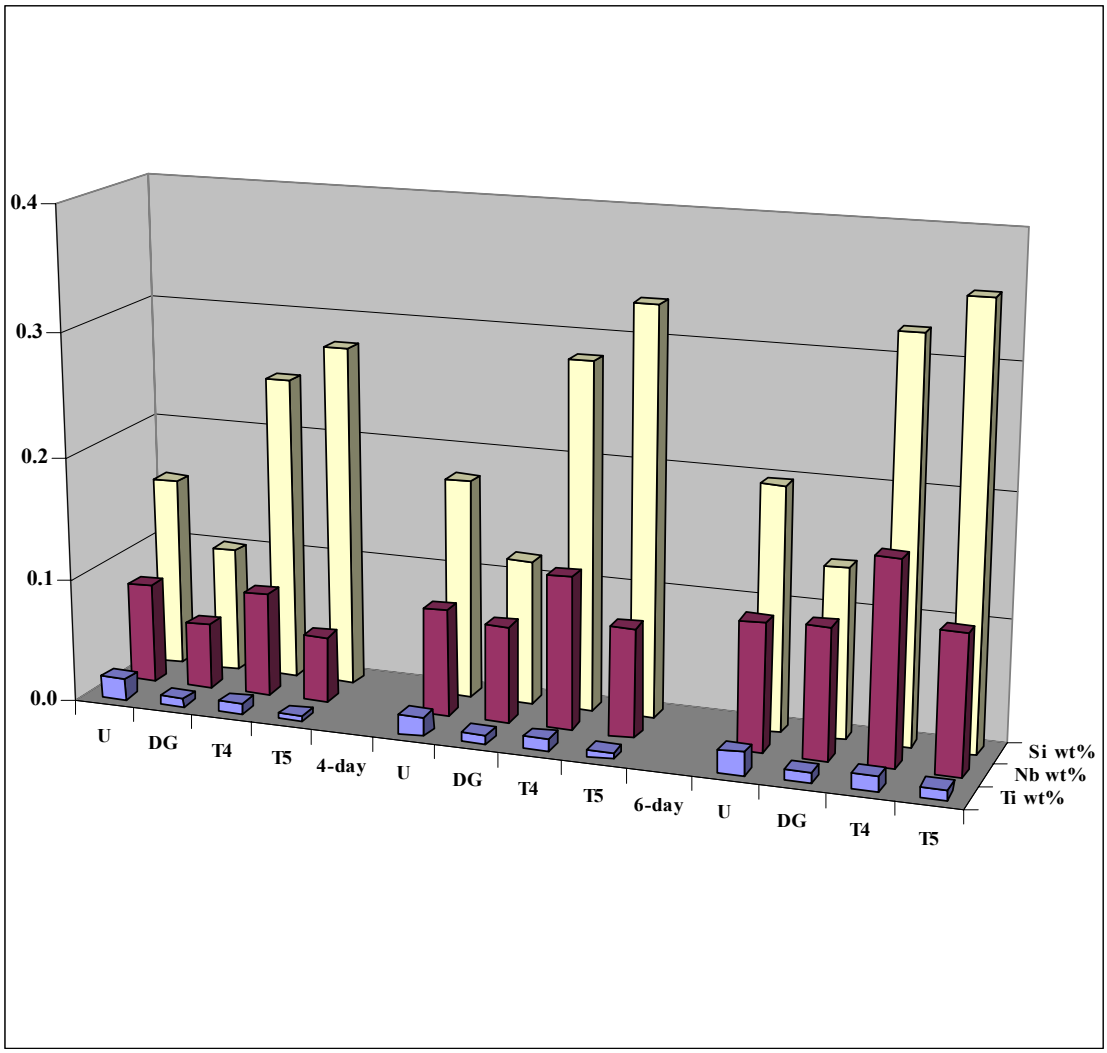

Figure 3.12. Leaching of Si, Ti, and Nb from CST as a result of shaking with simulant 2 (basic solution with 0.16 M Na_2CO_3 and 0.0025 M H_2O_2).

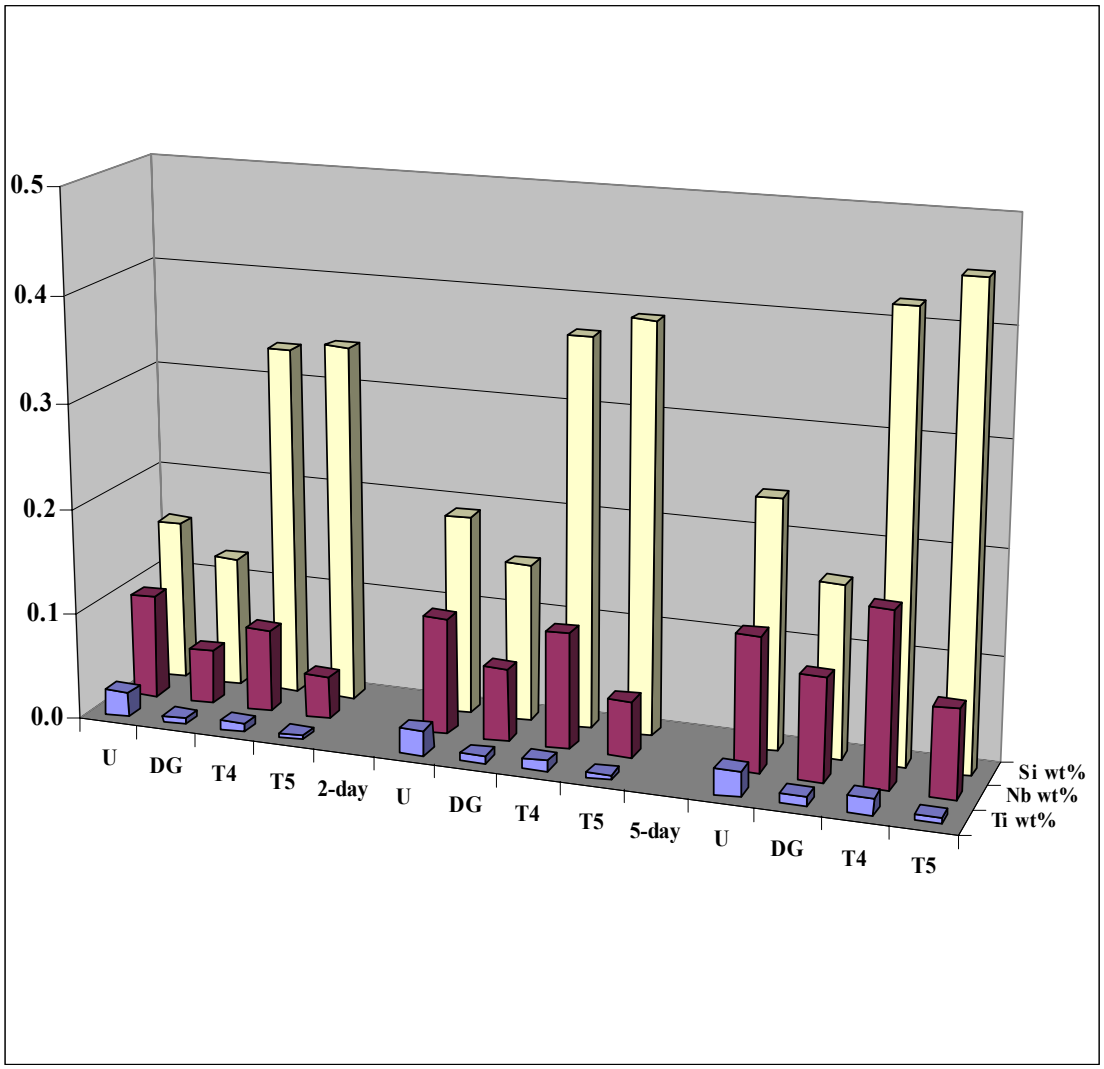

Figure 3.13. Leaching of Si, Ti, and Nb from CST as a result of shaking with simulant 5 (basic solution with 0.0025 M H_2O_2).

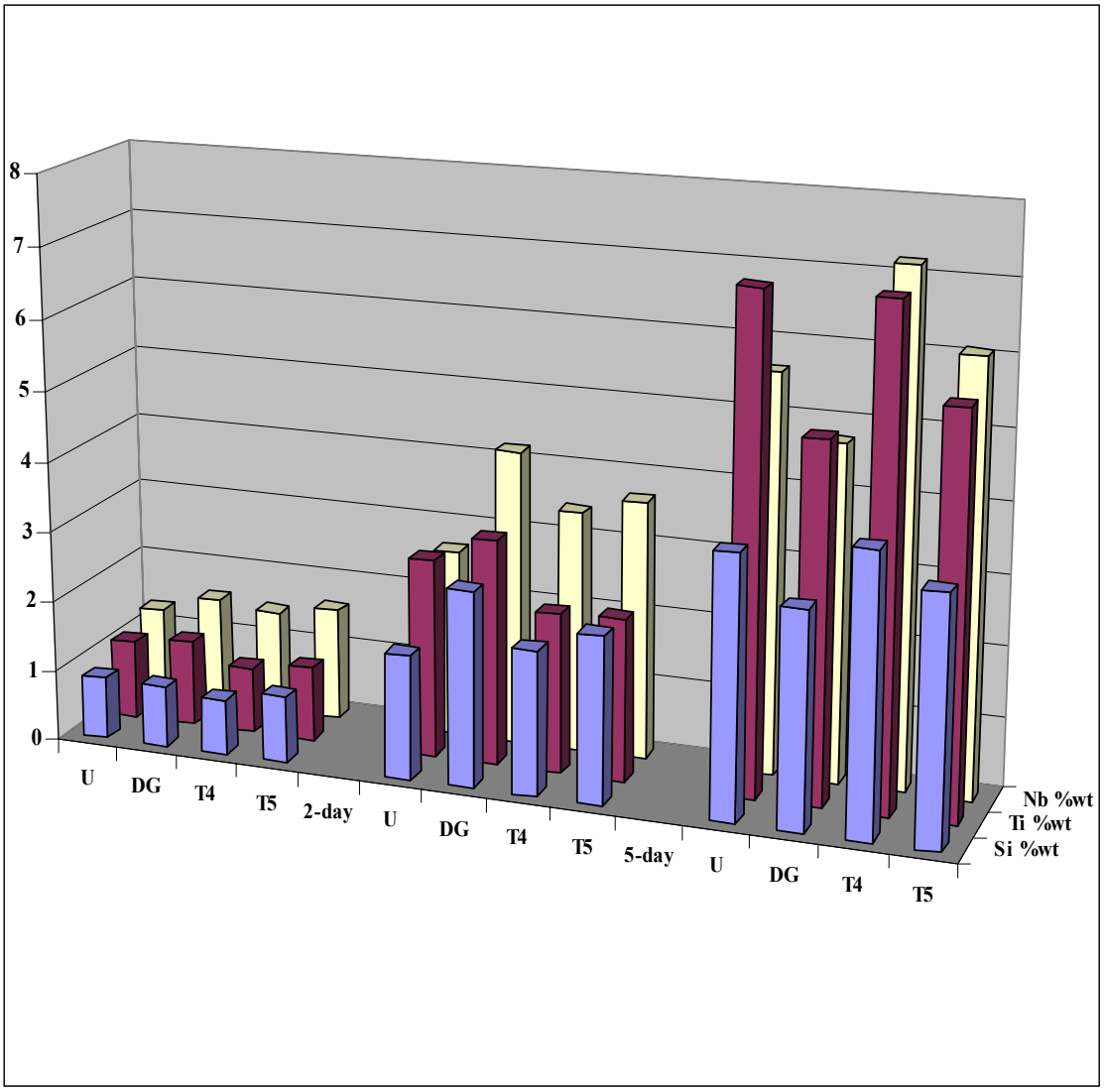

Figure 3.14. Leaching of Si, Ti, and Nb from CST as a result of shaking with simulant 6 (basic solution with 0.1 M H_2O_2).

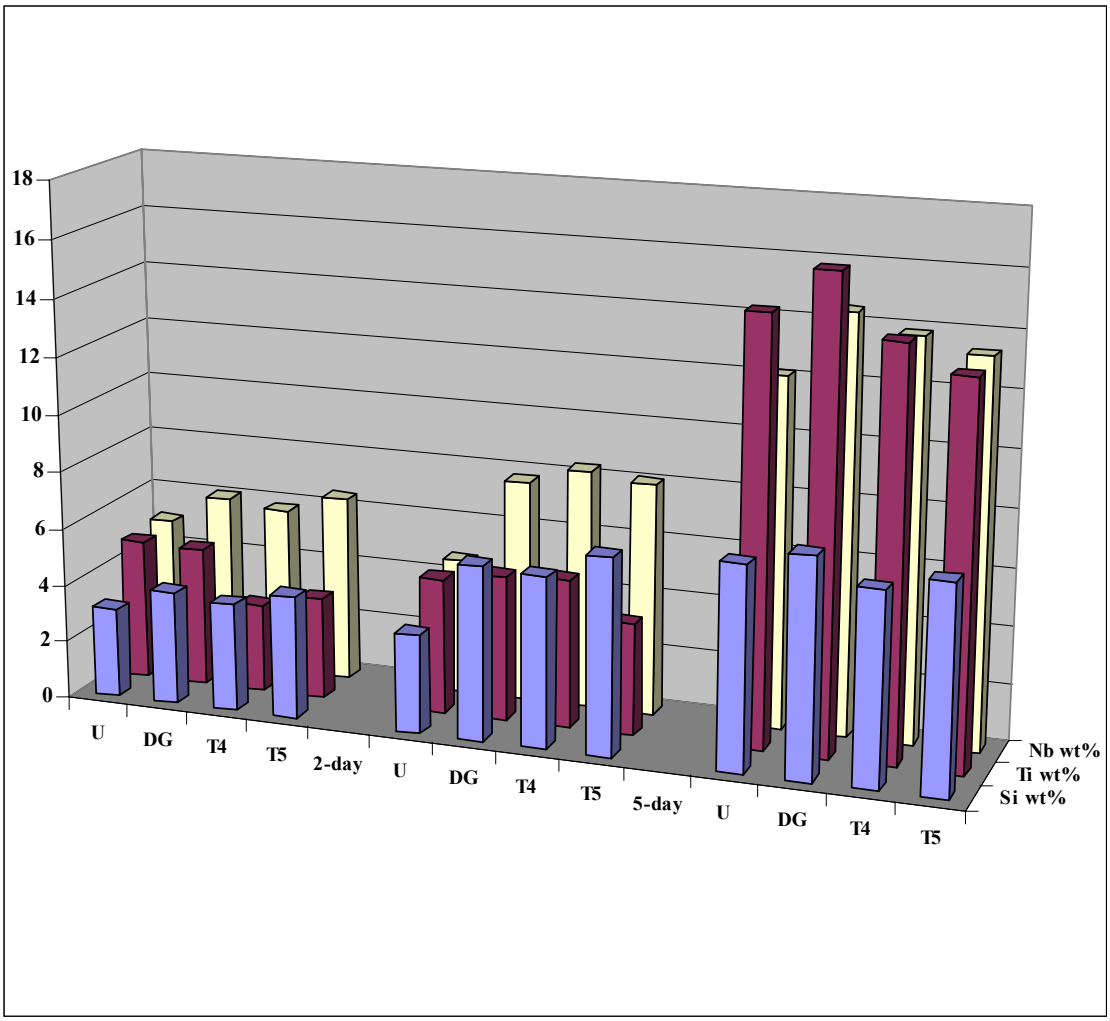

Figure 3.15. Leaching of Si, Ti, and Nb from CST as a result of shaking with simulant 7 (basic solution with 1 M H_2O_2).

The XRD patterns of four CST samples of CST before shaking with simulant are shown in Figure 3.16. All of the major peaks belong to the tetragonal phase. Four minor peaks (2 theta = 9,10, 15.9,29.7) belong to the minor phase (Nb/Ti oxide). From Figure 3.17 to Figure 21 show the XRD pattern of CST samples exposed to simulants with hydrogen peroxide. Hydrogen peroxide attacks the tetragonal phase and the intensity of XRD peaks changes proportionally to the exposure time, as well as the concentration of hydrogen peroxide. The intensity of XRD pattern of the tetragonal phase decreases, while that of the minor phase increases. The XRD patterns shown in Figure 3.21 indicate that after five days of exposure to simulant with 1M of hydrogen peroxide, most of the tetragonal phase in the CST samples has disappeared. TEM has identified the minor phase in the CST as Nb-Ti oxide phase with a Nb/Ti ratio close to 2.

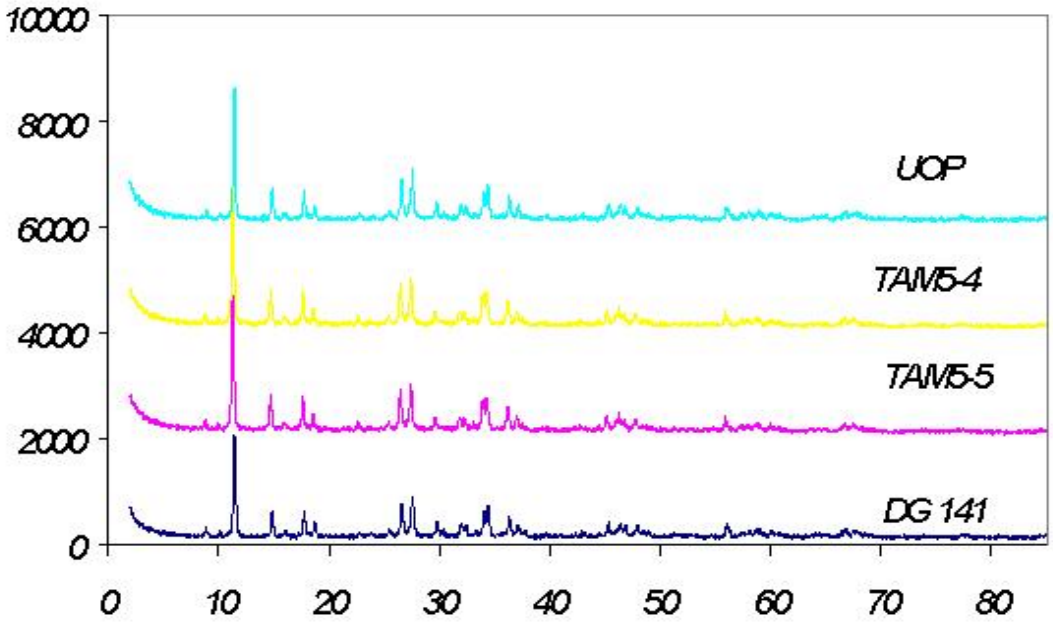

Figure 3.16. XRD pattern of CSTs before shaking with basic simulant.

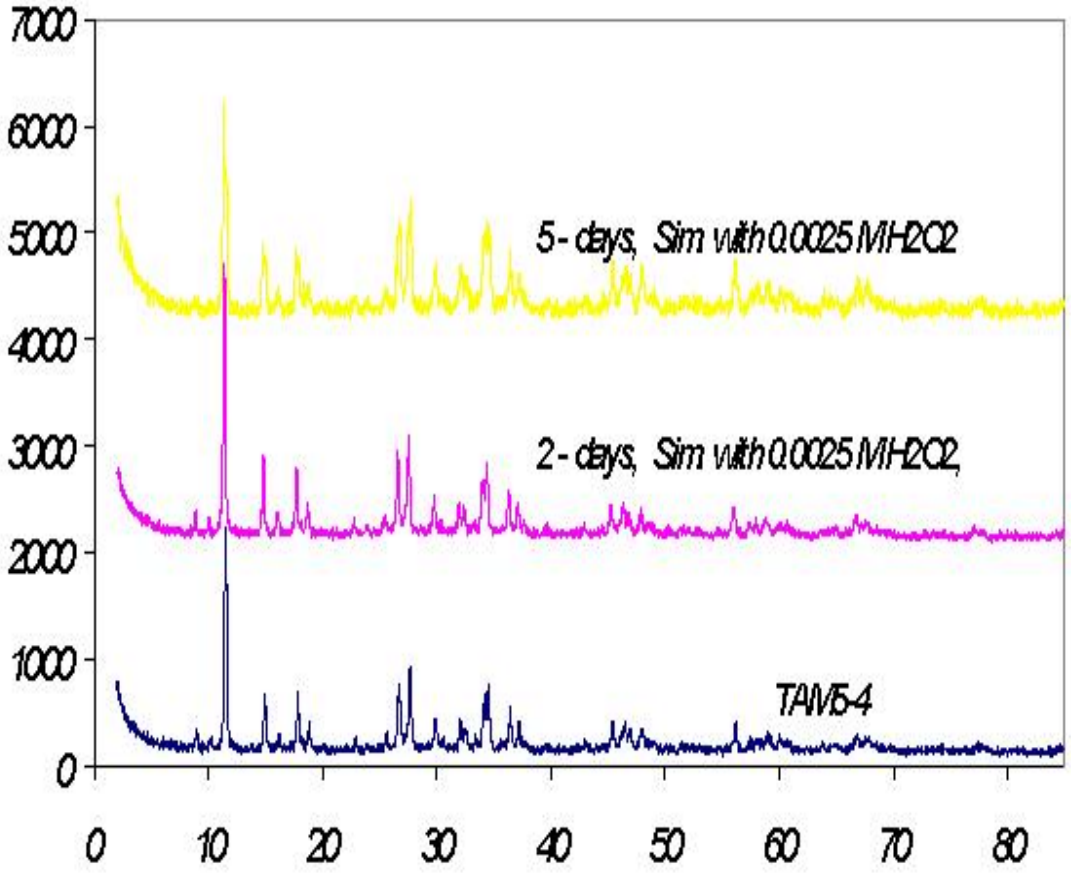

Figure 3.17. Effect on the XRD pattern of CST as a result of shaking with basic simulant containing 0.0025 M H_2O_2.

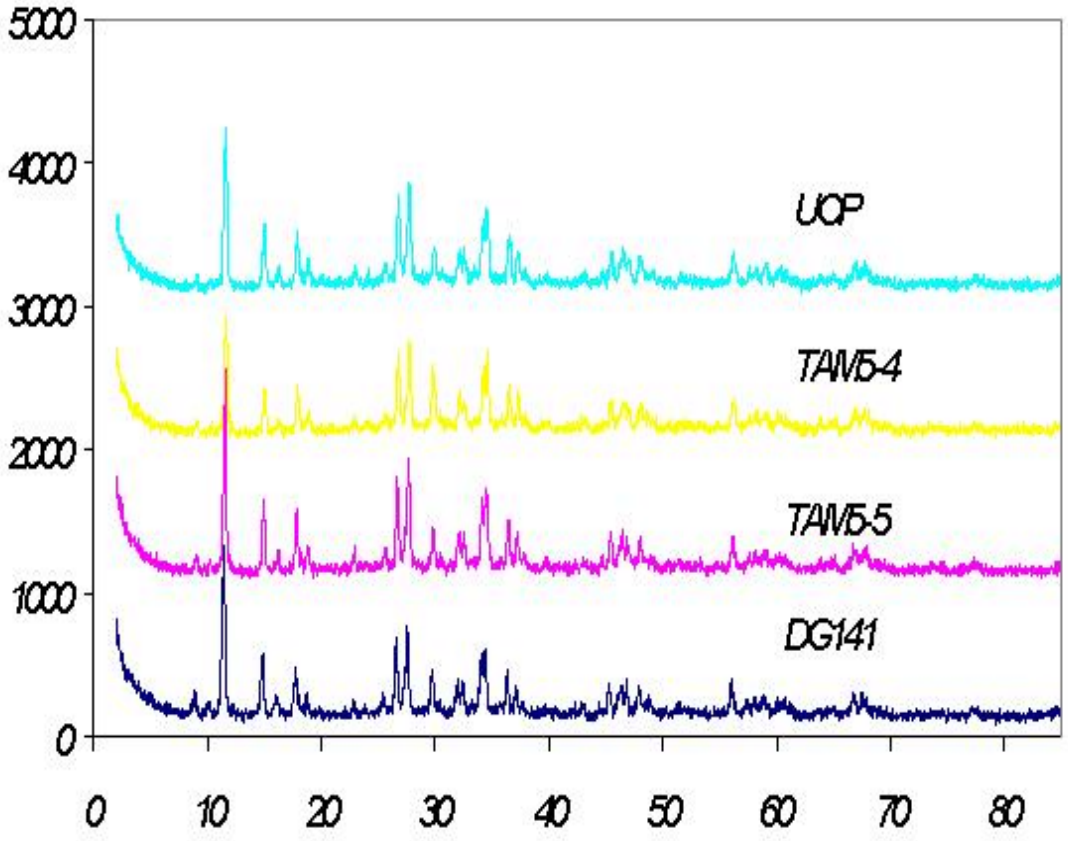

Figure 3.18. Effect on the XRD pattern of CST as a result of shaking with basic simulant containing 0.1 M H_2O_2 for 2 days.

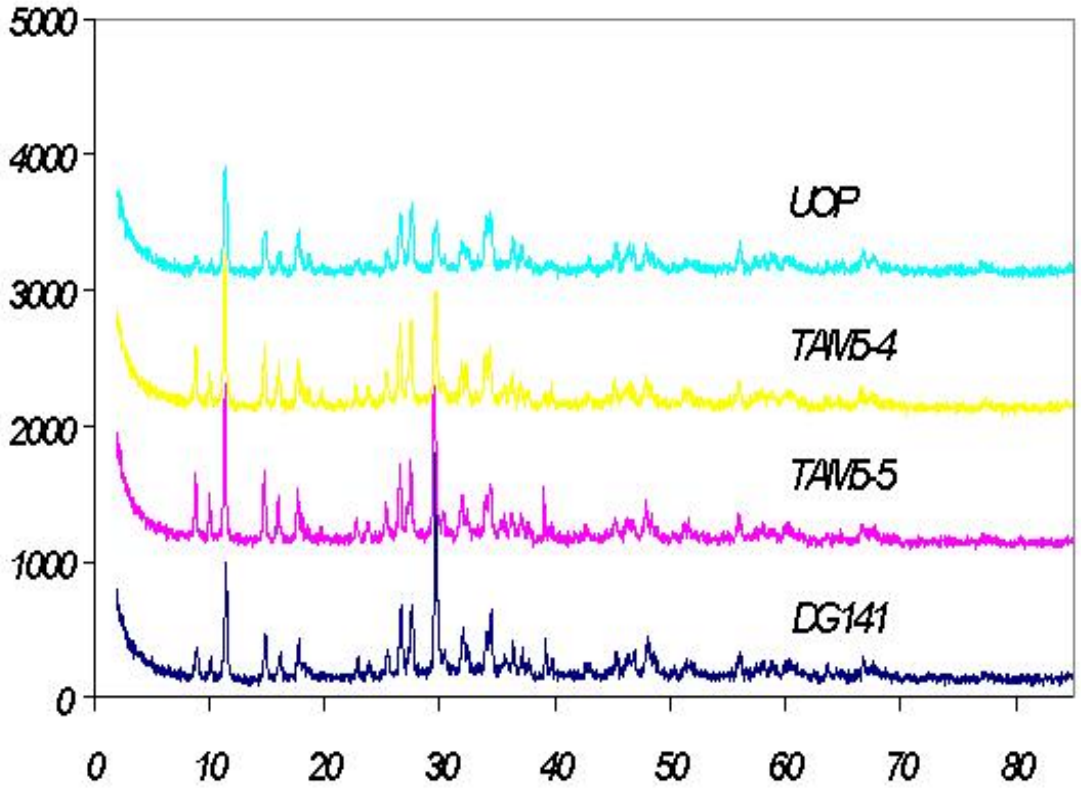

Figure 3.19. Effect on the XRD pattern of CST as a result of shaking with basic simulant containing 1 M H_2O_2 for 2 days.

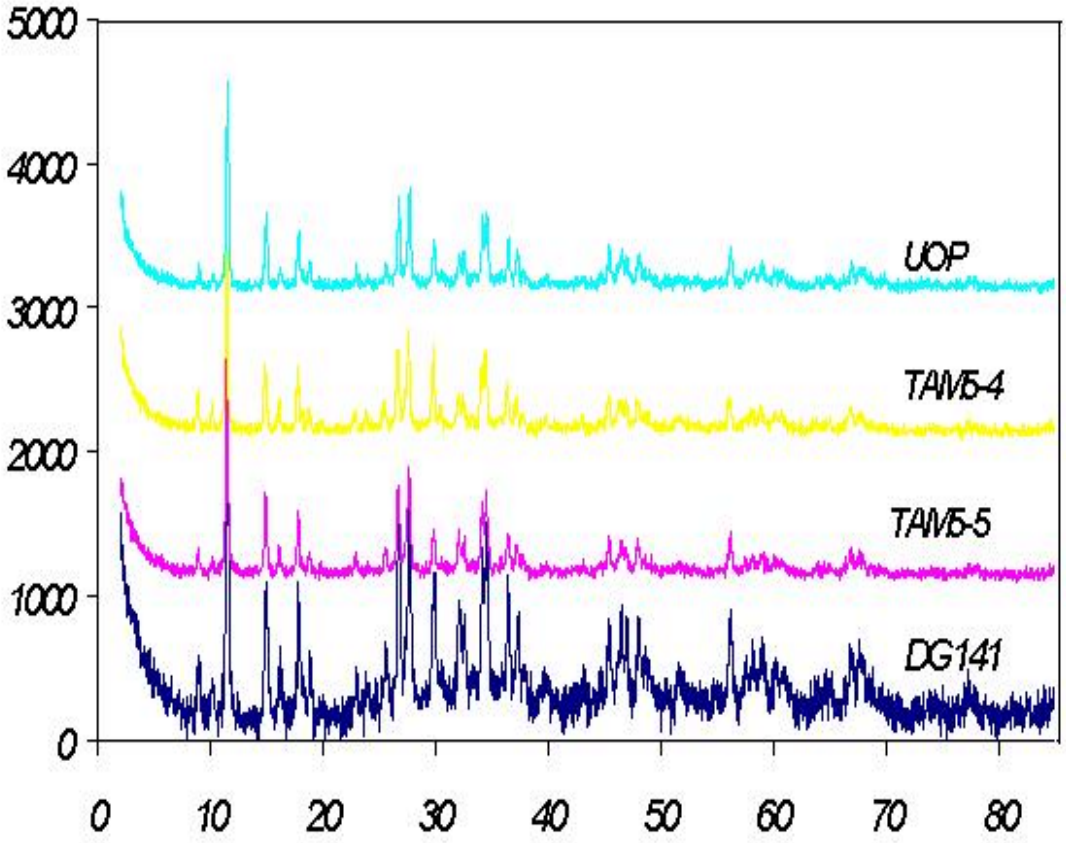

Figure 3.20. Effect on the XRD pattern of CST as a result of shaking with basic simulant containing 0.1 M H_2O_2 for 5 days.

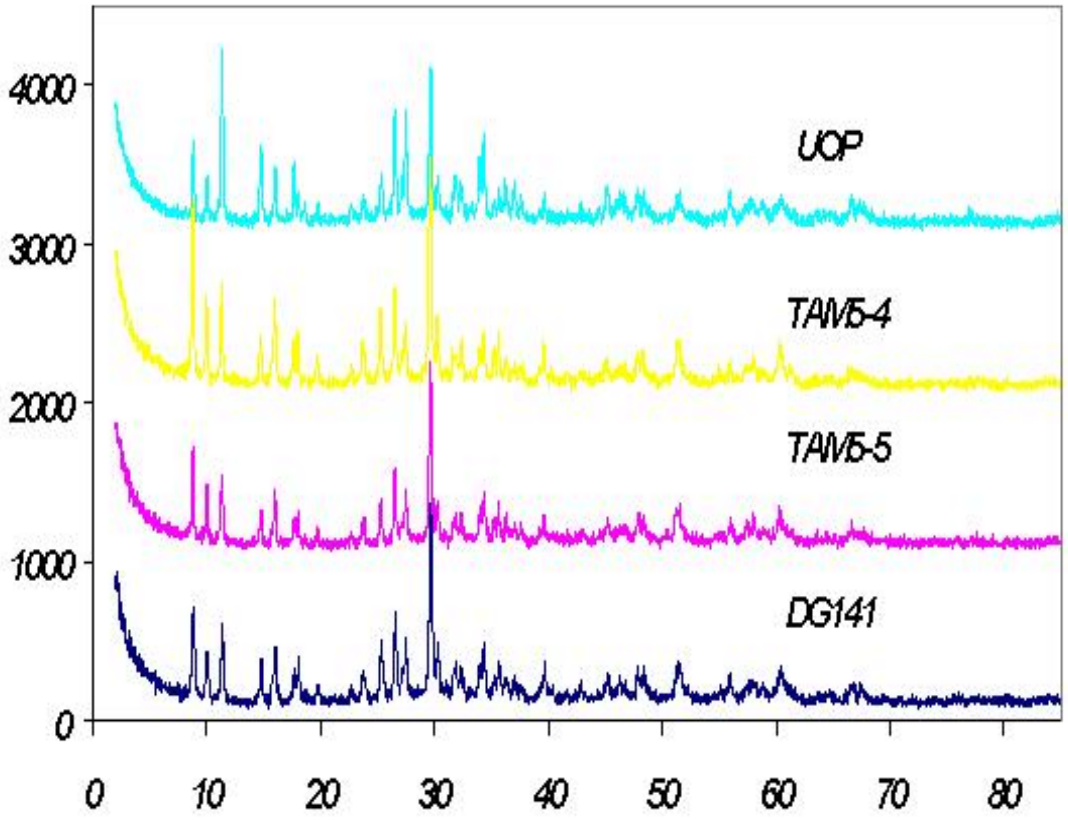

Figure 3.21. Effect on the XRD pattern of CST as a result of shaking with basic simulant containing 1 M H_2O_2 for 5 days.

CHAPTER IV

EQUILIBRIUM MODEL FOR CST GRANULES

4.1 Introduction

By using data obtained from ion exchange experiments in simple solutions and data obtained from knowledge of the structure of TAM5, Zheng et al. (1997) developed the ZAM equilibrium model for the IE-910 powder to estimate the equilibrium behavior of the CST particles in radioactive waste solutions. A set of model reactions were also proposed for multicomponent ion exchange of group I metals by TAM5. Furthermore, these model equations produced good predictions for the equilibrium compositions and the cesium distribution coefficients in highly complex solutions, which is difficult to perform equilibrium experiments, by using Bromley's model for estimating activity coefficients of multicomponent electrolytic solutions.

The IE-911 granules are made by combining the IE-910 powder with a binder. Thus, a correction factor has been applied to the values predicted from the ZAM model to account for the presence of binder. Because the binder is estimated to be 30 % of the particles, a correction factor 0.7 was used to multiply the predicted values obtained from the ZAM model. The 70 % correction indicates the IE-910 powder is diluted with the addition of 30 % binder. However, experimental equilibrium isotherms determined at Savannah River Site waste by McCabe (1997) indicated that the 70 % correction of ZAM model significantly underestimates the actual IE-911 cesium K_d values. Therefore, for design purpose, the ZAM model should be modified based on the simple experiments

of IE-911 granules to correctly account for the equilibrium behavior of granules in the complex waste solutions.

There has been no output data of sodium equilibrium in the ZAM model. The sodium K_d value, which is calculated form the equilibrium model, was added in the output data of the K-ZAM (Kim-Zheng-Anthony-Miller) model.

Zheng (1996) found that the solid phase loadings for the K^+ were greater than the equilibrium ion exchange capacity of TAM 5 in a 1.6 M $NaNO_3$ experiment, which indicated that some of the potassium precipitated as a salt. The salt was determined to be KNO_3 based on the solubility and XRD data. The crystallization was observed only in the solution that contains TAM5 and the conclusion by Zheng (1996) was that crystallization of KNO_3 is induced by TAM5. The solubility product of KNO_3 with TAM5 was estimated from the potassium isotherm in 1.6 M $NaNO_3$. The value was fixed as 0.19 mol/L in the ZAM moldel. This value can be changed with the other factor such as ionic strength. Therefore, the solubility product of KNO_3 was added in the input file of the K-ZAM model, which make able to change the value easily.

4.2 Ion Exchange Capacity of IE-911 Granules

Practically, an ion exchanger can be considered as a reservoir of ions, which can be exchanged, and can be characterized in a quantitative way by its capacity. Therefore, The number of counter ions, which can be exchanged, is more important than the number of associated groups. The total amount of exchangeable sodium ion in the IE-911 granule can be measured by titration with hydrogen ion. In such a titration, the ion

exchanger comes to equilibrium with the solution to which the hydrogen ion is added. The ion exchange process of sodium ion in the IE-911 can be monitored by recording the pH of the supernatant solution while the titration is in progress. The amount of sodium ions released by IE-911 is stoichiometrically equivalent to the amount of hydrogen ions added. After the exchangeable sodium ions are exchanged with hydrogen ions, the pH of the supernatant should decrease with further addition of hydrogen ions.

Different amount of 0.1 N HCl solutions was added to the deionized distilled water (DDW) in 24 plastic vials to make 20 ml of solution and mixed with 0.2 g of IE-911 (lot No.: 999096968100002). These samples were mixed by shaker for 24 hours, and allow to be settled for 1 hour. Then, the pH was measured by using an ORION 720A pH meter. HCl control solutions, which have the same concentrations with samples but not mixed with IE-911, were also analyzed to compare the pH of the solution. The result of titration is shown in Figure 4.1. The result showed that the sample reached almost same pH with solution without IE-911 at the HCl titration range from 6.25 to 7.5 meq/g CST, which means that the total ion exchange capacity is ranged form 6.25 to 7.5 meq/g CST. This value is larger than that of Zheng's (1996) result with TAM5 powder, which was 4.8 meq/g CST. This discrepancy is probably coming from the property of TAM5 powder, which can be easily hydrolyzed. Zheng (1996) also concluded that the total ion exchange capacity of TAM5 may be greater than 4.8 meq/g CST, if there was not the partial hydrolysis of the TAM5 material.

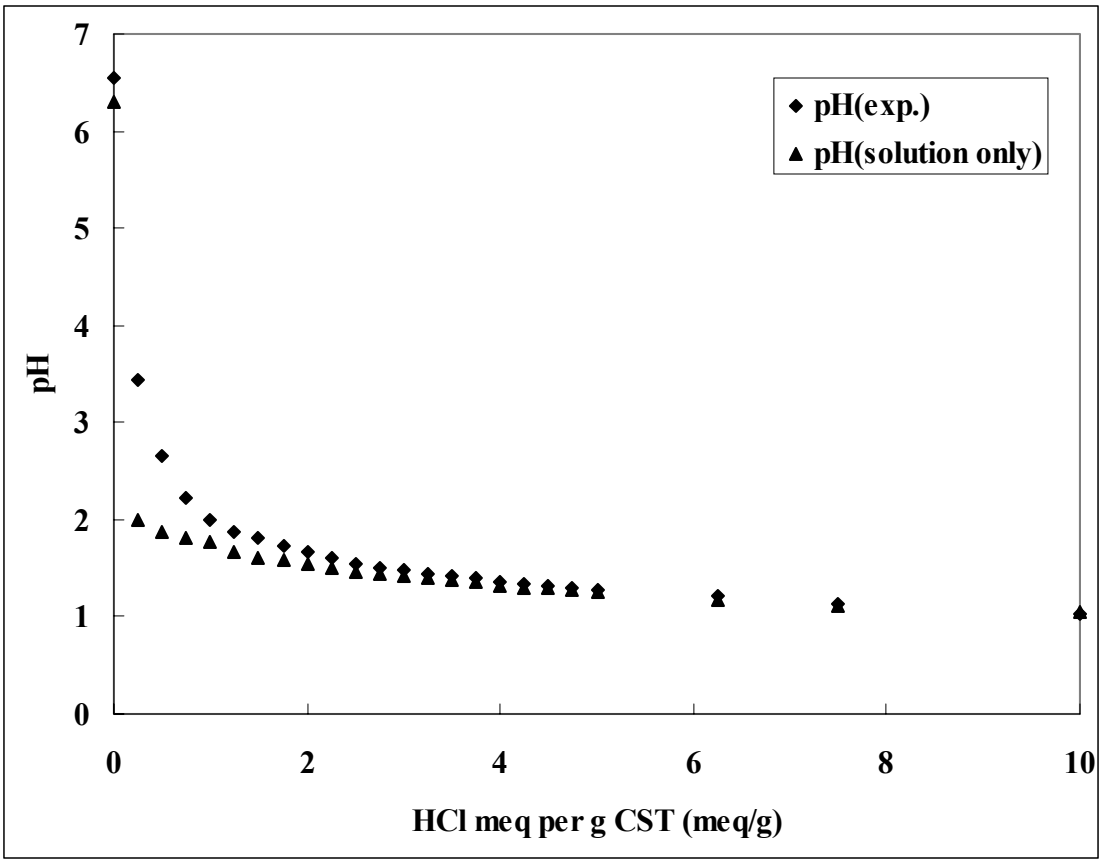

Figure 4.1. Titration curve of IE-911 granules by HCl in deionized distilled water to estimate the total capacity of granules.

The ICAP analysis of sodium in the IE-911 granules was also conducted to determine the sodium concentration in the IE-911 granules. One hundred mg of three solid samples, i.e., IE-911 granules (lot No.: 999096968100002) with Na^+ form, IE-911 granules with H^+ form, and TAM5-5 powder were dissolved in 48 % HF solution. These samples were diluted to 10,000 times, then measured the sodium with the ICAP. Sodium concentration can be calculated by equation 4.1, which is represented as:

$$[Na^+](\text{meq/g}) = \frac{C \times DF}{w \times MW \times 1{,}000} \qquad (4.1)$$

where C is measured concentration of sodium in μg/g, DF is dilution factor, w is weight of solid sample in g, and MW is molecular weight of sodium in 23 g/mol. Table 4.1 shows the results.

Table 4.1. The ICAP analysis result for sodium in the TAM5 solid

	C (μg Na^+/g CST)	Na^+ concentration (meq/g)
IE-911 Na^+ form	1.57 ± 0.21	6.84 ± 0.92
IE-911 H^+ form	0.31 ± 0.02	1.36 ± 0.09
TAM5-5 powder	1.07 ± 0.12	4.67 ± 0.52

It should be noted that the sodium concentration of TAM5-5 powder was 4.67± 0.52 meq/g, which is equal to the result by Zheng (1996), i.e., 4.8 meq/g. The sodium concentration for the IE-911 with Na^+ form was given as 6.845 ± 0.92 meq/g, which is in the range of the titration result.

4.3 K-ZAM Model for IE-911 Granules

By studying the structure of TAM5 and the titration experiments, Zheng et al. (1997) revealed that there were two major types of exchange sites in TAM5, which was represented as $Na_2X^{II}X^{I}Na$, where X^{I} and X^{II} represent the ion exchange sites with different exchange characteristics. Before the model can be used to predict the equilibrium composition of the ion exchange with IE-911 granules, the model parameters, i.e., equilibrium constant, and heat of reaction, need to be determined. The equilibrium equation for cesium in the basic solution, which exchanges with $Na_2X^{II}X^{I}Na$, can be written as:

$$Cs^+ + Na_2X^{II}X^{I}Na \Leftrightarrow Na_2X^{II}X^{I}Cs + Na^+ \qquad (4.2)$$

If the solid phase can be assumed as an ideal phase, which means solid phase activity coefficients are not needed, the equilibrium constant of equation 4.2 can be written as the following equation.

$$K_{eq} = \frac{Q_{Na_2X^{II}X^{I}Cs}\,\gamma_{Na^+}\,C_{Na^+}}{Q_{Na_2X^{II}X^{I}Na}\,\gamma_{Cs^+}\,C_{Cs^+}} \qquad (4.3)$$

where Q represents the equilibrium concentration in the solid phase, C represents the equilibrium concentration in the liquid phase, and γ represents activity coefficient in liquid phase. The experimental data for cesium isotherm in the standard solutions (Latheef, 1999) were used to compare with the cesium concentrations, which predicted by the ZAM model by adjusting the equilibrium constant. The objective function was the error sum of square between the simulated distribution coefficient and the experimental data. The relative error between the predicted concentrations and experimental data were minimized when the equilibrium constant is 30,000. This value of equilibrium constant of cesium was used to improve the ZAM equilibrium for IE-911 granules. The calculated concentrations are compared with the measured values in Figure 4.2. The temperature effect on the equilibrium constant was also investigated by using the experimental data, which were collected from report by Taylor and Mattus (1999). The value of the heat of reaction for the model was calculated based on integration of Van't Hoff's equation (equation 2.7) by assuming that the heat of reaction is constant. The integration result, which uses the reference temperature, is as follows:

$$\ln K_{eq} = \ln K_{ref} - \frac{\Delta H^o}{R}\left(\frac{1}{T} - \frac{1}{T_{ref}}\right) \qquad (4.4)$$

where K_{ref} is the equilibrium constant at the reference temperature T_{ref}, ΔH^o is the heat of reaction. The heat of reaction can be estimated from slope of ln K_{eq} vs. $(1/T-1/T_{ref})$ plot.

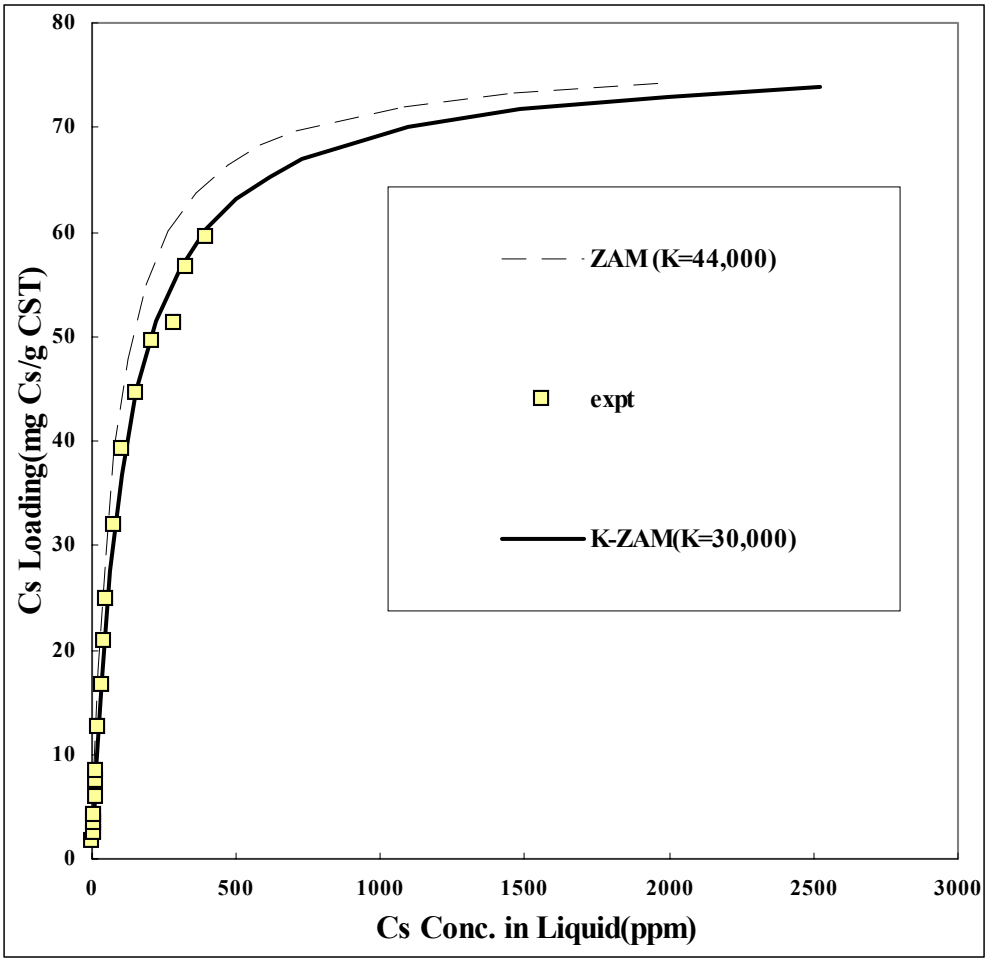

Figure 4.2. Cesium isotherm in a standard solution. The experimental data was compared with estimated data with the variance of the equilibrium constant.

Figure 4.3 shows the estimation of heat of reaction for equation 4.2, the exchange of Cs^+ with $Na_2X^{II}X^{I}Na$. The heat of ion exchange is -33.22 ± 3.7 KJ/mol for the IE-911 granules but for the IE-910 powder Zheng (1996) reported a value of -21.760 ± 0.03 KJ/mol. After the modification of the parameters in the model, the K-ZAM model was used to estimate the cesium K_d values for temperatures in the range of 30 ^oC to 120 ^oC. Table 4.2 shows the composition of SRS supernate simulant, which was used as the simulant for the experiments and predictions. Figure 4.4 illustrates the improvement in the predictability of the model. The predictions for distribution coefficients for potassium, rubidium and strontium have not been modified in the K-ZAM model. The K-ZAM model does an excellent job of predicting the distribution coefficients for the average waste simulant as illustrated in Figure 4.4.

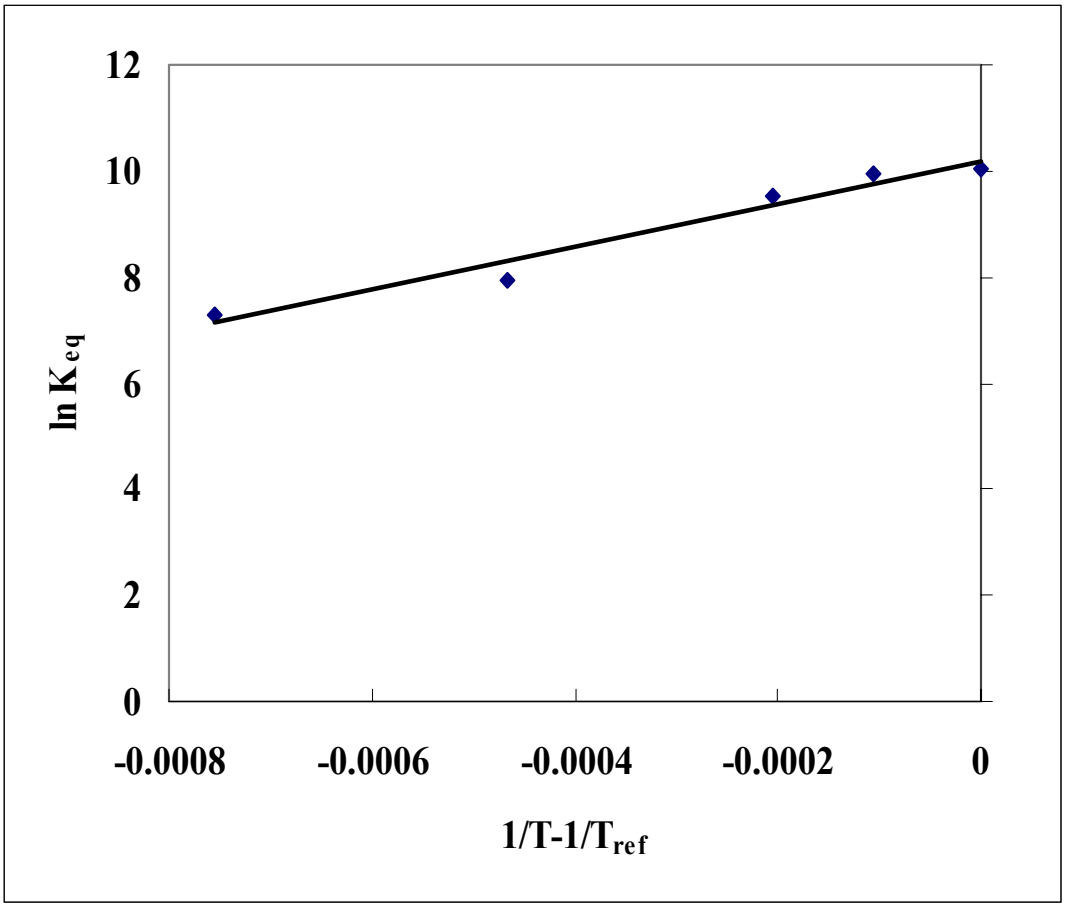

Figure 4.3. The estimation of the heat of ion exchange of Cs^+ with $Na_2X^{II}X^{I}Na$ in a SRS average solution. The equilibrium constants are based on the experimental data, which were collected from the report by Taylor and Mattus (1999).

Table 4.2. Composition of SRS simulant

Component	Concentration(M)
Na^+	5.6
K^+	0.015
Cs^+	0.00038
OH^-	1.91
NO_3^-	2.14
NO_2^-	0.52
$Al(OH)_4^-$	0.31
CO_3^{2-}	0.16
SO_4^{2-}	0.15
Cl^-	0.025
F^-	0.032
PO_4^{3-}	0.01
$C_2O_4^{2-}$	0.008
SiO_3^{2-}	0.004
MoO_4^{2-}	0.0002

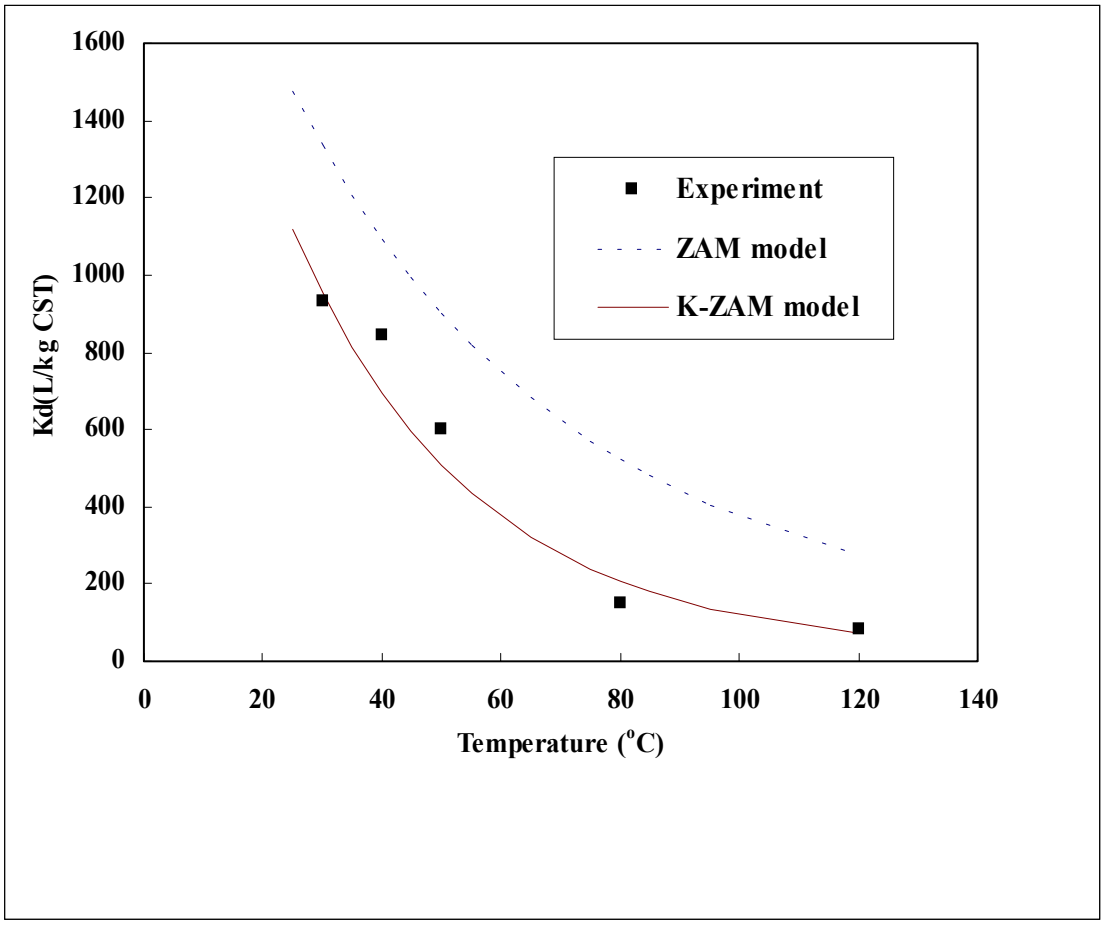

Figure 4.4. Illustration of the improvement in the ZAM equilibrium model for IE-911 granules.

CHAPTER V

SINGLE-LAYER COLUMN MODELING

5.1 Introduction

Several different approaches have been investigated for removing radioactive ions such as ^{137}Cs and ^{90}Sr in aqueous wastes with high concentrations of sodium ions. Through collaborating efforts at Texas A&M University, Sandia National Laboratory and UOP Associates, TAM5, an inorganic ion exchange material, was synthesized that selectively removes cesium from concentrated nuclear waste solutions (Anthony et al., 1993,1994,2000,2002). In an ion exchange treatment facility, UOP IONSIV® IE-911 granules, the commercial form of TAM5, would be packed into a series of fixed-bed columns. The cesium breakthrough curve for the columns is strongly dependent on the effective diffusivities within the particle. Effective diffusivities in early laboratory work were determined by modeling the breakthrough curves with fundamental column models, which incorporated the effects of axial dispersion, resistance to film diffusion and resistance to intra-particle diffusion. Huckman et al. (1999) proposed the use of a batch experimental technique to determine effective diffusivities. This approach was much simpler than the use of column experiments, because the method was easier, faster, and cheaper to perform than column experiments. However, there were some definite experimental challenges to obtaining excellent data, and one had to be sure the resistance to film diffusion was negligible. Numerical methods were also used to

estimate the values of the effective diffusivities. In spite of many numerical methods, the design of fixed-bed columns is still complicated and difficult.

To eliminate the complexity of computation, experiments were conducted by many researchers using shallow bed columns and rapid flows of solutions passing through a thin layer of ion exchangers. These studies, included experimental work with phenol-formaldehyde resin exchanger (Boyd et al., 1947), sulfonated cross-linked polystyrene in bead forms (Reichenberg, 1953) , zeolites (Ames, 1961,1962), and chitosan ion exchangers (Yosida et al., 1994). The differences in concentration at the inlet and outlet of the shallow bed were assumed to be negligible to meet the boundary condition of infinite solution volume, which enable an analytical solution of the balance equations. The shallow bed method requires a very high flow rate and a large solution throughput to meet the boundary condition of infinite solution volume. That's why resistance to film diffusion was assumed to be negligible, which is the normal case for rapid flow over pellet materials. However, if the flow around the particles is slow, then film resistance to diffusion should be included in the calculation of effective diffusivity for the granules. Yosida et al. (1994) used sodium chloride to desorb bovine serum albumin (BSA) in the resin phase. And then, they analyzed the solution for BSA with UV-Visible Recording Spectrophotometer UV-260. Boyd et al (1947), Reichenberg (1953), and Ames (1961,1962) used a radioactivity measurement, which estimated the amount of radioactive tracer in the solid by beta and gamma counting procedures. Radioactivity measurement is very convenient but is less accurate than direct measurement of samples.

In this work Cs concentrations of less than 20 ppm were used, and at values less than 20 ppm, the assumption of a linear isotherm is valid. Taking advantage of this fact, a simple mathematical model for a single-layer column was presented. This model was then used to estimate the values of effective diffusivities for IE-911 granules. The work described herein is concerned with the use of a series of single-layer columns to characterize both intra-particle and film resistance through the CST granules. A simple apparatus was designed to collect the experimental data. The cesium loading was determined by analyzing the solid, instead of analyzing the solution as were done in the batch and column reactors. The experimental data for the single-layer column will be used to estimate effective diffusivities for a standard solution and for a SRS waste simulant. The effective diffusivities of Cs, which were determined by the previous batch studies and column studies, are compared with those obtained from the current single-layer column modeling work.

5.2 Modeling Equations

When compared to the mass transfer rate of the ions, the rate of ion exchange at the site is usually fast enough to be considered as instantaneous. Thus, mass transfer is assumed to be the rate-determining step in ion exchange (Helfferich, 1962). Since this is the case, equilibrium at the ion exchange site is assumed. The physical properties of the fluid are considered to be constant since the concentration of cesium is low. Based on the above assumptions, ion exchange of cesium can be described by a mathematical model, which is composed of the following four equations; 1) a constitutive equation

that describes the diffusive flux, 2) a differential mass balance over a particle, 3) an isotherm describing the solid/liquid equilibrium, and 4) a bulk liquid differential material balance.

Although the Nernst-Planck equation is highly useful for explaining diffusion due to gradients in electrolytic solutions, the equation itself is too complex to obtain an analytical solution. Furthermore, since the solution is a concentrated solution of sodium ions, there is very little change in the electrical charges within the particle. Thus, Fick's law is applicable and the most commonly used equation to describe the diffusion flux, where the flux is proportional to the concentration gradient, and the diffusion coefficient is assumed to be constant. Huckman et al. (1999) and Gu et al.(1997) show that for the highly concentrated DOE wastes this is an excellent assumption. Therefore, Fick's law (equation 5.1) was used as a constitutive equation for this study.

$$J_i = -D_e \frac{dC_i}{dr} \qquad (5.1)$$

where, D_e is the effective intra-particle diffusion coefficient, C_i is the concentration of i in the pores of the particles, and r is the radial distance from the center of the particle. It should be noted that the use of effective diffusivity requires the assumption that the pore structure and particle represents a quasi-homogeneous phase when in reality it is an inhomogeneous particle with micro- and macro-pores.

Among the four balances as described above, the differential material balances play an important role in determining the overall form of the model. The most

commonly used models for particle material balances are a single-phase homogeneous model, a two-phase homogeneous model, and a two-phase heterogeneous model. The single-phase homogeneous model, where the particles are considered as a uniform composition with only one diffusion mechanism through the particle phase, is used in a limited number of cases as a simple approximation and is appropriate for modeling diffusion within the IONSIV® IE-910 powder, the commercial form of TAM5 powder, which is considered to be a single-phase material with micro-pores. The two-phase heterogeneous model is the most realistic model for the IONSIV® IE-911 granule, which is the composite material manufactured by combining the TAM5 powder with a binder. Hence, there are resistances to diffusion in the macropores and greater resistances in the micropores. This model is often called a micro-macro pore model. The heterogeneous model is described by particle material balances for the macropores and crystal material balances for the micropores. These two material balances describe the initial diffusion through the macropore between the crystals followed by diffusion into the micropores of the crystals. The crystal phase is assumed to be a single homogeneous phase. Thus, the diffusion property in the micropores of the crystal should be available before the effective diffusivity in the macropores is estimated. Although the two-phase heterogeneous model is highly realistic and accurate for modeling the ion exchange process, its complexity results in the use of simpler models, such as the two-phase homogeneous model. Furthermore, if resistance to macropore diffusivity is dominant then the use of the two-phase homogeneous model is justified (Latheef et al., 2000).

In the two-phase homogeneous model, resistance to diffusion occurs only in the macropores where the pores are full of liquid and the diffusivity is the same in all of the pores. The liquid in the pore is assumed to be in local equilibrium with the solid phase in the particle. If Fick's law (equation 5.1) with a constant diffusivity is used as a constitutive equation for the diffusion flux, the two-phase homogeneous model for the material balance is written as equation (2.22) as previously referred.

The initial and boundary conditions are

$$
\begin{aligned}
&at \quad t = 0, \quad C = C_0, \quad C_p = 0 \\
&at \quad r = 0, \quad \frac{\partial C_p}{\partial r} = 0 \\
&at \quad r = R_p \quad D_e \frac{\partial C_p}{\partial r}\Big|_{Rp} = k_f (C - C_p\big|_{Rp}) \qquad (5.2)
\end{aligned}
$$

where C is cesium concentration in the bulk solution, the C_o is initial cesium concentration, Cp is the concentration in the pores of the particles, R_p is the particle radius and k_f is the film mass-transfer coefficient.

The equilibrium behavior between the liquid phase and solid phase in the pore is described by an equilibrium isotherm. The most widely used isotherm equation is the Langmuir isotherm. While the Langmuir equations have a theoretical basis and are derived from kinetic models (Holland and Anthony,1989), its application in ion exchange is empirical. Thus, the experimental data are fit with the Langmuir isotherm to provide the mathematical relationship between the solid loading and liquid concentration in the pore. However, when it is used in the partial differential equation (PDE), the non-

linearity of the Langmuir isotherm makes it difficult, if not impossible, to solve the PDE analytically. Frequently, for ion exchange reactions conducted isothermally at low liquid concentration (<20 ppm), the ion exchange equilibrium can be described by a linear isotherm.

$$q = K_d C_p \qquad (5.3)$$

where the K_d is the distribution constant. The linear isotherm is not only accurate enough to analyze the relationship between liquid concentration in the pore and solid loading at low concentration, but its use also makes it easy to solve the PDE analytically. Fortunately, in almost all cases, the Cs concentration in the Department of Energy (DOE) wastes is sufficiently low that the use of linear isotherms in the treatment of DOE wastes can be justified.

The type of the ion exchange equipment, such as batch or column, determines the form of the bulk liquid material balance. In the plant-scale ion exchange facilities, almost all ion exchange devices are fixed or pulsed-bed columns. Thus, the simulation of the fixed bed column is fundamental to design of an industrial scale ion exchange system. However, the bulk liquid balance equation for the fixed-bed column is so complicated that it is impossible to obtain an analytical solution without further simplification. Therefore, earlier column modeling work focused on the prediction of breakthrough curves by employing simplifications (Garg and Ruthven, 1973). Recently, with the development of computation capability, numerical methods to simulate the

fixed bed application in ion exchange have been proposed (Latheef et al., 2000; Hritzko et al., 2000). However, the fixed bed system is still complicated and difficult to be analyzed.

For a simpler and easier method, Huckman et al.(1999) conducted ion exchange experiments in a batch system. For a batch reactor system, the film resistance is assumed to be insignificant. Furthermore, the bulk liquid differential balance of the batch reactor system may be simpler than a column ion exchanger, but it is also impossible to obtain an analytical solution for non-linear isotherms. The best way to simplify the mathematical modeling for ion exchange is to eliminate the time difference of the concentration of the bulk liquid. If the time difference of liquid concentration is small enough to be ignored, the bulk material balance equation can be eliminated from the PDE system. That is why the shallow bed columns were used in research conducted in the fifties and sixties by Boyd et al (1947) and Reichenberg (1953). A variation of the shallow bed column experimental system is the single-layer column ion exchanger, where the column consists of two separate single layers of IONSIV® IE-911 granules, has been invented and evaluated by our research group. The concentration variation across the radial direction, which was checked by a dye experiment, was negligible. The concentration difference between each single-layer column did not exceed 3 % in our system. When a column length is extremely short, the small difference between the bulk concentration of the inlet stream and the outlet stream is negligible, which means the time difference of the bulk solution is insignificant, thus, the bulk balance equation can

be eliminated from the PDE system. This concept is analogous to differential reactors used in determining kinetic rate expressions.

When the bulk balance equation is eliminated, the particle balance (equation 2.22) with a linear isotherm (equation 5.3) is a partial differential equation (Pinsky, 1991) with an inhomogeneous boundary condition (equation 5.2). The analytical solution is given in equation (5.4) and Carslaw and Jaeger (1957).

$$C_p(r,t) = C_0 + \frac{1}{r}\sum_{n=1}^{\infty} B_n Sin\,(r\sqrt{\lambda_n})e^{-\lambda_n D t} \qquad (5.4)$$

where the eigenvalue $\lambda_{n,}$ is the solution of equation (5.5). The B_n and D are calculated from equations (5.6) and (5.7), respectively.

$$(1 - \frac{k_f R_p}{D_e}) = R_p\sqrt{\lambda_n}\,Cot\,(R_p\sqrt{\lambda_n}) \qquad (5.5)$$

$$B_n = \frac{-C_0 R_p k_f Sin\,(R_p\sqrt{\lambda_n})}{\frac{1}{2}(R_p - \frac{Sin\,(2R_p\sqrt{\lambda_n})}{2\sqrt{\lambda_n}})\lambda_n D_e} \qquad (5.6)$$

$$D = \frac{D_e}{[\varepsilon_p + (1-\varepsilon_p)K_d]} \qquad (5.7)$$

The analytic solution of (equation 5.4) represents the variation of cesium concentration in the pores. However, it is too difficult to measure the variation of liquid

concentration in the pore. Therefore, the cesium loaded onto the pore and solid of the IONSIV® IE 911 granules is measured as a function of time. The space-average particle concentration, which represents the amount of cesium loaded onto the pore and solid of the IONSIV® IE 911 granules as a function of time is calculated by equation (5.8)

$$\Psi(t) = \frac{1}{V_p}\int_0^{V_p} \varepsilon_p C_p dV + \frac{1}{V_p}\int_0^{V_p} (1-\varepsilon_p) q dV \qquad (5.8)$$

where V_p is the particle volume. The solid concentration, q, in equation (5.8) is calculated from a linear isotherm (equation 5.3). The integration of equation (5.8) along with equations (5.3) ~(5.7) is given by equation (5.9)

$$\Psi = \varepsilon_p (C_0 - \sum_{n=1}^{\infty} C_n e^{-\lambda_n Dt}) + (1-\varepsilon_p) K_d (C_0 - \sum_{n=1}^{\infty} C_n e^{-\lambda_n Dt}) \qquad (5.9)$$

where C_n is calculated from equation (5.10)

$$C_n = \frac{6C_0 (k_f \sin(R_p \sqrt{\lambda_n}))^2}{R_p (R_p - \frac{\sin(2R_p\sqrt{\lambda_n})}{2\sqrt{\lambda_n}}) \lambda_n D_e} \qquad (5.10)$$

For the case where the film mass transfer resistance is negligible, namely k_f is extremely large, the eigenvalues λ_n's, from equation (5.5) become

$$\sin(R_p\sqrt{\lambda_n}) = 0, \quad or \quad R_p\sqrt{\lambda_n} = n\pi \quad n = 1,2,\ldots \tag{5.11}$$

From equations (5.9)~(5.11) and the assumption that the amount of cesium in the pores is negligible compare to the amount of cesium in the solid gives equation (5.12), which is the same equation Boyd et al. (1947) derived, where the particle diffusion was the sole rate-controlling process.

$$F = \frac{q}{q_\infty} = 1 - \frac{6}{\pi^2}\sum_{n=1}^{\infty}\frac{e^{-n^2 Bt}}{n^2} \tag{5.12}$$

$$where \qquad B = \pi^2 D_e / R_p^2$$

where F is the fractional attainment of equilibrium, q_∞ is the amount of cesium load on the solid after infinite time. While equation (5.9) can be used in the general single-layer system, it should be stressed that equation (5.12) is applicable only for the special case when the film mass-transfer resistance and cesium concentration in the pore of the particle are negligible. It should be also noted that the F is a calculable mathematical function of Bt in the equation (5.12). Furthermore, if the diffusion coefficient does not vary with F over the range of time involved, Bt may be plotted against the experimental values of t and a straight line passing through the origin should be obtained. Yoshida el al. (1994) presented the parallel transport of a protein by surface and pore diffusion within a highly porous ion exchanger using the shallow bed method. Although Yoshida

et al considered the surface and pore diffusivities, which occur in parallel within the particles, it does not appear that they considered any resistance to film diffusion.

5.3 Experimental Setup

A single-layer column was designed for the experimental study of ion exchange of Cs from a simulated nuclear waste solution. To operate properly, the velocity of the bulk solution should be fast enough to maintain the same bulk concentration of the outlet stream as that of the inlet stream. Analysis of the exit and entrance streams verified that this criterion was satisfied. However, if IONSIV® IE-911 granules contact the fast stream for long periods, particle attrition may occur. Therefore, a key design criterion was to keep the fast stream, while at the same time compensating for the effect of attrition. A single-layer column was constructed according to the schematic diagram shown in Figures 5.1a, 1b, and 1c. Two single-layer columns were used in series. Filter paper, double-stick-carpet tape and Teflon tape were the materials used for making 'column wrap'. The ring- spacers were cut from the double-stick carpet tape and glued together to obtain the correct thickness. The spacer was then glued on to a filer paper and 100 mg of the IONSIV® IE-911 granules were spread evenly inside the spacer ring. Another filter paper was placed and glued on the top. The second spacer was then glued on top of the second filter paper and added IONSIV® IE-911 granules. Then the third filter paper was glued on the top. A piece of Teflon tape was used to wrap the assembly of two thin-layer columns, which were then placed in a commercially available filter holder. All experiments were performed at 25 ^{0}C and were considered to be isothermal.

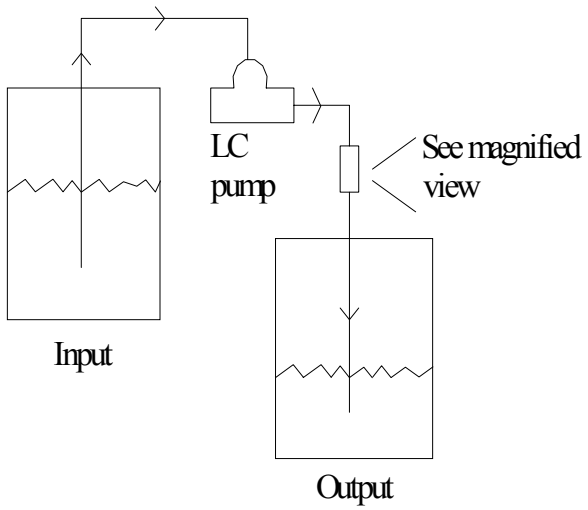

Figure 5.1a. Schematic diagram of the single-layer column reactor used for the experiment on IONSIV® IE-911 granules.

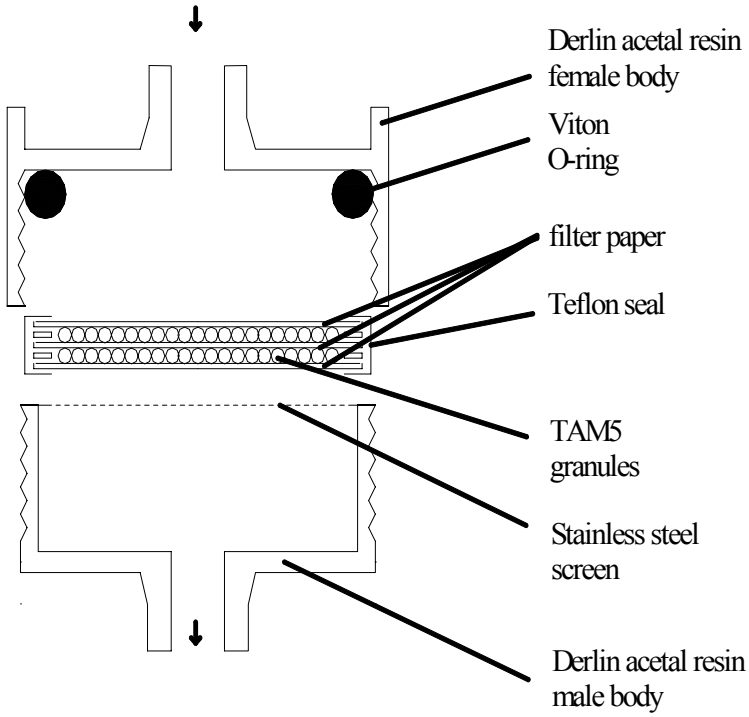

Figure 5.1b. Detailed Schematic diagram of the single-layer column reactor with the connection unscrewed.

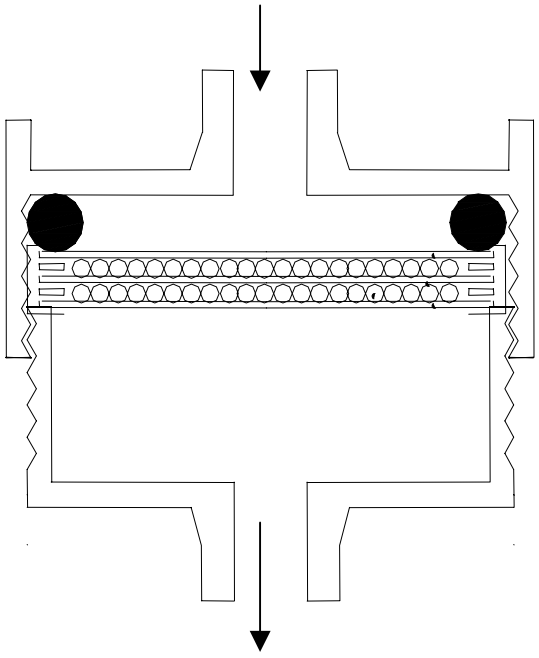

Figure 5.1c. Detailed Schematic diagram of the single-layer column reactor with the connection screwed.

The layer in the column was 390 μm long, which is approximately the same diameter of the IONSIV® IE-911 granules, and 1.6 cm in diameter. Two single-layer columns, where the two single-layer columns were connected to each other in series, were used as the column system. Two types of simulant solutions were prepared, a standard solution and a SRS average solution. The DOE wastes have some common properties such as strong basicity, very high concentrations of sodium, and very low concentrations of cesium. To simplify the effect of other ions while keeping common properties, a standard simulant for cesium was prepared. Thus, the criteria for the composition of a standard simulant was for the sodium and hydroxyl ion concentrations to be close to the values of the DOE wastes. Also, a more complex solution labeled SRS average solution was used. The composition of SRS average solution is based on the real waste located at Savannah River Site. The compositions of the standard and SRS average solutions were previously shown in chapter III and chapter IV. The simulant was pumped to the upper part of the single-layer column with a fixed rate of 4 ml/min. After a certain time-interval, the column holder was disconnected from the LC pump. Using a plastic syringe with 30 ml of deionized distilled water, the columns in the holder were flushed to remove the ion exchange solution. This manual procedure (disconnecting the flow and the injection of water for stopping the ion exchange process) required less than two seconds. The columns were then washed with 10 ml of acetone to

remove most of the water from the columns. While in the holder the columns were air-dried overnight. The columns were removed from the holder and the Teflon tape wrapper was also removed. The top filter paper was then carefully pealed off and granules from the top column were transferred into a weighed 30 ml plastic vial with the aid of a water jet from a wash bottle. One ml 50% HF was added to the vial to dissolve the CST granules. More water was added until the weight of the content reached 10 g. The spacer and the second filter paper were removed and the granules of the second column were processed similarly. The solutions were analyzed separately for Cs and Ti. The cesium in the solution was analyzed using a Varian AA 30 Atomic Spectrometer. One ml of the solution was diluted to 100 ml and titanium was analyzed using a Thermo Jarrel Ash Poly Scan 61 E Inductively Coupled Argon Plasma (ICAP) Spectrometer.

5.4 Model Parameters

For the model, the IONSIV® IE-911 granules are assumed to be spherical and of uniform size. The physical properties of the IONSIV® IE 911 granules and single-layer column are shown in Table 5.1. The average particle diameter of the granules was calculated using the following equation taken from Perry and Green (1997).

$$\frac{1}{d_p} = \sum \frac{y}{d_{p,y}} \qquad (5.13)$$

where y is the weight fraction of the material with diameter, $d_{p,y}$.

Table 5.1. Physical Properties of IE-911(lot No. : 2081000056) granules and single-layer column reactor

Properties	Value
Pellet Diameter, d_p (μm)	380
Pellet Porosity, ε_p	0.24
Pellet Density, ρ_p (g/cm^3)	2.0
Feed Velocity, u (m/s)	3.316×10^{-4}
Volumetric Flowrate E (mL/min)	4
Bed Diameter, d_B (cm)	1.6

The ion exchange isotherms for cesium using IONSIV® IE-911 granules were determined experimentally in a standard solution (Huckman, 1999) and in a SRS waste solution (Walker et al., 1998). The distribution coefficients for the linear isotherms in the standard solution and the SRS waste solution were reported as 553 ± 34.6 ml Cs/g CST and 1706 ± 97.9 ml Cs/g CST, respectively. Since the distribution coefficients are only half of equilibrium constants, they are functions of the solution concentrations. The particle to fluid mass transfer coefficient k_f, was estimated by a correlation equation (2.21), which was first suggested by Wilke and Hougen (1945). The molecular diffusivity of cesium at infinite dilution was reported as 2.06×10^{-9} m^2/s (Lide, 1996). According to the Stokes-Einstein relation, the diffusivity is inversely proportional to the viscosity of the solution. Therefore, the corrected values of 1.30×10^{-9} m^2/s, 6.13×10^{-10}

m^2/s were used for the molecular diffusivities of cesium in the SS and SRS average waste solutions.

5.5 Simulation Result

The analytical solution (equation 5.4) is represented as a sum of an infinite series. The eigenvalues of equation (5.5) should be calculated to get the result of the infinite series (equation 5.4). The number of eigenvalues n, are infinite and the eigenvalue decreases to zero as n increases to infinity. Therefore, only the eigenvalues, which affect the value of the pore concentration in the particle C_p, were calculated and used in equation (5.4). To determine the number of eigenvalues n, various simulations were conducted where n is 10, 100 and 1000 for the standard simulant and in the SRS average simulant. As n is decreased from 100 to 10, the resulting value of the pore concentration changed significantly while there was no change of the pore concentration when n was increased to 1000 from 100. With the result of the simulation, the number of eigenvalues was determined as 100. Figure 5.2 shows the calculated cesium concentrations along the particle radius as a function of time for a SRS average waste simulants with 20 ppm Cs in the feed. The physical parameters such as film-mass transfer coefficient and effective diffusivity were chosen as 1.8×10^{-5} m/s as calculated by use of equation (2.21), and 1.2×10^{-10} m^2/s, respectively. The increase of the pore concentration appears to be primarily caused by the increase of time and also by the increase of the particle radius. The effective diffusivity of 1.2×10^{-10} m^2/s was obtained by Huckman et al. (1999) for binary ion exchange with Cs-Rb in a basic solution with 1

molar sodium. However, even with this high value the calculation illustrates that a long time, i.e., 18 days, is required to obtain a fully loaded particle that is at equilibrium.

As compared to the batch ion exchange system, which is operated with vigorous mechanical stirring, the single-layer column ion exchange system is not subjected to mechanical degradation. Furthermore, IONSIV® IE-911 granules, the composite material manufactured by combining TAM5 powder with a binder, have been studied and demonstrated that the binder is not affected by the standard simulant or the SRS average simulant in the fixed-bed reactor. However, studies of IONSIV® IE-911 granules have revealed that the binder is affected by a highly caustic simulant, which may result in shrinkage of the binder and formation of a more brittle material (Nyman et al., 2001). In addition, the procedure of preparing the sample solution for analysis of the Cs after ion exchange, such as washing the granules with the DDW or acetone and dissolving the granules with HF solution, may be considered as a difficult procedure which could introduce errors in the analysis of the solid phase. Thus, it is necessary to eliminate or compensate for these errors, if they exist. In this study, the amount of Ti, which is the major component of the CST, is not leached from the CST structure during the ion exchange experiment as shown by the data in Table 5.2

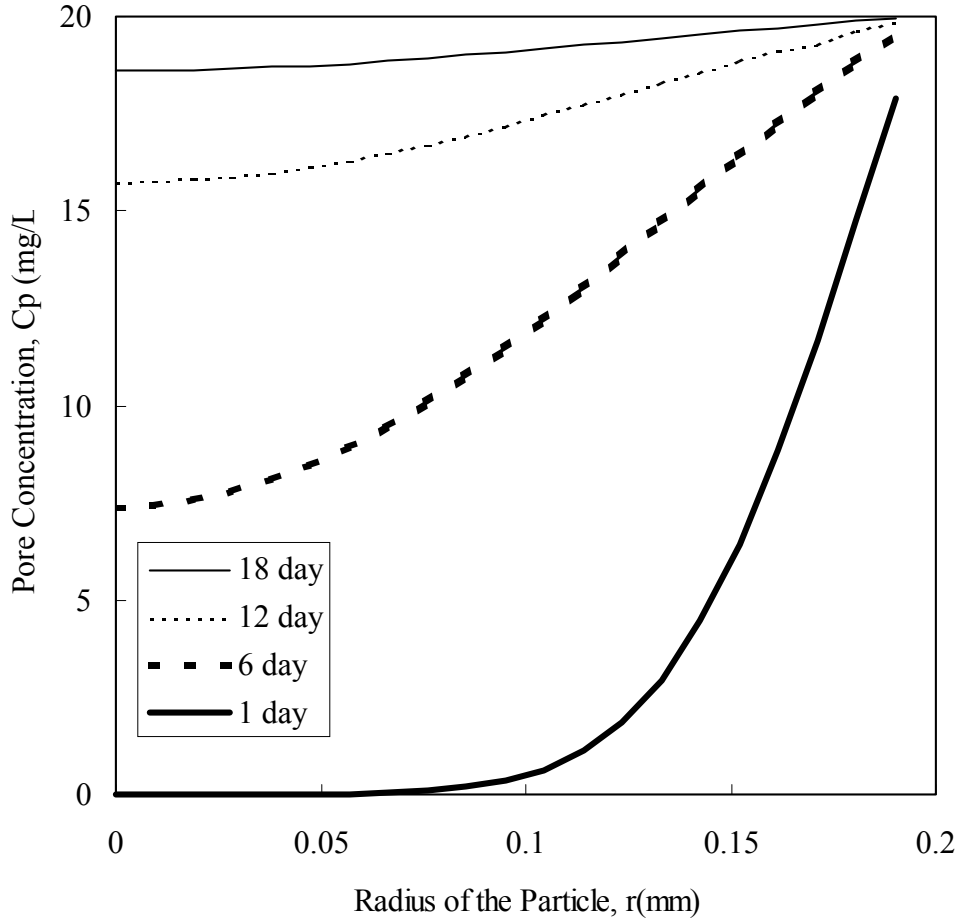

Figure 5.2. The simulation result of the variation of pore concentration with respect to time and particle radius in the SRS average waste solution. The k_f was 1.8 x 10^{-5} m/s, D_e was 1.2 x 10^{-10} m^2/s, and eigenvalue n, was 100. The center of the particle is when r = 0 mm and the surface of the particle is when r = 0.19 mm.

Table 5.2. Titanium left in columns with 100 mg CST after ion exchange

Time (min)	Ti (mg)
1	15.350
3	15.465
5	15.605
9	15.265
14	15.670
20	16.215
30	15.330
45	18.560
50	16.695
70	15.895
115	15.640
172	15.305
290	14.805
960	14.765
1440	15.260
2880	15.025
4560	14.945
Average	15.576 ± 0.893

For IONSIV® IE-911 granules, the titanium content can be used to determine the amount of CST in the granule particles. Therefore, the amount of Ti in a 100 mg sample of the particles is used to provide data on the attrition or the loss of the CST as a function of time. Table 5.2 gives the results of these analyses for Ti in the SRS average solution.

The results show that the amount of CST, which is determined by the amount of Ti, remained essentially constant during the experiments. A relatively high amount of Ti was obtained for the sample exposed to the wastes for 45 min., which is probably caused by human error in the experiment. The results indicate that no particular trend in particle attrition or loss was observed during the experiment.

5.6 Determining the Effective Diffusivities for Standard Solution and SRS Average Waste

The system of balances previously described (equation 2.22 and equation 5.1 through 5.3) involves three parameters: 1) film mass-transfer coefficient k_f, 2) equilibrium isotherm q = f (Cp), 3) effective diffusivity D_e. Among them, the equilibrium isotherm was determined experimentally by using a linear isotherm (equation 5.3). Although the film mass-transfer coefficient may be used as an adjustable parameter, the film mass-transfer coefficient and the effective diffusivity are highly correlated. Latheef (2000) also revealed that it had a minimal effect for the column system. Thus, the film mass-transfer coefficient was estimated using an existing correlation (equation 2.21) and used as a constant throughout the system. In this work, therefore, the effective diffusivity was used as the only adjustable parameter in determining the concentration of Cs in the IONSIV® IE-911 granules, which was compared with the experimental results. The variations of space-average particle concentration in the standard and SRS average waste solutions, which are obtained from equation (5.9), were simulated with the different values of the effective diffusivity for Cs

in the IE 911 granule. The effective diffusivities of Cs were estimated by minimizing the squared error between the model predicted values and the experimental data. Figures 5.3 and 5.4 show that the sum of errors squared for the standard solution and SRS average solution are minimized when the effective diffusivities of Cs are $1.56 \pm 0.14 \times 10^{-11}$ m^2/s and $0.68 \pm 0.09 \times 10^{-11}$ m^2/s, respectively. The standard solution was designed to eliminate the effect of other ions while keeping the common properties of the DOE wastes such as strong basicity, very high concentration of sodium, and low concentration of cesium. Compared to the SRS average solution, the standard solution has similar characteristics, but the viscosity is less than the SRS average waste. The viscosities of the standard solution and SRS average waste solution are 1.59 cP and 3.36 cP, respectively. According to the well-known Stokes-Einstein relation, the diffusivity is inversely proportional to the viscosity of the solution (Reid et al., 1987). Thus, the difference of the effective diffusivities in the waste solutions may be explained by the difference of the viscosities.

If the special case, where the film resistance is ignored and the particle diffusion is the sole rate-controlling process, is considered, the equation (5.12) may be used to estimate the effective diffusivities of Cs. The resulted effective diffusivities of Cs for the standard solution and SRS average solution are minimized when the effective diffusivities of Cs was found to be $1.30 \pm 0.18 \times 10^{-11}$ m^2/s and $0.63 \pm 0.11 \times 10^{-11}$ m^2/s, respectively.

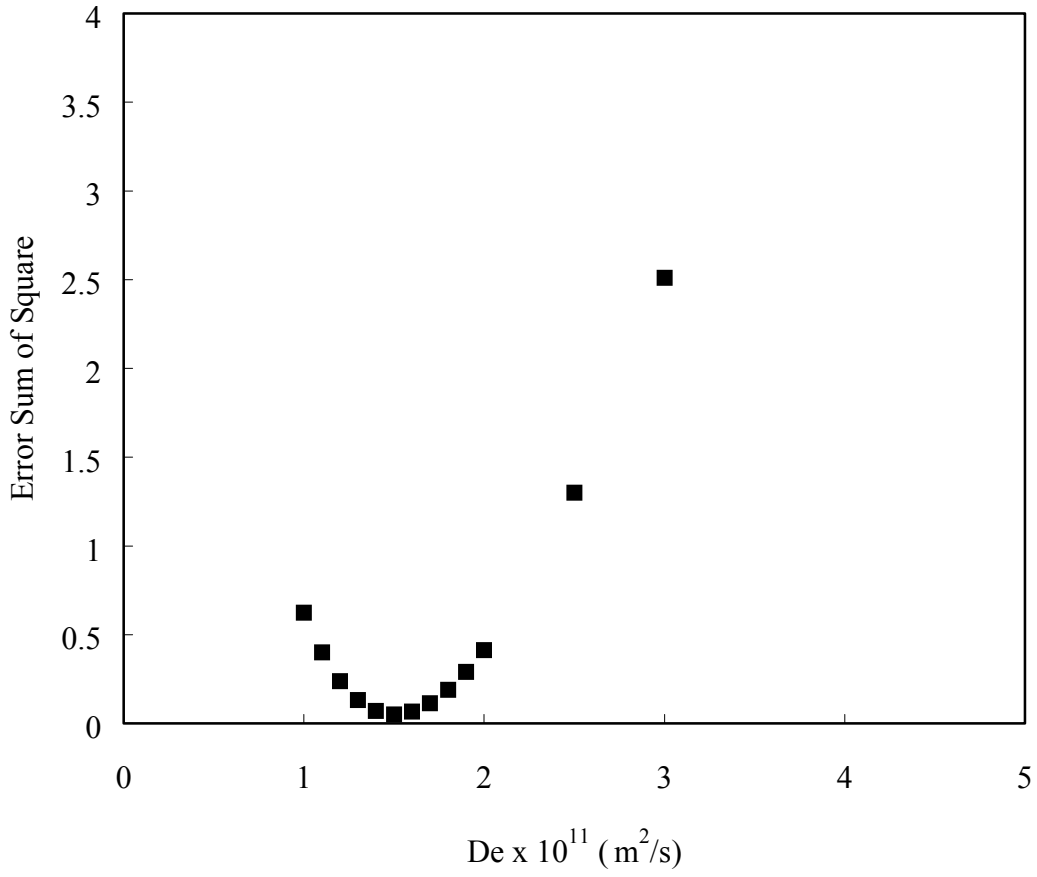

Figure 5.3. The variation of the error sum of square with respect to the effective diffusivity for the standard solution. The best-fit Cs effective diffusivity is obtained when the effective diffusivity is 1.56 x 10^{-11} m^2/s.

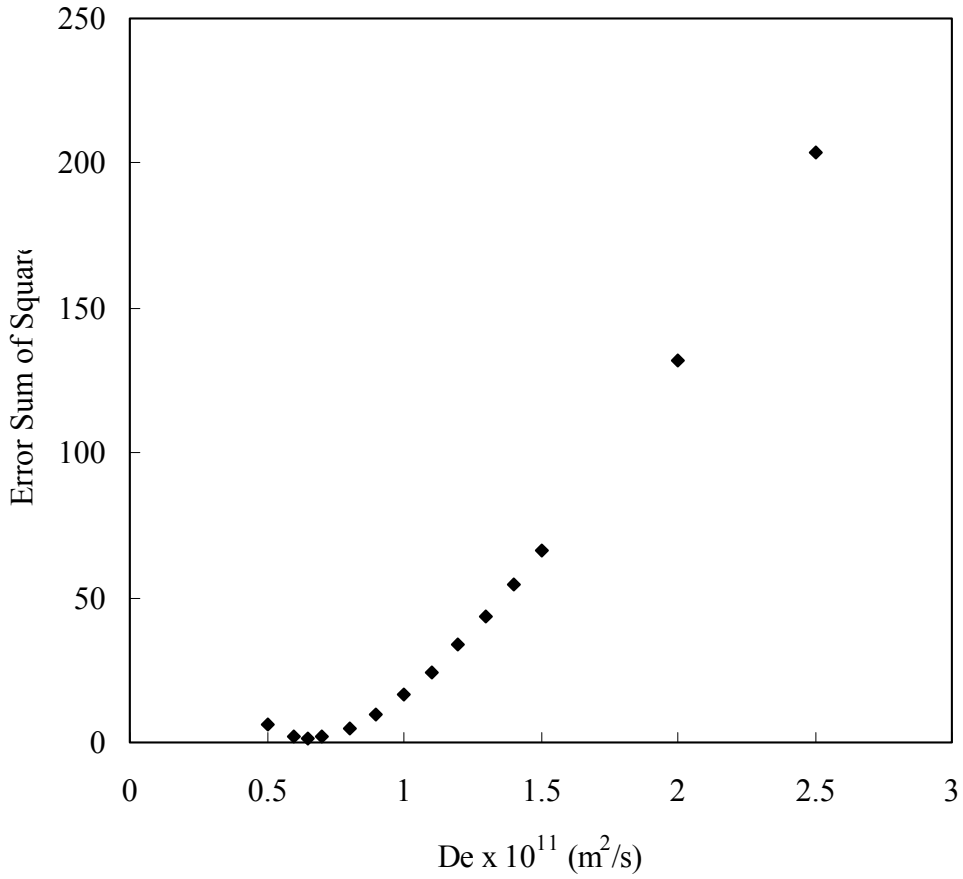

Figure 5.4. The variation of the error sum of square with respect to the effective diffusivity for the SRS average solution. The best-fit Cs effective diffusivity is obtained when the effective diffusivity is 0.68×10^{-11} m^2/s.

Although the ion exchanger and solutions are different, it should be noted that the consistent results of effective diffusivities for cesium, 1.55 x 10^{-11} m^2/s for erionite and 1.66 x 10^{-11} m^2/s for clinoptilolite, which were determined by using shallow bed, were reported by Ames (1961). These consistent results likely due to the similarity of the framework between zeolotes and CST, i.e., three-dimensional materials with shape-selective and size-exclusion properties, which are generally referred to as molecular sieves (Solztak, 1989).

Previous values of the effective diffusivity of Cs in the standard solution, which were determined from fitting the two-phase homogeneous model to batch kinetic data and to fixed-bed column kinetic data, were 3.0 ± 1.0 x 10^{-11} m^2/s (Huckman,1999) and 4.5 ± 1.0 x 10^{-11} m^2/s, respectively (Latheef et al., 2000). For the case of SRS average waste solution no data for a batch study have been reported. However, values reported from WSRS using a fixed bed column ranged from 2.0 x 10^{-11} to 6.0 x 10^{-11} m^2/s (Huckman et al., 2001). The smaller value was obtained for experiments conducted at high fluid velocities, whereas the higher value was obtained at low velocities. Figures 5.5 and 5.6 illustrate the calculated concentrations compared with data for the single-layer column for the standard and the SRS average, waste solutions. The predicted Cs concentrations of IE 911 granules were well fitted with experimental values, where the R-square value was 0.995, when the effective diffusivity of Cs is 1.56 ± 0.14 x 10^{-11} m^2/s in the standard solution. This value is almost one-half the value obtained from batch experiments and a third smaller than values obtained from column experiments.

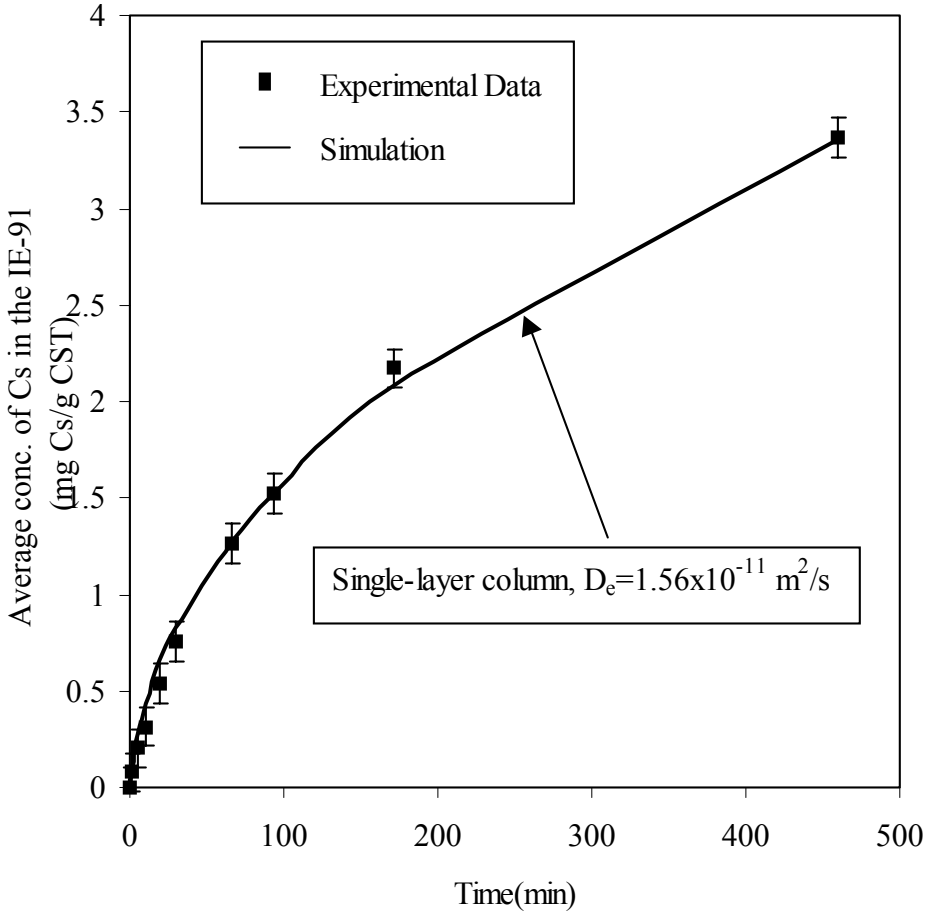

Figure 5.5. Experimental data for the standard solution and single-layer simulations at effective diffusivity of $1.56 \pm 0.14 \times 10^{-11}$ m^2/s.

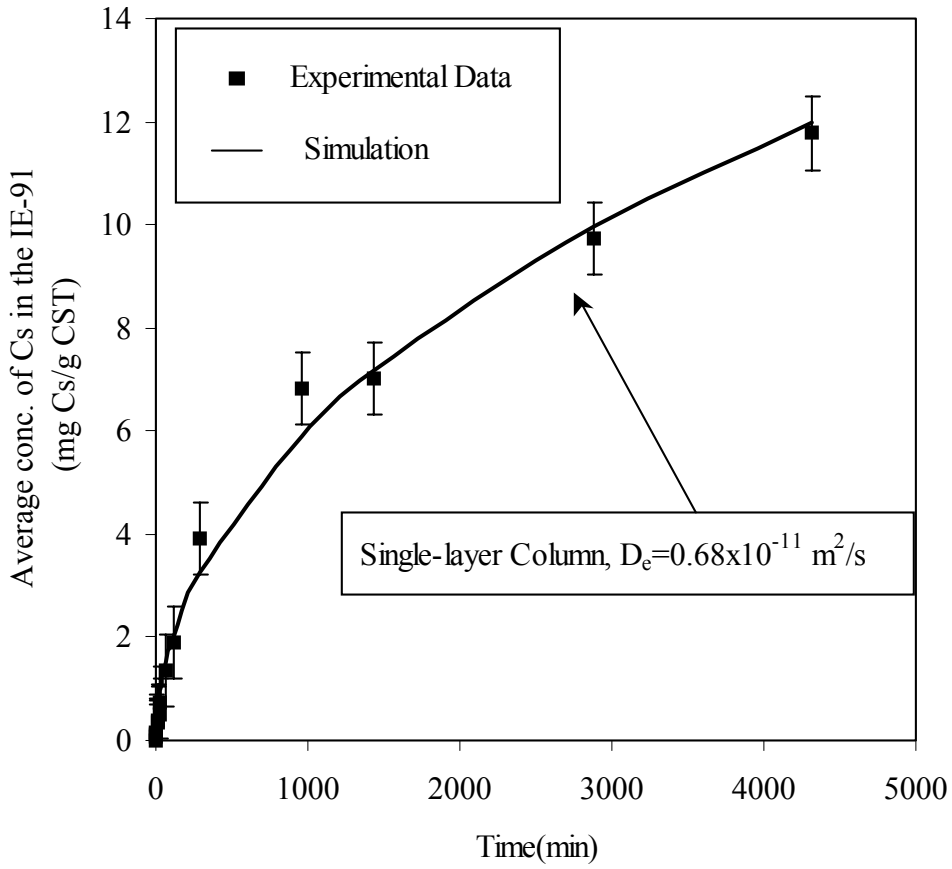

Figure 5.6. Experimental data for the SRS average waste solution and single-layer simulations at effective diffusivity of $0.68 \pm 0.14 \times 10^{-11}$ m^2/s.

The predicted Cs concentration of SRS average solution is also well fitted with experimental data, where the R-square value was 0.992. However, the effective diffusivity estimated for SRS average solution was $0.68 \pm 0.09 \times 10^{-11}$ m^2/s, which is much smaller than the value of experiment conducted at high fluid velocities of the column model. Table 5.3 shows the summary of the effective diffusivities of Cs in various conditions.

Table 5.3. The summary of the effective diffusivities of Cs in various conditions

Solution	D_e (m^2/s)	Condition
SS	$3.0 \pm 1.0 \times 10^{-11}$	Batch reactor (Huckman, 1999)
	$4.5 \pm 1.0 \times 10^{-11}$	Column reactor (Latheef et al., 2000)
	$1.56 \pm 0.14 \times 10^{-11}$	Single-layer (This work, equation 5.9)
	$1.30 \pm 0.18 \times 10^{-11}$	Single-layer (Large k_f or no mass transfer resistance, equation 5.12)
SRS avg.	$2.0 \sim 6.0 \times 10^{-11}$	Column reactor (Huckman et al., 2001)
	$0.68 \pm 0.09 \times 10^{-11}$	Single-layer (This work, equation 5.9)
	$0.63 \pm 0.11 \times 10^{-11}$	Single-layer (Large k_f or no mass transfer resistance, equation 5.12)

CHAPTER VI

PULSE COLUMN MODELING

6.1 Introduction

In a commercial facility, UOP IONSIV® IE-911, the commercialized granular form of TAM5, would be packed into a series of fixed-bed columns. Although the actual ion exchange technology use column reactors, the batch reactor kinetics of both TAM5 powder and IE-911 granules have been studied by several researchers because batch kinetics is simpler, easier, faster and cheaper to perform than column experiments (Nguyen, 1994; Gu et al., 1997; Huckman, 1999). Furthermore, the results of these studies provide fundamental understanding of the diffusion process to be used in more complex column models. Based on the batch studies, several researchers designed and modeled the continuous carousel process with packed column in series, which incorporated the effects of axial dispersion, resistance to film diffusion and resistance to intraparticle diffusion, to utilize CST for the treatment of DOE wastes stored at the Savannah River Site (Hritzko et al., 2000; Huckman et al., 2001).

Su et al. (2001) studied the leaching of niobium and silicon from UOP IONSIV® IE-911 and concluded that the precipitation of aluminosilicates from the SRS simulants onto the IONSIV® IE-911 particles could occur. These precipitates of a hexametric niobium could form and lead to plugging of ion exchange column, which could be serious deficiency for the ion exchange technique (Krumhansl et al., 2001). To solve this problem, an alternative column designs that had the potential to avoid column

plugging were evaluated (Yen et al., 2001). One of the most promising design is the counter-current ion exchange (CCIX) column, based on a moving bed of ion exchange media where fresh ion exchange media is pulsed into the column from the end that feed solution exits the column while used ion exchanger is removed from the column at the end that the feed solution enter the column. Thus, the feed and ion exchanger are moving in opposite directions through the column.

This research is focused on the mathematical model and design process for a CCIX column, which is used to simulate the performance of UOP IONSIV® IE-911 granules for removal of cesium in the complex nuclear solution at Savannah River Site (SRS). The effective diffusivities of the Cs^+ ion, which were determined by the previous batch studies and column studies, were used to analyze the performance of the pilot test of CCIX column at Severn Trent Service (STS).

6.2 Modeling Equations

An ion exchange or adsorption process involves several steps that transfer the ion species from the bulk of the fluid phase to the specific sites within the interior of the pellets as well as steps that replace the counter ions in the ion exchange sites. In most cases, ion exchange reaction is much faster than the various mass transfer steps and can be ignored when formulating the overall rate expression. Thus, mass transfer is assumed to be the rate-determining step in ion exchange. Furthermore, the assumption that the ion change is considered an isothermal process is applied universally, because the enthalpy change associated with the ion exchange reaction is usually small (Helfferich,

1962). Since the concentration of cesium is low, the physical properties of the fluid are considered to be constant. Based on the above assumptions, the four key elements, which are: 1) a constitutive equation that describes the diffusive flux, 2) a differential particle phase mass balance, 3) an isotherm describing the solid/liquid equilibrium, and 4) a bulk liquid differential material balance ion exchange process, have been determined to make a mathematical model in this study.

Fick's law (equation 5.1) was used as a constitutive equation. Two-phase homogeneous model (equation 2.22) was used as a differential particle phase mass balance in this model. As a boundary condition of particle phase mass balance, equation (5.2), which simply states that the concentration of ions is symmetry across the center of the granules and the flux of ions at the particle surface is equivalent to the flux of ions across the thin film around the particle, was selected in this work.

The equilibrium behavior between the ion in the solid phase and ion in the pore-filled liquid phase can be described by the Langmuir isotherm, which is the most widely used isotherm equation. While the Langmuir isotherm has a theoretical basis and are derived from kinetic models (Holland and Anthony,1989), its application in ion exchange is purely empirical. Thus, the experimental data are fit with the Langmuir isotherm to provide the mathematical relationship between the solid loading and liquid concentration in the pore. For SRS average waste, experimental data were used with the following Langmuir isotherm (Walker et al., 1998)

$$q = \frac{q_t K_d C_p}{1 + K_d C_p} \tag{6.1}$$

where qt is the maximum loading and K_d is the Langmuir constant.

The type of the ion exchange equipment, such as batch or column, determines the form of the bulk liquid material balance. Thus, the CCIX column, where the fresh ion exchanger is pulsed into the column from the end of the column whereas the spent ion exchanger is removed from the other end of the column, determines the bulk material balance. The distinctive feature of the CCIX from regular bed column is that a certain part of bed is moved periodically and counter-currently to the solution containing the radioactive wastes. Therefore, the mathematical model of the CCIX reactor starts from modeling of the fixed bed column reactor. For the simple case of single-phase plug flow in a packed bed of a cylindrical column, the bulk balance equation can be described as equation (6.2).

$$\frac{\partial C_i}{\partial t} = -v_i \frac{\partial C_i}{\partial x} + D_L \frac{\partial^2 C_i}{\partial x^2} - \frac{3}{R_P} k_f \left[C_i - C_{Pi}\big|_{r=R_P} \right] \tag{6.2}$$

where v_i is interstitial velocity, D_L is axial dispersion coefficient. Note that the radial dispersion is ignored since the bed diameter is almost always several orders of magnitude greater than the pellet diameter. The boundary conditions were given by Danckwerts(1953) as shown in equation (6.3)

$$\frac{\partial C_i}{\partial x}\Big|_{x=0} = \frac{v_i}{D_L}(C_i\Big|_{x=0} - C_i^0)$$
$$\frac{\partial C_i}{\partial x}\Big|_{x=L} = 0 \qquad (6.3)$$

where C_i^0 is the feed concentration and L is the length of the reactor. These boundary conditions simply express the fact that the rate of feed is equal to rate of the combined flow and diffusion at the entrance and the concentration derivative should be zero at the exit of the column.

Because of the lack of computation ability, the initial column models were focused on theoretical prediction of breakthrough curves by employing simplifying assumptions. For example, asymptotic solutions to the macro-micro column model, which was presented by Garg and Ruthven (1973), assumed plug flow, isothermal conditions, and negligible film resistance and momentum analysis, which was conducted by Kim (1990), assumed plug flow and a linear isotherm. Recently, with the progress of computation performance, numerical methods to simulate the fixed-bed application in ion exchangers have been proposed (Latheef et al., 2000; Hritzko el al., 2000). They employed orthogonal collocation on gradient-directed finite elements (OCFE), which combines orthogonal collocation (Finlayson, 1972) that transforms the set of partial differential equations (PDEs) into a set of ordinary differential equations (ODEs), with the high accuracy of the finite element method. In the application of OCFE, the whole domain is divided into a specified number of sub-domains and orthogonal collocation is applied to each domain. This method transforms the system of PDEs into a system of

algebraic differential equarions (ADEs) that has to be solved using a special integration package. The integration package used in this study is DASSL, which uses fifth-order Adams/Moulton algorithm (Petzold, 1982). In our modeling work of CCIX column, the discontinuities of the concentration profile in the sub-domains occur as the fresh ion exchanger is pulsed into the column, which moves in an opposite direction with the feed solution. The discontinuities are handled by moving the concentrations at the bottom column collocation points into the direction of the collocation points for the top column and then setting the concentrations at the newly pulsed column collocation points equal to zero, since the newly pulsed column is loaded with fresh ion exchanger.

6.3 Experiment

The CCIX pilot-scale column experiment and procedure, which were performed at the STS facilities in Tampa, Florida, were described in a reference (Wester et al., 2001). Only a few comments will be given here. The IE-911 granules were used as adsorbent for cesium and SRS average solution, whose composition shown in Table 4.2, was used as the waste simulant. The column was about 22 ft long and 2 in. in diameter. The column was pulsed hydraulically approximately once per day so that the ion exchanger bed moved about 12 in. when the bed was pulsed. Samples were collected from five points along the column. The supernate was analyzed by inductively coupled plasma mass spectrometry (ICP-MS).

The model parameters, i.e., particle diameter, particle density, film mass transfer coefficient etc., were used as in chapter 5.3. The Suzuki and Smith (1972) correlation

for the axial dispersion coefficient (equation 2.16) was used to estimate the axial dispersion in the CCIX reactor.

6.4 Simulation Results

In a column reactor, the composition of the outlet stream and its change with time depend on the properties of the ion exchanger, the composition of the feed, and the operating conditions. Although it is not perfect to characterize the performance of the ion exchange reaction in the column, simplifications and semi-empirical approximations are used to predict the performance of the column, and to find the probable range of optimum operating conditions for various process conditions. As one of the estimation method of column capacity, the overall capacity, which is the amount of cesium taken up prior to exhaustion of the ion exchanger, can be used. The breakthrough curve can be used to determine the overall capacity (Helfferich, 1962). The breakthrough capacity, which is the amount of cesium removed from the solution prior to the breakthrough, can also be determined by breakthrough. However, since the breakthrough capacity depends on the nature of process and the operating conditions, the conditions should be specified in the breakthrough capacity. Figure 6.1 shows the specific example of breakthrough curve for IE-911 granules in the SRS average solution, whose composition is in Table 4.2, with 19 ppm cesium at 5.9 column volume (CV)/hr, when the effective diffusivity is 6.0×10^{-11} m^2/s (Huckman et al, 2001).

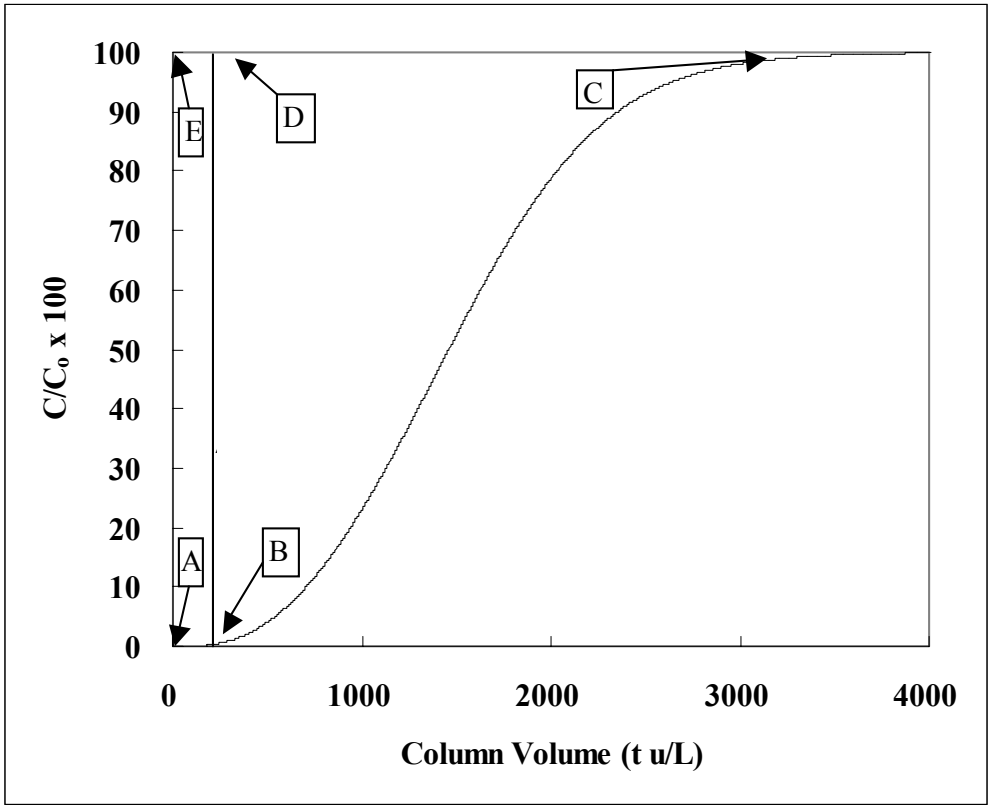

Figure 6.1. The example of breakthrough curve for IE-911 in the SRS average solution. Flow rate = 2.8×10^{-8} m^3/s, velocity = 9.5 cm/min, column diameter = 0.015m, column length = 0.1 m.

The overall capacity is proportional to the area ABCDE, while breakthrough capacity is proportional to the area ABDE. The degree of column utilization, which is defined as the ratio of the breakthrough and the overall capacity, can also be calculated. The upper area of the breakthrough curve was calculated as 1506 while the maximum upper area was 4095. Thus, the simulation result shows the 36 % of total capacity was used. The treated cesium amount, which can be calculated from the upper area multiplied by column volume and initial cesium concentration, was calculated as 0.498 g. The amount of adsorbed cesium, which can be calculated from the amount of treated cesium divided by used amount of ion exchangers, was 28 mg / g CST.

From an optimal design point of view, one should keep the overall capacity and column utilization large, while using a small amount of ion exchanger. There are two design options in determining the time of a moving bed, i. e., moving the bed with constant time interval or constant concentration at certain height of column. If the bed is moving with same interval, the operation of pulse moving is easy but the outlet concentration should be analyzed more often so as not to let the cesium flow out without treatment. If the bed is moving at certain concentration, the analysis of bed is easy but the exact time for moving the bed is difficult to estimate.

Figure 6.2 shows simulation result of pulsed column where 25 % of the bed is moving counter-currently with simulant every 84 hours. The discontinuities, which occur when the column is moving, show that the bed is moving when the column volume reaches 500, while the cesium concentration is increase at the moving point as the time increases.

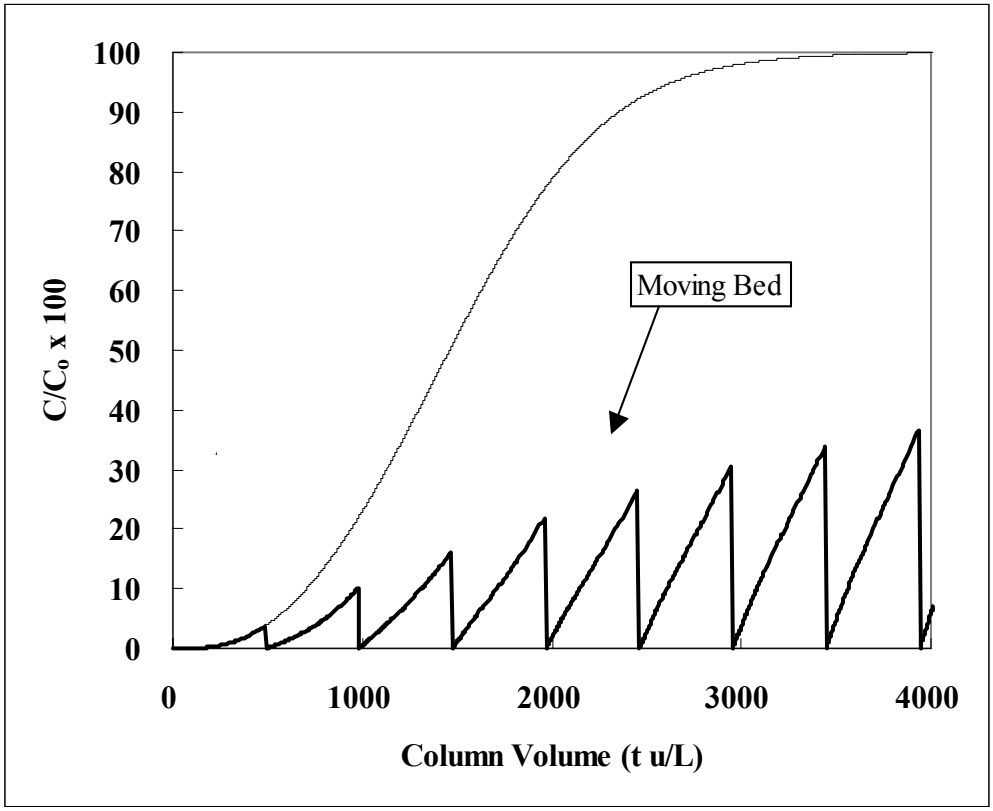

Figure 6.2. The simulated breakthrough curve for SRS average solution with pulsed column where 25 % of the bed is moved every 84 hours.

Therefore, while the first discarded ion exchanger is almost fresh ion exchanger, the last discarded ion exchanger is almost exhausted ion exchanger. The upper area of the breakthrough curve was 3643, which was 89 % usage of the total capacity of the column reactor. The amounts of treated and adsorbed cesium were 1.20 and 34.1mg/ g CST, respectively. Although the used amounts of IE-911 granules of the pulsed bed were 2 times than that of normal fixed-bed operation, cesium concentration was maintained below 40 % of initial concentration throughout the operation and the utilization of the bed was 62 % larger for the pulsed bed than that of the fixed-bed operation.

Figure 6.3 shows the simulation results of pulsed column where 25 % of the bed is moving counter-currently with simulant when the cesium concentration reaches 90 % of initial concentration at the 25 % length from the top of the column. The concept of the design of this column is the safe and economic operation instead of convenience of pulse operation. The upper area of the breakthrough curve was 3671, which was 90 % utilization of the total capacity of the column reactor. The amounts of treated and adsorbed cesium were 1.21 and 34.3mg/ g CST, respectively. This simulation showed that the utilization of the bed for the moving bed at constant concentration was almost same value as that of the moving bed at constant time while the cesium concentration was maintained below 30 % of initial concentration throughout the operation constantly, which was lower values than maximum value of the moving bed at constant time.

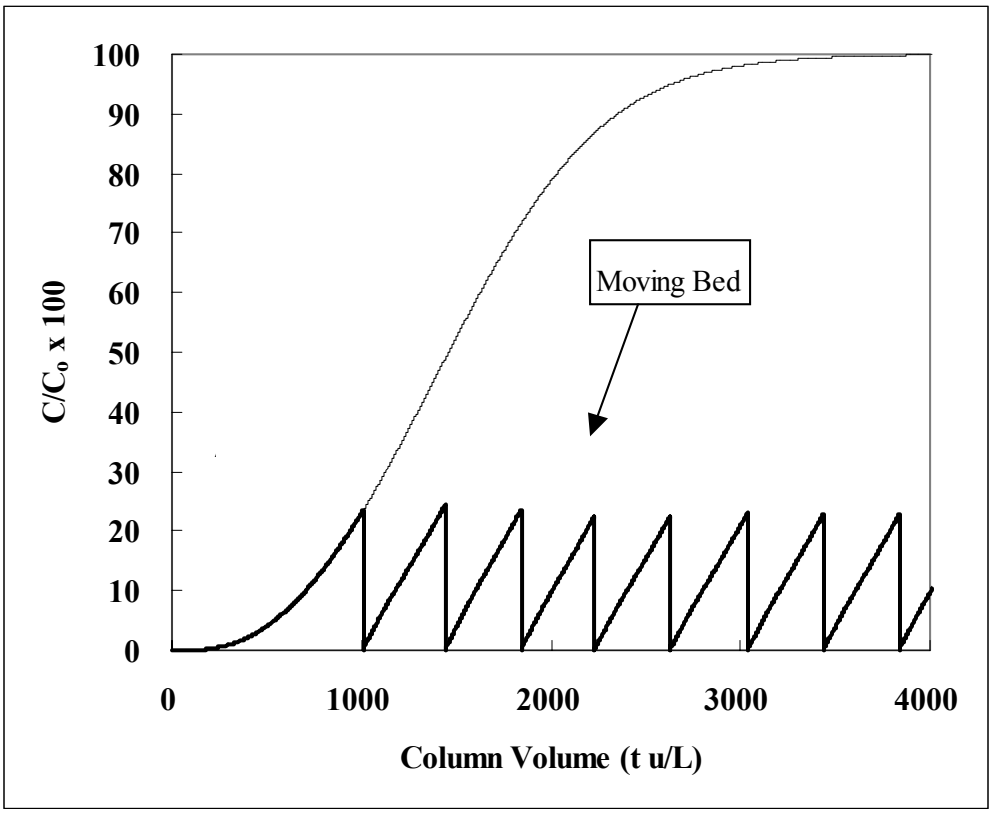

Figure 6.3. The simulated breakthrough curve for SRS average solution with a pulse column where 25 % of the bed is moving the cesium concentration reaches 90 % of initial concentration at the 25 % length from the top of the column.

Figure 6.4 shows the concentration distribution of cesium along the column reactor as a function of time in the pilot-scale plant when the effective diffusivity is 2.0×10^{-11} m^2/s. It should be noted that the breakthrough curve for the pilot-scale experiment couldn't be obtained, because the 18 days of operation was too short to detect the cesium concentration at the outlet of the column, which is clearly shown in Figure 6.4. Figure 6.5 shows the variation of cesium concentration along the column length before and after the pulsed move of ion exchanger. As shown in Figure 6.5, the non-zero cesium concentration is found only at the top column even after three days. The pulsed moving of 6.25 % of column decreases cesium concentration slightly at the top part of the column.

Figure 6.6 shows the comparison of the experimental data with the simulation data of the pilot-scale plant. Although there was some variance in the experimental data, the predicted cesium concentrations were close to the experimental data when the effective diffusivity is in the range from 1.0×10^{-11} m^2/s to 6.0×10^{-11} m^2/s

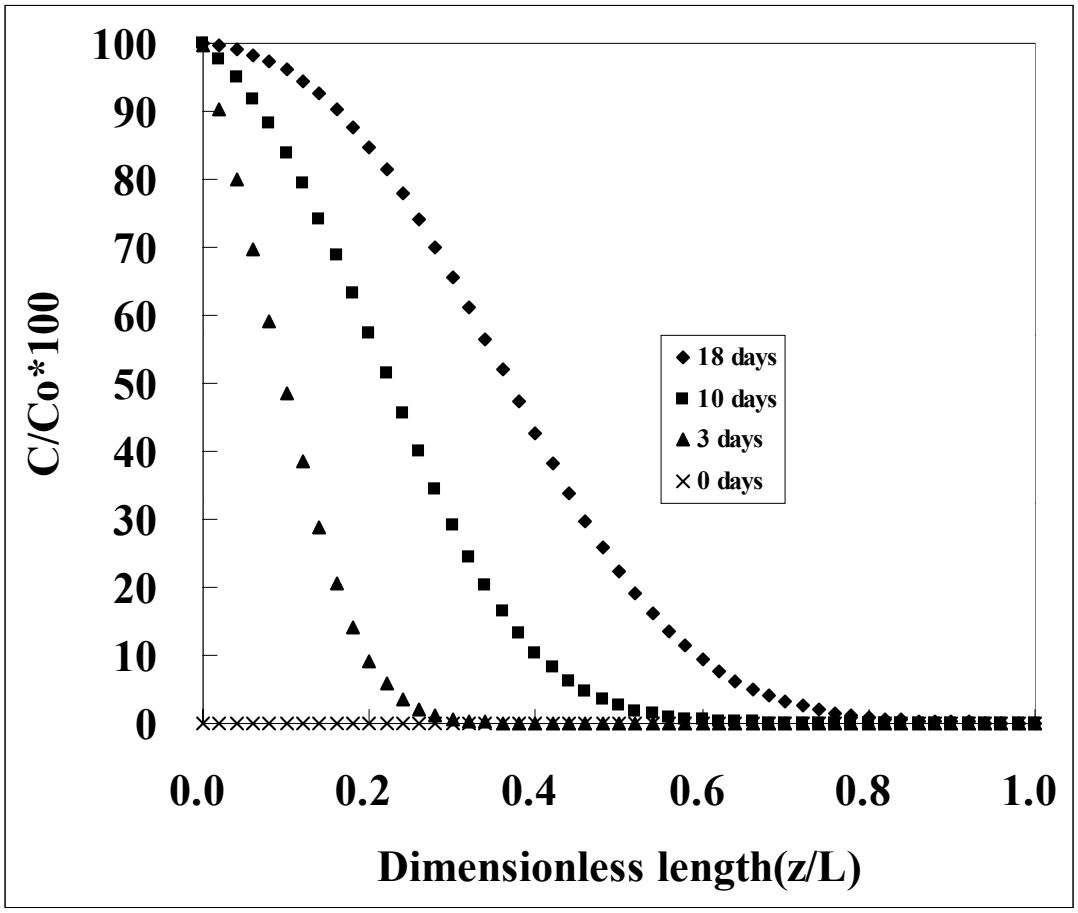

Figure 6.4. The simulated Cs concentration variation along the pilot-scale column reactor with the effective diffusivity of 2.0×10^{-11} m^2/s.

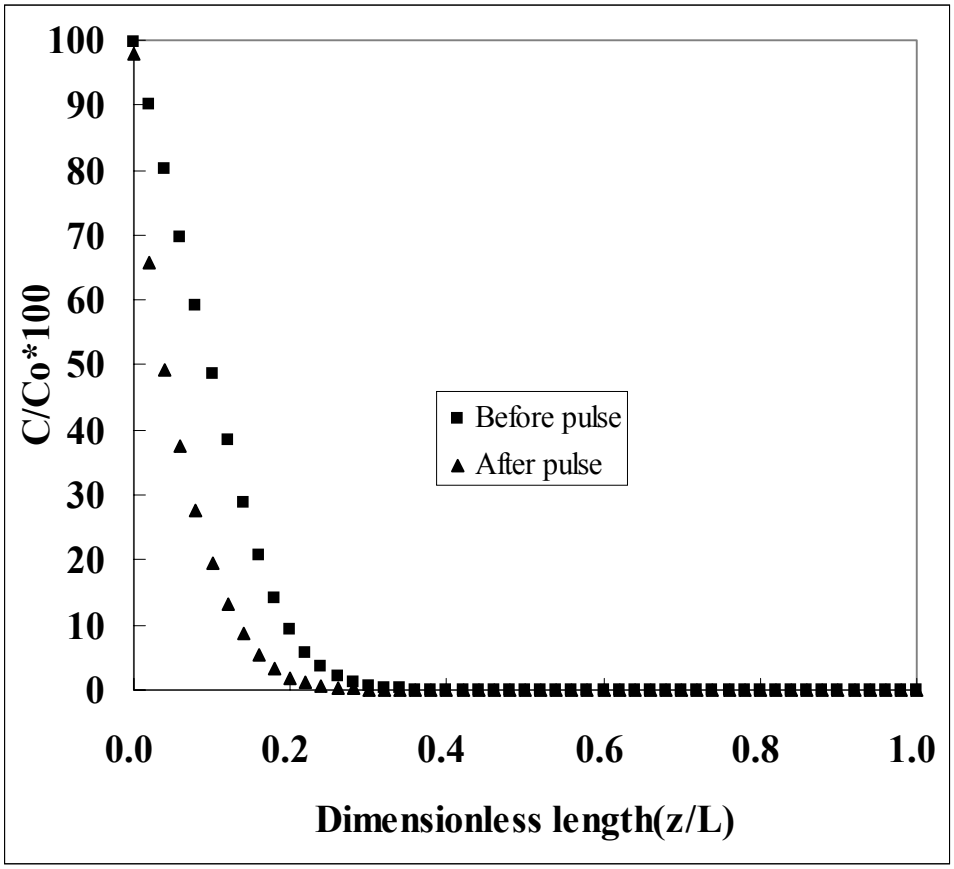

Figure 6.5. The simulated Cs concentration variation when the column was first pulsed 6.25% after 3days of testing with the effective diffusivity of 2.0×10^{-11} m^2/s.

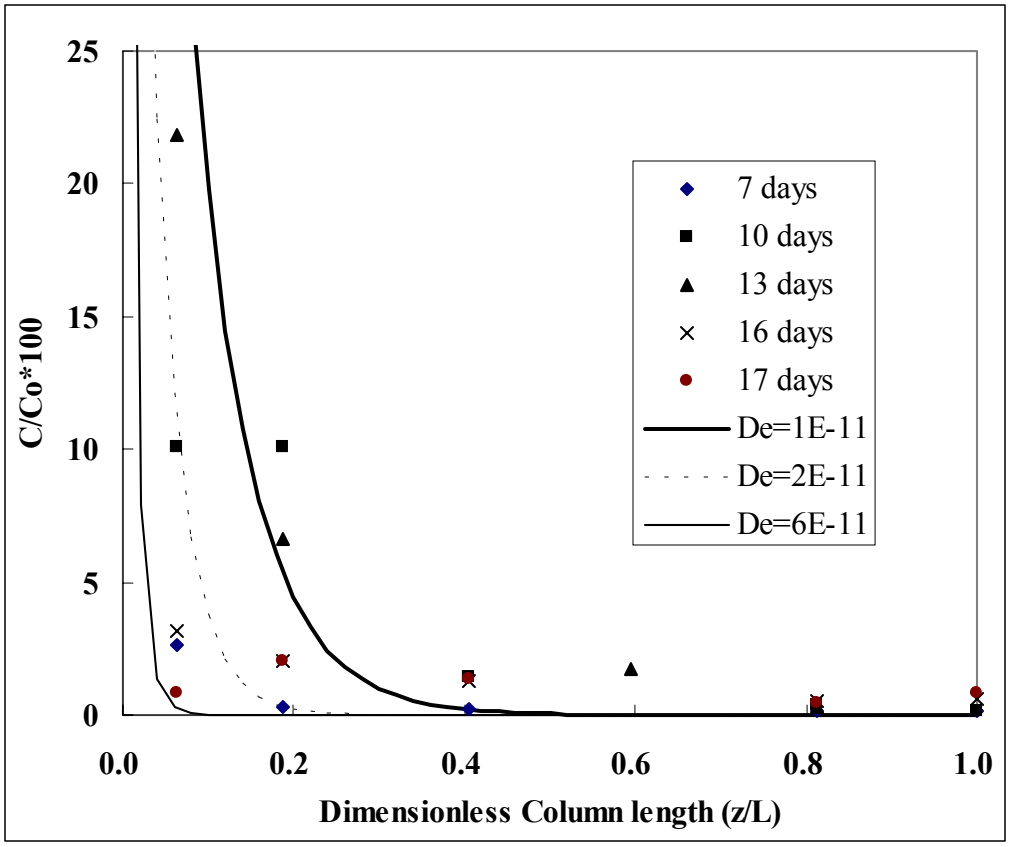

Figure 6.6. The comparison of simulated Cs concentration with the experimental data of the pilot-scale pulsed column where 6.25% of column packing was removed every day.

CHAPTER VII

CONCLUSIONS AND RECOMMENDATIONS

The main objectives of this research was to investigate the effect of various chemicals on cesium loading of IONSIV® IE-910 and to develop a mathematical model to simulate ion exchange performance for cesium using the UOP IONSIV® IE-911 granules for various ion exchange systems such as counter-current ion exchange (CCIX) column and single layer column. In order to complete these objectives, previous ZAM equilibrium model provided by Zheng (1996), which was developed based on data collected from experiments with IE-910 powder, was examined and used to predict the ion exchange performance of IE-910 for cesium and its distribution coefficients for radioactive simulants.

In Chapter III, the increase of carbonate in the simulant results in increase of cesium distribution coefficient. However, the increase of oxalate to the range of 0.0016 M doesn't affect the cesium distribution coefficient. A careful examination of data reveals that hydrogen peroxide at very low concentration has a degrading effect on CST. At higher concentration of hydrogen peroxide, i.e., 1 M or higher, the cesium distribution coefficient was decreased significantly. The XRD pattern changed for higher hydrogen peroxide concentration, indicating the dissolution of the tetragonal crystal structure, which is the phase in TAM5 that is selective for cesium.

The ZAM equilibrium model was extended to IE-911 granules to predict the performance of commercialized CST in the radioactive solutions. The equilibrium

predictions from the K-ZAM model for IE-911 granules were compared to experimental data measure for cesium distribution coefficient in an SRS average solution. The model did an excellent job of predicting the cesium distribution coefficients for the SRS average waste simiulant.

The novel single-layer column reactor, where the bulk concentration outside the packed particle is constant, was investigated. The condition of constant bulk concentration eliminates the need for a bulk liquid differential balance equation from the PDE system, which makes it possible to solve the balance equations analytically. This simple mathematical model of the single-layer column experiment allowed an easy estimation of the effective diffusivity for Cs in the IE 911 granules loaded in the simple standard solution, which contains only NaOH, $CsNO_3$ and $NaNO_3$ and complex simulant representative of the waste solutions at the SRS.

Based on the Ti analysis in the IE 911 granules, no particular trend in particle attrition or loss was observed during the experiment.

From a comparison of simulation with the experimental data, the effective diffusivities of Cs determined for the standard solution and SRS average waste were $1.56 \pm 0.14 \times 10^{-11}$ m^2/s, and $0.68 \pm 0.09 \times 10^{-11}$ m^2/s, respectively. From the comparison of effective diffusivities in the simple and complex waste solutions, one may notice that the differences of the effective diffusivities in the waste solutions is explained by the well-known Stokes-Einstein relation, where the effective diffusivity is inversely proportional to the viscosity of the solution.

A numerical method based on the orthogonal collocation method was used to design the CCIX where the fresh CST is pulsed into the column at certain period or at certain concentration of cesium, and to simulate the concentration profile of cesium in the CCIX loaded with IE-911 granules.

Two design options in determining the moving bed, i. e., moving the 25 % of bed with constant time interval of 84 hrs or with 90 % of initial cesium concentration at 75 % column height from the bottom of column, were investigated in the lab-scale fixed bed reactor. The simulation for lab-scale moving bed showed that the utilizations of ion exchanger for both cases were larger than that of normal fixed-bed operation.

Simulation results showed that cesium removal behavior in the pilot-scale test of CCIX experiment, where the column length is 22 ft and the IE-911 is pulsed 1 ft in every 24 hours, was close to the simulation result when the effective diffusivity is in the range from 1.0 to 6.0×10^{-11} m^2/s.

The results of this research point to the following recommendations for future work, which is that the K-ZAM model should be developed more to include various ions in predicting equilibrium performance, and the there should be more research for single-layer column to explain why the effective diffusivities from the single-layer column yields values less than the values obtaining from the batch and column reactors.

NOTATION

A,B = ions in the liquid phase

$\bar{A}$, $\bar{B}$ = ions in the solid phase

$a_{A,B}$ = the activities of A, B

A_m = Debye-Huckel constant

a_p = external surface area of the particles per packed volume

B_i = Bromley parameters for ion i

C = liquid phase concentration

C_i = bulk liquid phase concentration of i

C^o = feed concentration in bulk liquid phase

C^o_i = feed concentration in bulk liquid phase of i

C^∞_i = feed concentration in bulk liquid phase of i

C_{Pi} = pore liquid concentration of i

DF = dilute factor

D_c = effective diffusivity of crystal phase

D_s = effective diffusivity of macropore phase

D_e = effective diffusivity

D_L = axial dispersion coefficient

D_m = molecular diffusivity

D_P = intraparticle diffusion coefficient (same as D_e)

d_p = particle diameter

$d_{p,y}$ = particle diameter with weight fraction y

H_c = Herny's constant at micropore phase

H_s = Herny's constant at macropore phase

ΔH^o = enthalpy change

I = the ionic strength

J_i = liquid phase diffusive flux of i

J_i^s = solid phase diffusive flux of i

K_{eq} = the thermodynamic equilibrium constant

K ≡ Langmuir isotherm constant

K_{dA} = distribution coefficient of A

k_f = film mass transfer coefficient

L = length of reactor

MW = molecular weight of sample

m_i = the molality of ion i

N_i = flux of ion i

P = pressure

$Q_{A,B}$ = solid phase concentration of A,B from equilibrium isotherm

q = solid phase concentration

q_i = solid phase concentration of i

q_∞ = maximum solid phase concentration

R = gas constant

R_C = crystal radius

R_s = Radius of macropore particle

r = radial direction to center of particle

R_p = particle radius

S_c = surface area of micropore phase

S_s = surface area of macropore phase

s = radial direction to center of crystal

T = temperature

t = time

u = superficial velocity

V = volume of liquid

w = weight of sample

x = spatial direction along length of column

y = weight fraction

$Z_{A,B}$ = the charge values of A,B

z_i = valence of specie i

Greek Letters

δ_i = Bromley parameters for ion i

η = dimensionless macrosphere radial position

ε_B = bed porosity

ε_c = porosity of micropore phase

ε_s = porosity of macropore phase

ε_P = pellet porosity

γ_i = activity coefficient of i

$\gamma_{\pm}$ = mean activity coefficient of an electrolyte in the liquid

τ = tortuosity factor

τ_i = dimensionless time

$\nu_{A,B}$ = stoichiometric coefficient of A,B

ν_i = interstitial velocity

ν = kinematic viscosity

LITERARURE CITED

Ames, Jr. L. L., "Cation Sieve Properties of the Open Zeolites Chabazite, Mordenite, Erionite and Clinoptilolite, " *The American Mineralogist.,* **46**,1120 (1961).

Ames, Jr. L. L., "Effect of Base Cation on the Cesium Kinetics of Clinoptilolite, " *The American Mineralogist.,* **47**, 1310 (1962).

Amphlett, C. B., *Inorganic Ion Exchangers*, Elsevier, London (1964)

Anthony, R. G., C. V. Philip, and R. G. Dosch, "Selective Adsorption and Ion Exchange of Metal Cations and Anions with Silico-Titanates and Layered Titanates, " *Waste Manage.,* **13**, 503 (1993).

Anthony, R. G., R. G. Dosch, D. Gu, and C. V. Philip, "Use of Silicotitanates for Removing Cesium and Strontium from Defense Waste, " *Ins. Eng. Chem. Res*., **33**,2702 (1994).

Anthony, R. G., R. G. Dosch, and C. V. Philip, "Method of Using Novel Silicotitanates, " U.S. Patent 6,110,378 (2000).

Anthony, R. G., R. G. Dosch, and C. V. Philip, "Silico-Titanates and Their Methods of Making and Using, " U.S. Patent 6,479,427 (2002).

Barrer, R. M., and D. C. Sammon, "Exchange Equilibria in Crystals of Chabazite, " *J. Chem. Soc.*, **4**, 2838 (1955).

Barrer, R. M., and J. Falconer, "Ion Exchange in Felspathoids as a Solid State Reaction, " *Proc. R. Soc. London, Ser. A*, **236**, 2838 (1956).

Boyd, G. E., A. W. Adamson, and L. S. Myers, Jr., "The Exchange Adsorption of Ions from Aqueous solutions by Inorganic Zeolites. II. Kinetics, " *Jour. Am. Chem. Soc*., **69**, 2836 (1947).

Bromley, L. A., "Thermodynamic Properties of Strong Electrolytes in Aqueous Solutions, " *AIChE J.*, **19**, 313 (1973).

Bunker, B. C., "Evaluation of Inorganic Ion Exchangers for Removal of Cs from Tank Wastes, " Technical Report TWRSPP-94-085, Pacific Northwest National Laboratory, Richland, WA (1994).

Carslaw, H. S., and J. C. Jaeger, *Conduction of Heat in Solids,* Oxford University Press, London, p. 237 (1959).

Collins J. L., B. Z. Egan, K. K. Anderson, C. W. Chase, J. E. Mrochek, J. T. Bell, and G. E. Jernigan, "Evaluation of Selected Ion Exchangers for the Removal of Cesium from MVST W-25 Supernate, " Technical Report ORNL/TM-12938, Oak Ridge National Laboratory, Oak Ridge, TN (1995).

Crittenden, J. C.,B. W. C. Wong, W. E. Thacker, V. L. Snoeyink, and R. L. Hinrichs, "Mathematical Model of Sequential Loading in Fixed-Bed Adsorbers, " *J. Water Poll. Cont. Fed.*, **52**, 2780 (1980).

Danckwerts, P. V., "Contiuous Flow Systems- Distribution of Residence Times, " *Chem. Eng. Sci.,* **2**, 1 (1953).

DeMuth, S. F., "Cost Benefit Analysis for Separation of Cesium from Liquid Radioactive Waste by Crystalline Silico-titanate Ion Exchange Resin, " Technical Report LA-UR-96-966, Los Alamos National Laboratory, Los Alamos, NM (1996).

Denbigh, K., *The Principles of Chemical Equilibrium*, Cambridge University Press, Cambridge (1981).

DePaoli, S. M., and J. J. Perona, "Model for Sr-Cs-Ca-Mg-Na Ion-Exchange Uptake Kinetics on Chabazite, " *AIChE J.,* **42**, 3434 (1996).

Fettig, J., and H. Sontheimer, "Kinetics of Adsorption on Activated Carbon: I single solute System, " *J. Environ. Eng..,* **113**, 764 (1987).

Fink, S. D., T. B. Peters, D. D. Walker, M. J. Banes, R. A. Pierce, M. A. Norato, and W. R. Wilmath, "Demonstration of Cesium Removal Technologies Using High-Level Waste in Support of the Salt Processing Project at the Savannah River Site, " Technical Report WSRC-MS-2002-00059, Westinghouse Savannah River Co., Aiken, SC (2002).

Finlayson, B. A., *The Method of Weighted Residuals and Variational Principles*, Academic Press, London (1972).

Fowler, J. R., "Acid Hydrolysis of Tetraphenylborate, " Technical Report DPST-83-1099, Westinghouse Savannah River Co., Aiken, SC (1983).

Fowler, V. L., and J. J. Perona, "Evaporation Studies on Oak Ridge National Laboratory Liquid Low-Level Waste, " Technical Report ORNL/TM-12243, Oak Ridge National Laboratory, Oak Ridge, TN (1993).

Furusawa, T., and J. M. Smith, "Diffusivities from Dynamic Adsorption Data, " *AIChE J.* **19**, 401 (1973).

Gains, G. L., H. C. Thomas, "Adsorption Studies on Clay Minerals. II. A Formulation of the Thermodynamics of Exchange, " *J. Chem. Phys.*, **21**, 714 (1953).

Garg, D. R., and D. M. Ruthven, "Theoretical Prediction of Break-through Curves for Molecular Sieve Adsorption Columns- I. Asymptotic Solutions, " *Chem. Eng. Sci*., **28**, 791 (1973).

Gu, T., G. Tsai, and G. T. Tsao, "New Approach to a General Nonlinear Multicomponent Chromatography Model, " *AIChE J.*, **36**, 784 (1990).

Gu, D., L. Nguyen,C. V. Philip, M. E. Huckman, R. G. Anthony, J. E. Miller, and D. E. Trudell, "Cs^+ Ion Exchange Kinetics in Complex Electrolyte Solutions Using Hydrous Crystalline Silicotitanates, " *Ind. Eng. Chem. Res.,* **36**, 5377 (1997).

Helfferich, F., *Ion Exchange*, McGraw-Hill, New York (1962).

Holland, C. D., and R. G. Anthony, *Fundamentals of Chemical Reaction Engineering*, Prentice Hall, Englewood Cliff, NJ (1989).

Horvath, A. L., *Handbook of Aqueous Electrolyte Solutions: Physical Properties, Estimation and Correlation Methods*, Ellis Horwood Limited, England (1985).

Hritzko, B. J., D. D. Walker, and N.-H. L. Wang, "Design of a Carousel Process for Cesium Removal Using Crystalline Silicotitanate, " *AIChE J*., **46**, 552 (2000).

Huckman, M. E., "Ion Exchange Kinetics of Cs+, SrOH+, and Rb+ for the Hydrous Crystalline Silico-Titanates, UOP IONSIV IE910 and UOP IONSIV IE911, " PhD Dissertation, Texas A&M University, College Station, TX (1999).

Huckman, M. E., I. M.Latheef, and R. G. Anthony, "Ion Exchange of Several Radionuclides on the Hydrous Crystalline Silicotitanates, UOP IONSIV IE-911, " *Sep. Sci. Tech.*., **34**, 1145 (1999).

Huckman, M. E., I. M.Latheef, and R. G. Anthony, "Designing a Commercial Ion-Exchange Carousel to Treat DOE Waste Using CST Granules, " *AIChE J*., **47**, 1425 (2001).

Johnstone, J. K., "The Sandia Solidification Process: Consolidation and Characterization, Part 1. Consolidation Studies, " Technical Report SAND78-0663, Sandia National Laboratory , Albuquerque, NM (1978).

Kilpatrick, L. L., "Solubility of Sodium Oxalate and Sodium Tetraphenylborate in DWPF Supernate, " Technical Report DPST-84-314, Westinghouse Savannah River Co., Aiken, SC (1984).

Kim, D. H., "Single Effective Diffusivities for Dynamic Adsorption in Bidisperse Adsorbents," *AIChE J.* **36**, 302 (1990).

Koh, J.-H., P. C. Wankat, and N.-H. L. Wang, "Pore and Surface Diffusion and Bulk-Phase Mass Transfer in Packed and Fluidized Beds, " *Ind. Eng. Chem. Res.,* **37**, 228 (1998).

Komiyama, H., and J. M. Smith, "Surface Diffusion in Liquid-Filled Pore, " *AIChE J.*, **20**, 1110 (1974).

Krumhansl, J. L., P. C. Zheng, C. Jove-Colon, H. L. Anderson, R. C. Moore, F. M. Salas, T. M. Nenoff, and D. A. Lucero, , "A Preliminary Assessment of IE-911 Column Pretreatment Options," Technical Report SAND2001-1002, Sandia National Laboratory, Albuquerque, NM (2001).

Kurath, D. E., L. A. Bray, K. P. Brookes, G. N. Brown, S. A. Bryan, C. D. Carlson, K. J. Carson, J. R. DesChane, R. J. Elovich, and A. Y. Kim, "Experimental Data and Analysis to Support the Design of an Ion-Exchange Process for the Treatment of Hanford Tank Waste Supernatant Liquids," Technical Report PNNL-10187, Pacific Northwest National Laboratory, Richland, WA (1994).

Latheef, I. M, "Ion Exchange Column Studies for the Selective Separation of Radionuclides Using the Hydrous Crystialline Silicotitanate, UOP IONSIV® IE-911, " Ph. D. Dissertation, Texas A & M University, College Station, TX (1999).

Latheef, I. M., M. E. Huckman, and R. G. Anthony, "Modeling Cesium Ion Exchange on Fixed Bed Columns of Crystalline Silicotitanate (CST) granules, " *Ind. Eng. Chem. Res*., **39**, 1356 (2000).

Lee, D. D., J. R. Travis, and M. R. Gibson, "Hot Demonstration of Proposed Commercial Cesium Removal Technology: Progress Report, " Technical Report ORNL/TM-13363, Oak Ridge National Laboratory, Oak Ridge, TN (1997).

Lee, L. M., and L. L. Kilpatrick, "A Precipitation Process for Supernate Decontamination, " Technical Report DP-1636, Westinghouse Savannah River Co., Aiken, SC (1982).

Lide, D. R. (editor-in-chief), *Handbook of Chemistry and Physics 77th Edition*, CRC Press, New York (1996).

Ma,Y. H., and T. Y. Lee, "Transient Diffusion in Solids with a Bipore Distribution," *AIChE J.* **22**, 147 (1976).

Ma,Y. H., "The Kinetics of Sorption in a Bipore Adsorbent Particle," *AIChE J.* **24**, 531 (1978).

Ma, Z., R. D. Whitley, and N.-H. L. Wang, "Pore and Surface Diffusion in Multicomponent Adsorption and Liquid Chromotography Systems," *AIChE J.* **42**, 1244 (1996).

Marsh, S. F., Z. V. Svitra, and S. M. Bowen, "Effects of Soluble Organic Complexants and Their Degradation Products on the Removal of Selected Radionuclides from High-Level Wastes," Technical Report LA-13000, Sandia National Laboratories, Albuquerque, NM (1993).

McCabe, D. J., "Crystalline Silicotitanate Examination Result", Technical Report WSRC-RP-94-1123, Westinghouse Savannah River Co., Aiken, SC (1995).

McCabe, D. J., "Examination of Crystalline Silicotitanate Applicability in Removal of Cesium from SRS High Level Waste", Technical Report WSRC-RP-97-0016, Westinghouse Savannah River Co., Aiken, SC (1997).

Miller, J. E., and N. E. Brown, "Development Properties of Crystalline Silicotitanate (CST) Ion Exchangers for Radioactive Waste Applications," Technical Report SAND97-0771, Sandia National Laboratory, Albuquerque, NM (1997).

Moore, M., " First Puzzlement; Then Action, " *Bull. At. Sci.* **49**,314 (1993).

Nguyen, L.T., "A Kinetic Model for Ion Exchange Between Cesium and Sodium Using Silico-Titanates, " M.S. Thesis, Texas A&M University, College Station, TX (1994).

Nyman, M., T. M. Nenoff, and T. J. Headley, "Characterization of UOP IONSIV IE-911," Technical Report, SAND 2001-0999, Sandia National Laboratory, Albuquerque, NM (2001).

Perry, R. H., D. W. Green, and J. O. Maloney, Eds., *Perry's Chemical Engineers' Handbook 7th Edition*, McGraw-Hill, New York, p.6-39 (1997).

Petzold, L.R., "A Description of DASSL: A Differential/Algebraic System Solver," Technical Report SAND82-8637, Sandia National Laboratory, Albuquerque, NM (1982).

Philip, C. V., and R. G. Anthony, "Synthesis and Characterization of New Crystlalline Silicotitanate, " *International Symposium on Industrial Applications of Zeolites*, Technological Institute of Brugge, Belgium (2000).

Philip, C. V., S. H. Kim, M Philip, and R. G. Anthony, "The Effect of Hydrogen Peroxide on a CST Under Cesium Ion Exchange Conditions" *Sep. Sci. Tech*., 38, 3009 (2003).

Pinsky, M. A. *Partial Differential Equations and Boundary Value Problems with Applications,* Mc-Graw Hill, New York (1991).

Pitzer, K. S., "Ion Interaction Approach: Theory and Data Correlation, " *Activity Coefficients in Electrolyte Solutions*, Pitzer, K. S. ed., CRC press, Boca Baton, FL (1991).

Polzer, W. L., and H. R. Fuentes, "The Use of a Heterogeneity-Based Isotherm to Interpret the Transport of Radionuclides in Volcanic Tuff Media, " *Radiochim. Acta.*, **44/45**,361 (1988).

Polzer, W. L., M. G. Rao, H. R. Fuentes, and R. J. Beckman, "Thermodynamically Derived Relaionship Between the Modified Langmuir Isotherm and Experimental Parameters," *Environ. Sci. Technol.*, **26**,1780 (1992).

Reichenberg, D, "Properties of Ion-Exchange Resin in Relation to their Structure. III. Kinetics of Exchange," *Jour. Am. Chem. Soc*., **75**, 589 (1953).

Reid, R. C., J. M. Prausnitz, and B. E. Poling, *The Properties of Liquid and Gases*, McGraw Hill, New York (1987).

Ritcey, G. M., and A. W. Ashbrook, *Solvent Extraction, Principle and Applications to Process Metallurgy*, Elsevier, New York (1984).

Robinson, R. A., and R. H. Stokes, *Electrolyte Solutions: The Measurement and Interpretation of Conductance, Chemical Potential and Diffusion in Solutions of Simple Electrolytes*, Butterworths, London (1970).

Robinson, S. M. W. D. Arnold, and C. H. Byers, "Mass-Transfer Mechanisms for Zeolite Ion Exchange in Wastewater Treatment," *AIChE J.,* **40**, 2045 (1994).

Ruckenstein, E., A. S. Vaidyanathan, and G. R. Youngquist, "Sorption by Solids with Bidisperse Pore Structures," *Chem. Eng. Sci.* **26,** 1305 (1971).

Ruthven, D. M., and K. F. Loughlin, "The Diffusional Resistance of Molecular Sieve Pellets," *The Canadian Journal of Chemical Engineering*, **50**, 550 (1972).

Satterfield, C. N., Mass Transfer in Heterogeneous Catalysis, MIT press, Cambridge, MA (1970).

Sherwood, T. K., R. L. Pigford, and C. R. Wilke, *Mass Transfer*, Mcgraw-Hill, New York (1975).

Silva, V. M. T. M., and A. E. Rodrigues, "Adsorption and Diffusion in Bidisperse Pore Structures, " *Ind. Eng. Chem. Res.*, **38**, 4023 (1999).

Sladek, K. J., E. R. Gilliland, and R. F. Baddour, "Diffusion on Surfaces. II. Correlation of Diffusivities of Physically and Chemically Adsorbed Species, " *Ind. Eng. Chem. Fund.*, **13**, 100 (1974).

Smith, E. H., and W. J. Weber, Jr., "Modeling Activated Carbon Adsorption of Target Organic Compounds from Leachate-Contaminated Groundwaters, " *Environ. Sci. Technol.*, **22**, 313 (1988).

Smith, J. M., and H. C. Van Ness, *Introduction to Chemical Engineering Thermodynamics*, McGraw Hill, New York (1987).

Sokolova, E. V., R. K. Ratsvetaeva, V. I. Andrianov, Yu. K. Egorov-Tismenko, and Yu. P. Men'shikov, "The Crystal Sructure of a New Natural Sodium Titanosilicate, " *Sov. Phys. Dokl.*, **34**, 583 (1989).

Solztak, R., *Molecular Sieves: Principles of Synthesis and Identification,* Van Nostrand Reinhold, New York (1989).

Su, Y., L. Li, J. S. Young, and M. L. Balmer, "Investigation of Chemical and Thermal Stabilities of Cs-Loaded UOP IONSIV® IONSIV IE-911 Ion Exchanger, " Technical Report PNNL-13392-2, Pacific Northwest National Laboratory, Richland, WA (2001).

Suzuki, M, and J. M. Smith, "Axial Dispersion in Beds of Small Particles," *Chem. Eng. J.*, **3**, 256 (1972).

Suzuki, M., *Adsorption Engineering*, Elsevier, Amsterdam (1990).

Taylor, R. A, and C. H. Mattus, "Thermal and Chemical Stability of Crystalline Silicotitanate Sorbent, " Technical Report ORNL/TM-1999/233, Oak Ridge National Laboratory , Oak Ridge, TN (1999).

Turner, G. A., "The Flow Structure in Packed Beds, " *Chem. Eng. Sci.*, **7**, 156 (1958).

U. S. Department of Energy, "Committed to Results: DOE's Environmental Management Program, " Technical Report DOE/EM-0152P, Washington, DC (1994).

U. S. Department of Energy, "Tank Focus Area: Annual Report FY2000, " Technical Report DOE/EM-0564, Washington, DC (2000).

Wakao, N., and T. Funazkri, "Effect of Fluid Dispersion Coefficients on Particle-to-Fluid Mass Transfer Coefficients in Packed Beds : Correlation of Sherwood Numbers, " *Chem. Eng. Sci.*, **33**, 1375 (1978).

Wakao, N., and S. Kaguei, *Heat and Mass Transfer in Packed Beds*, Gordon and Breach Science Publishers, New York (1982).

Walker, D. D., and M. A. Schmitz, "Technical Data Summery: In Tank Percipitation Processing of Soluble High-Level Waste," Technical Report DPSTD-84-103, Westinghouse Savannah River Co., Aiken, SC (1984).

Walker, D. D., W. D. King, D. P. Diprete, L. L. Tovo, D. T. Hobbs, and W. R. Wilmarth, "Cesium Removal from Simulated SRS High Level Waste Using Crystalline Silicotitanate," Technical Report. WSRC-TR-98-00344, Westinghouse Savannah River Company, Aiken, SC (1998).

Walker, D. D., "Cesium Sorption/Desorption Experiments with IONSIV® IE-911 in Rdioactiove Waste," Technical Report WSRC-TR-2000-00362, Westinghouse Savannah River Co., Aiken, SC (2000).

Walker, Jr. J. F., and E. L. Youngblood, "Design Alternatives Report for the Cesium Removal Demonstration, " Technical Report ORNL/TM-12939, Oak Ridge National Laboratory , Oak Ridge, TN (1995).

Walker, Jr. J. F., P. A. Taylor, and D. D. Lee, "Cesium Removal from High-pH High-Salt Wastewater Using Crystalline Silicotitanate Sorbent," *Sep. Sci. Tech.*, **34**,1167 (1999).

Weber, W. J., Jr., and C. K. Wang, "A Microscale System for Estimation of Model Parameters for Fixed Bed Adsorbers," *Environ. Sci. Technol.*, **21**,1096 (1987).

Wen, C. Y., and L. T. Fan, *Models for Flow Systems and Chemical Reactions*, Marcel Dekker, New York (1975).

Wester, D., R. Leugemors, F. Fondeur, P. Taylor, R. Dennis, T. Hong, and J. Pike, "Pilot-Scale Test of Counter-Current Ion Exchange (CCIX®) Using UOP IONSIV® IE-911, " Technical Report PNNL-13625; EW4010000, Pacific Northwest National Laboratory, Richland, WA (2001).

Wilke, C. R., and O. A. Hougen, “Mass Transfer in Flow of Gases through Granular Solids Extended to Low Modified Reynolds Numbers, ” *Tans. Am. Inst. Chem. Eng.*, **41**, 445 (1945).

Yen, S. N., J. A. Pike, R. A. Jacobs, M. R. Poirier, B. M. Sahawneh, and R. K. Leugemors, “Evaluation of Alternate Ion Exchange Designs for CST Non-Elutable Ion Exchange Process, ” Technical Report WSRC-TR-2001-00133, Westinghouse Savannah River Company, Aiken, SC (2001)

Yoshida, H., M. Yoshikawa, and T. Kataoka, “Parallel Transport of BSA by Surface and Pore Diffusion in Strongly Basic Chitosan, ” *AIChE J.,* **40**, 2034 (1994).

Zemaitis, J. F., D. M. Clark, M. Rafal, and N. C. Scrivner, *Hankbook of Aqueous Electrolyte Thermodynamics: Theory & Application*, Design Institute for Physical Property Data, New York (1986).

Zheng, Z., D. Gu, R. G. Anthony, and E. Klavetter, “Estimation of Cesium Ion Exchange Distribution Coefficients for Concentrated Electrolytic Solutions When Using Crystalline Silicotitanates,” *Ind. Eng. Chem. Res.*, **34**, 2142 (1995).

Zheng, Z., “Ion Exchange in Concentrated Solutions Utilizing Hydrous Crystalline Silicotitanates, ” PhD Dissertation, Texas A&M University, College Station, TX (1996).

Zheng, Z., C. V. Philip, R. G. Anthony, J. L. Krumhansl, D. E. Trudell, and J. E. Miller, “Ion Exchange of Group I Metals by Hydrous Crystalline Silicotitates,” *Ind. Eng. Chem. Res.*, **35**, 4246 (1996).

Zheng, Z., R. G. Anthony, and J. E. Miller, “Model Multicomponent Ion Exchange Equilibrium Utilizing Hydrous Crystalline Silicotitanates by Multiple Interactive Ion Exchange Site Model,” *Ind. Eng. Chem. Res.*, **36**, 2427 (1997).

VITA

Sung Hyun Kim was born in Seoul, Korea on March 20, 1968, to Chang Woon Kim and Kum Ja Jin. In 1991, He received a Bachelor of Science degree in chemical engineering from Korea University in Korea. He continued his studies at the graduate school of his alma mater and received a Master of Science degree in 1993. The title of the thesis is "A Study of Improvement of Conversion Efficiency by Granulating Fine Coal Particles in the Fluidized Bed Combustor". He spent the following 6 years working as a researcher for Korea Kumho Petrochemical Company in Korea. In 1999 he began graduate studies towards his Ph. D. at Texas A & M University in College Station, Texas.

He can be reached through the following address: 394-24, Kuro-Dong, Kuro-Gu, Seoul, Korea.